Davies, P. J., McKenzie, J. A., Palmer-Julson, A., et al., 1991
Proceedings of the Ocean Drilling Program, Initial Reports, Vol. 133

4. SITES 811/825[1]

Shipboard Scientific Party[2]

HOLE 811A

Date occupied: 17 August 1990

Date departed: 17 August 1990

Time on hole: 21 hr, 43 min

Position: 16°30.977′S, 148°9.436′E

Bottom felt (rig floor; m, drill-pipe measurement): 947.9

Distance between rig floor and sea level (m): 10.89

Water depth (drill-pipe measurement from sea level, m): 937.1

Total depth (rig floor; m): 1162.9

Penetration (m): 213.6

Number of cores (including cores with no recovery): 23

Total length of cored section (m): 214.5

Total core recovered (m): 213.2

Core recovery (%): 99.4

Oldest sediment recovered:
Depth (mbsf): 214.5
Nature: foraminifer nannofossil ooze
Age: middle Miocene

HOLE 811B

Date occupied: 17 August 1990

Date departed: 19 August 1990

Time on hole: 1 day, 22 hr, 43 min

Position: 16°30.948′S, 148°9.454′E

Bottom felt (rig floor; m, drill-pipe measurement): 948.0

Distance between rig floor and sea level (m): 10.99

Water depth (drill-pipe measurement from sea level, m): 937.0

Total depth (rig floor; m): 1340.5

Penetration (m): 392.5

Number of cores (including cores with no recovery): 24

Total length of cored section (m): 199.3

Total core recovered (m): 15.5

Core recovery (%): 7.8

Oldest sediment recovered:
Depth (mbsf): 384.9
Nature: lithified bioclastic grainstone
Age: early to middle Eocene

HOLE 811C

Date occupied: 20 August 1990

Date departed: 20 August 1990

Time on hole: 10 hr, 39 min

Position: 16°30.942′S, 148°9.451′E

Bottom felt (rig floor; m, drill-pipe measurement): 947.8

Distance between rig floor and sea level (m): 11.02

Water depth (drill-pipe measurement from sea level, m): 936.8

Total depth (rig floor; m): 1003.0

Penetration (m): 55.2

Number of cores (including cores with no recovery): 6

Total length of cored section (m): 55.2

Total core recovered (m): 55.28

Core recovery (%): 100.1

Oldest sediment recovered:
Depth (mbsf): 55.20
Nature: foraminifer nannofossil ooze
Age: late Pliocene

HOLE 825A

Date occupied: 6 October 1990

Date departed: 7 October 1990

Time on hole: 1 day, 3 hr, 7 min

Position: 16°30.948′S, 148°9.458′E

Bottom felt (rig floor; m, drill-pipe measurement): 951.0

Distance between rig floor and sea level (m): 11.57

Water depth (drill-pipe measurement from sea level, m): 939.4

Total depth (rig floor; m): 1332.5

Penetration (m): 381.5

Number of cores (including cores with no recovery): 23

Total length of cored section (m): 186.0

Total core recovered (m): 54.4

Core recovery (%): 29.2

Oldest sediment recovered:
Depth (mbsf): 315
Nature: bioclastic grainstone
Age: early Miocene

HOLE 825B

Date occupied: 7 October 1990

Date departed: 8 October 1990

Time on hole: 1 day, 7 hr, 42 min

Position: 16°30.961′S, 148°9.457′E

Bottom felt (rig floor; m, drill-pipe measurement): 951.0

Distance between rig floor and sea level (m): 11.66

Water depth (drill-pipe measurement from sea level, m): 939.3

Total depth (rig floor; m): 1417.3

Penetration (m): 466.3

Number of cores (including cores with no recovery): 10

[1] Davies, P. J., McKenzie, J. A., Palmer-Julson, A., et al., 1991. *Proc. ODP, Init. Repts.*, 133: College Station, TX (Ocean Drilling Program).
[2] Shipboard Scientific Party is as given in list of participants preceding the contents.

Total length of cored section (m): 86.8

Total core recovered (m): 3.0

Core recovery (%): 3.5

Oldest sediment recovered:
Depth (mbsf): 453
Nature: bioclastic grainstone
Age: middle Eocene to early Miocene

Hard rock recovered:
Depth (mbsf): below 453
Nature: poorly foliated metasedimentary(?) or metavolcanic(?) rock

Principal Results: Site 811 was located on the western margin of the Queensland Plateau, 3.5 nmi east of Holmes Reef. Drilling penetrated a 385-m-thick sequence of calcareous (90% $CaCO_3$), platform-top sediments ranging in age from early-to-middle Eocene to Pleistocene. Based on benthic foraminifer assemblages, we estimated that the depositional site had been a middle bathyal paleobathymetric depth (600–1000 m) for at least the last 10 m.y. Below this datum level (below 200 mbsf), reworking and redeposition of shallower water deposits were indicated by the occurrence of larger benthic foraminifers. Below 270 mbsf, redeposited skeletal grains document the transition to a neritic environment, possibly fore- or back-reef. Sedimentation rates for the upper 270 mbsf were relatively low for a carbonate platform environment and ranged between 1.5 and 3 cm/k.y. Variations in the rate can be attributed to varying amounts of bank-derived carbonate detritus and the considerable removal of finer fractions by winnowing.

Seven seismic sequences can be identified, five of which equate well with the lithostratigraphic units defined from the drilling. Six major sedimentary units were recovered between the seafloor and 384.9 mbsf. The lithologic units are follows:

Sedimentary Unit I: depth, 0–33.15 mbsf; age, late Pleistocene to late Pliocene (1.8–2.5 Ma). The dominant lithologies are foraminifer oozes with nannofossils and nannofossil oozes with foraminifers intercalated with redeposited shallow-water carbonate sediments composed of unlithified bioclastic packstones with nannofossils and lithoclastic rudstones. The mixture of pelagic and bank-derived, fine-grained components identifies these sediments as periplatform oozes. Unit I has been divided into three subunits based on the distribution of the redeposited sediments:

Subunit IA: depth, 0–7.85 mbsf; age, late Pleistocene. The oozes contain pteropods and are intercalated with a series of 10- to 15-cm-thick unlithified foraminifer bioclastic packstone layers, which have been interpreted as calciturbidites.

Subunit IB: depth, 7.85–18.0 mbsf; age, approximately middle Pleistocene. Bioclastic packstone layers and pteropods are absent, but the fine-grained component consists of up to 75% fine-grained, bank-derived calcite particles.

Subunit IC: depth: 18.0-33.15 mbsf; age, late Pliocene (1.8–2.5 Ma). Two debris-flow deposits, comprising unlithified bioclastic packstones with nannofossils and unlithified lithoclastic rudstones and floatstones, are separated by a 7-m-thick interval of nannofossil foraminifer ooze. Moldic porosity in some lithoclasts suggests meteoric diagenesis during exposure of the carbonate bank source.

Sedimentary Unit II: depth, 33.15–147.5 mbsf; age, late Pliocene to late Miocene (2.4–8.75 Ma). Homogeneous nannofossil oozes with foraminifers to foraminifer oozes with nannofossils have been divided into two subunits based on variations in the source of the fine-grained fraction.

Subunit IIA: depth, 33.15–70.0 mbsf; age, early-to-late Pliocene (2.5–3.75 Ma). Although gravity flow deposits are absent, the fine-grained fraction of the ooze contains up to 75% bank-derived calcareous particles, which defines it as a periplatform ooze. This ooze grades into chalk at the base of the subunit.

Subunit IIB: depth, 70–147.5 mbsf; age, early Pliocene to late Miocene (3.75–8.75 Ma).

The oozes have a predominantly pelagic origin, contain more than 75% nannofossils, and are devoid of calciturbidite layers. The degree of induration decreases downward, grading from more chalky to unconsolidated at the base of the subunit.

Sedimentary Unit III: depth, 147.5–269.5; age, late-to-middle Miocene (8.75–12.5 Ma). Periplatform oozes and chalks alternate with numerous 10- to 70-cm-thick, bioclastic foraminifer wackestone, packstone, lithoclast floatstone, and rudstone layers, which usually fine upward and are considered turbidites. The degree of induration tends to increase downward; however, because of the extremely poor recovery in the lower 50 m of the unit (exclusive of good recovery in a 5-m interval cored using a vibrapercussive coring tool), it is impossible to delineate the exact level and nature of the change from ooze to chalk.

Sedimentary Unit IV: depth, 269.5–356.3 mbsf; age, middle-to-early Miocene (125–? Ma). A thick, redeposited sand and rubble package containing mostly skeletal grains, such as coral debris, alcyonarian spicules, mollusk fragments, small and larger benthic foraminifers (amphisteginids, miliolids, textularians), echinoids, crustaceans, bryozoans, and red algae documents passage from the middle bathyal environment of the overlying units into a neritic environment, possibly representing a fore- or back-reef environment. Very poor recovery of the neritic sediments and absence of good biostratigraphic markers limit our interpretation of this transition.

Sedimentary Unit V: depth, 356.3–365.9 mbsf; age, late Oligocene. A poorly recovered, unlithified to well-cemented, fine-grained skeletal packstone that contains abundant planktonic foraminifers in a micritic matrix composed of silt-size bioclastic particles documents that sedimentation at Site 811 occurred in a comparatively cold, open-water environment during the Oligocene.

Sedimentary Unit VI: depth, 365.9–392.5(?) mbsf; age, early-to-middle Eocene. Only a small pebble of shallow-water limestone was recovered from this unit (Section 133-811B-23X-CC; 384.9 mbsf), which may represent the sedimentary cover overlying the unrecovered seismic basement at this site.

Aragonite concentrations up to 38% were recorded between 0 and 10 mbsf, with traces detectable to depths of 30 mbsf. Dissolution of metastable carbonate phases is reflected in the interstitial water chemistry. Below 30 mbsf, the absence of aragonite and the monotonous interstitial water chemistry indicate that only a very minor amount of recrystallization is occurring at present.

The total organic carbon content of the sediments was low, and ranged from 0.1% to 0.45%. Volatile hydrocarbons, with methane concentrations ranging from 1.7 to 4.8 ppm and only trace amounts of ethane and propane, presented no safety problems.

Shipboard paleomagnetic studies failed to resolve any magnetic polarity reversals because of severe downhole contamination by (1) drill-string particles, (2) possible viscous drill-string magnetization, and (3) core disturbances.

Site 825 is located on the windward western margin of the Queensland Plateau, immediately east of Holmes Reef. This site was a reoccupation of Site 811 intended to reach our basement objective and to try to recover additional sediment from the poorly recovered intervals at Site 811. Hole 825A was washed to 200 mbsf after the retrieval of a 4.5-m APC mud-line core. APC/XCB drilling then penetrated to 381.5 mbsf before refusal. This was followed by RCB drilling of Hole 825B between 379.5 and 466.3 mbsf, with basement contact at approximately 453 mbsf.

The continental basement is a possible quartz-feldspar-mafic(?) metasediment or metavolcanic rock. Accurate identification of the rock type will require shore-based analysis of thin sections. We were unable to determine precisely the age of the bioclastic grainstone and rudstone representing the inner-shelf facies that transgressed over the basement, but sparse coccoliths indicate an age range from middle Eocene to early Miocene. Interpretation of age on the basis of the abundant larger benthic foraminifers obtained in Hole 825B will be forthcoming after shore-based thin-section analyses.

Five lithologic units (possibly six based on the recovery of a single pebble dated as early-to-middle Eocene) were defined for the Site 811 sedimentary sequence. The sediments recovered at Site 825 correspond to these units in part; however, with deeper penetration, Hole 825B extended below the level of the lowest lithologic Unit VI defined at Site 811. Thus, the same unit designations have been used for Site 825 sediments, with a redefinition of Unit VI on the basis of better recovery and an additional Unit VII that includes basement rock.

1. *Unit I:* depth, 0–4.5 mbsf; age, late Pleistocene. The mud-line core from Hole 825A contained nannofossil foraminifer micritic ooze with interbeds of thin foraminifer pteropod packstone layers, which has been interpreted as calciturbidites. These sediments correlate with the Pleistocene periplatform ooze of lithologic Subunit IA at Site 811. No sediments from Unit II were cored at Site 825.

2. *Unit III:* depth, 200.0–276.4 mbsf; age, middle Miocene. The sediments recovered in this interval are white micritic ooze and chalk with nannofossils and foraminifers alternating with white unlithified to partially lithified bioclastic packstone and floatstone. These sediments are similar to the series of deep-water periplatform ooze and chalk alternating with gravity flow deposits that were recovered at Site 811 in the same depth interval.

3. *Unit IV:* depth, 305.4–315.0 mbsf; age, late early Miocene. Unit IV contains white lithified bioclastic packstone with foraminifers and yellow indurated bioclastic rudstone with larger benthic foraminifers, coralline algae, and coral molds, as observed at Site 811. This unit represents deposition in a tropical fore- or back-reef environment at water depths of less than 50 m. No sediments from Unit V were recovered at Site 825.

4. *Unit VI:* depth, 408.4–453 mbsf; age, middle Eocene to early Miocene, probably late Oligocene. Unit VI contains white and pale yellow to yellow, alternating with pinkish, indurated well-sorted bioclastic grainstone and rudstone. The dominant bioclasts are coralline algae, echinoids, bryozoans, mollusks, and small branching corals. Primary intergranular porosity is well preserved, with only minimum moldic porosity. The interpreted depositional environment is temperate to subtropical waters on the inner neritic shelf. These sediments probably represent the transgressive facies overlying the continental basement.

5. *Unit VII:* depth, 453–466.3 mbsf; age, unknown. The basement rock is a dark gray, poorly foliated, well-lithified fine-grained quartz-feldspar-mafic(?) metasediment(?) or metavolcanic(?) containing more coarsely crystalline zones of quartz and feldspar. Thin, discontinuous quartz or feldspar veinlets are present, and disseminated pyrite is common.

Three WSTP runs were performed to obtain downhole temperatures and formation fluids. Temperature data indicate that the geothermal gradient at Sites 811/825 is 8.0°C/100 m, which is comparatively greater than 5° to 6°C/100 m observed at other Leg 133 sites. Geochemical analyses of WSTP and squeezed interstitial waters correspond to the profiles obtained at Site 811. The higher thermal gradient, together with the monotonous geochemistry of the interstitial fluids measured at Site 811 and confirmed by the Site 825 waters, indicate a massive fluid flow through the carbonate sediments. Physical property measurements of sediments recovered between 200 and 267 mbsf show high porosity (about 52%) and water content (about 40%), approximately 5% higher than normal for these depths. These measurements are consistent with the proposed fluid flow that essentially must be maintaining the higher water content by replacing water expelled with normal compaction.

BACKGROUND AND SCIENTIFIC OBJECTIVES

Operations at Sites 811/825 in the west-central Queensland Plateau (Fig. 1) represent the first attempt to drill in the Coral Sea since 28 December 1972, when Site 209 was drilled in 1428 m of water on the eastern margin of the Queensland Plateau (Burns, Andrews, et al., 1973).

Drilling at Site 209 defined three lithologic facies (Fig. 2). A basal upper bathyal-to-neritic, upper middle Eocene, glauconite-bearing bioclastic and foraminifer-rich sediment is overlain by an uppermost middle Eocene to upper Eocene section comprising terrigenous detritus and foraminifer ooze. The section indicates that some subsidence of the upper Eocene to upper Oligocene sediments may be the result of nondeposition and/or submarine erosion. This hiatus was followed by further subsidence until the present mid-bathyal depths and the deposition of almost pure foraminifer and nannofossil ooze from the late Oligocene to the present, with a period of apparent nondeposition or erosion in the middle Miocene. The most important conclusions to emerge from the drilling at Site 209 are as follows:

1. The site clearly records the subsidence history of the Queensland Plateau from shallow neritic depths in the late middle Eocene to its present mid-bathyal depth of 1428 m (Fig. 3); a major subsidence pulse began in the latest part of the middle Miocene.

2. The sediments are dominantly foraminifer ooze throughout, while the terrigenous content of the cores decreases in the upper units, particularly from the middle to the upper Eocene.

3. A major period of nondeposition or submarine erosion spans most of the Oligocene, after which deposition was almost entirely carbonate-dominated.

4. The Oligocene unconformity is thought to relate to circulation changes in the southwest Pacific.

Studies at Site 209 raised many questions. In particular, these studies showed an apparent marked lack of correlation between unconformities and seismic reflectors. Questions regarding the nature of the basement beneath the Queensland Plateau were not answered. Both factors still are pertinent today.

Sites 811/825 lie in approximately 938 m of water on the western margin of the Queensland Plateau approximately 3.5 nmi east of Holmes Reef. Site-survey seismic data (Fig. 4) together with stacked velocity plots from this site and DSDP Site 209 (Fig. 5) helped to identify four prominent sub-bottom reflectors, the lowest of which (horizon 7) at 1.74 s has been interpreted as basement. Reflector 6 may represent the boundary between the middle Miocene and Oligocene and also may reflect a major change in facies from shallow-water reef(?) sedimentation below to deeper water above. The sediments in the drill hole between reflectors 6 and 7 can be traced northward into a build-up that may form the site of derivation of the sediments at the drilling location. Reflector 5 separates two sequences of different character and may indicate the change from shallow to deeper water facies. Reflector 4 may be of late Miocene age.

On the basis of these factors, Site 811 presents an opportunity to define a complete record of plateau sedimentation throughout the Neogene and a record of the extent to which sea level affected sedimentation during the late Oligocene and early Miocene. The record may also define the beginning of shallow-water carbonate sedimentation on Queensland Plateau and, in particular, the time at which tropical reefs started to develop. Drilling at these sites should show whether the carbonate system at Holmes Reef began as a tropical or a temperate build-up. Finally, Sites 811/825 may define the origin of the Queensland Plateau by drilling into basement that is thought to be composed of probable(?) Paleozoic rocks (Mutter and Karner, 1980). Beneath the western one-third of the plateau, particularly near Sites 811/825, basement is progressively downfaulted westward toward the Queensland Trough. Basement rocks were almost certainly exposed and planated during Cretaceous and Eocene time.

The principal objectives of drilling at Sites 811/825 were as follows:

1. To determine the age and facies of periplatform deposits adjacent to a plateau-margin reef build-up.

2. To determine the sea level, paleoceanographic and paleoclimatic signals within a periplatform system; in particular, to define the history of the carbonate saturation of the ocean over the Queensland Plateau and to determine the onset of the East Australian Current over the plateau.

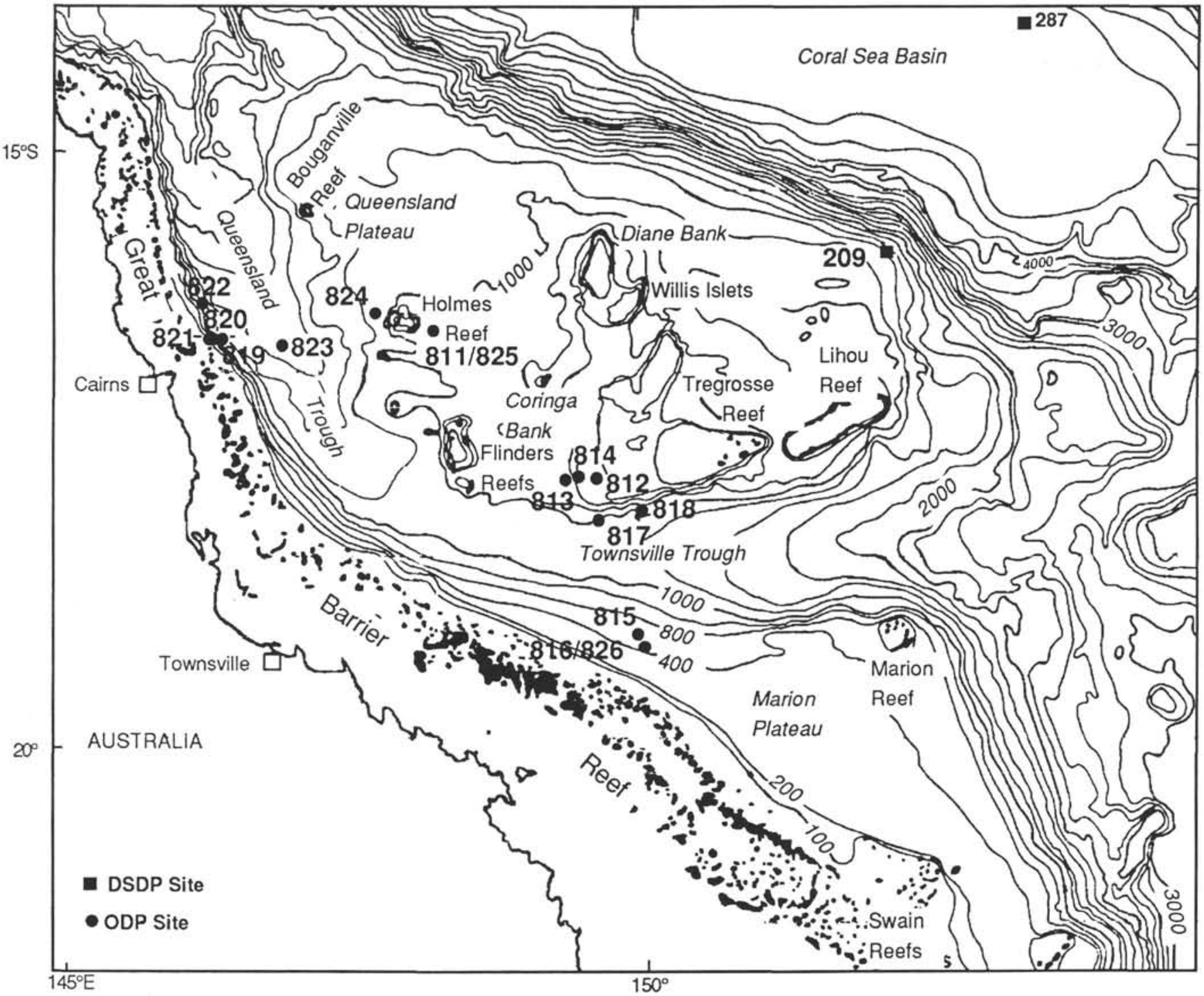

Figure 1. Position of Sites 811 and 825 and other Leg 133 sites in the western Coral Sea.

3. To understand sedimentation processes within a plateau carbonate system, specifically:

(1) the facies changes concomitant with plateau drowning,
(2) the timing and compositional differences between temperate and tropical sedimentation,
(3) the onset of reef sedimentation, and
(4) the attendant diagenetic signatures.

4. To determine the composition and age of basement.

Previously available data in the region include those collected by BMR since 1971, together with a few long regional Shell and GSI seismic lines. Better quality seismic data were collected in 1987 for the ODP site survey (BMR Lines 75/037); cores collected during that same cruise (75GC/22 and 75GC/23) define the surface sediments as foraminiferal oozes. We had no reason to expect hydrocarbon accumulations at the site. A shallow basement, the absence of structural closure, and a thin, thermally immature section precluded any possibility of hydrocarbon occurrence. Therefore, no major risks were anticipated, although a slight chance existed for encountering some minor biogenic gas.

SITE 811 OPERATIONS

Guam Port Call

Leg 133 officially began when the *JOIDES Resolution* put the first line ashore at Berth Victor 6 in Port Apra, Guam, at 1900L (all times in this section are local time, or L) 4 August 1990. Customs and immigration formalities were not concluded until 2400L. A change of crew, offloading the diamond coring system (DCS), loading and offloading ocean and air freight, and normal port call activities proceeded slowly during frequent rain. Rigging down the DCS system required longer than expected, and an attempt by Vetco/Baker/Hughes to inspect the 5-1/2-in. drill pipe ended after six stands because of delays. The American Bureau of Shipping completed an inspection of the explosives and radioactive material lockers and renewed our certificate for safe storage and handling. Divers welded straps over four notches in the

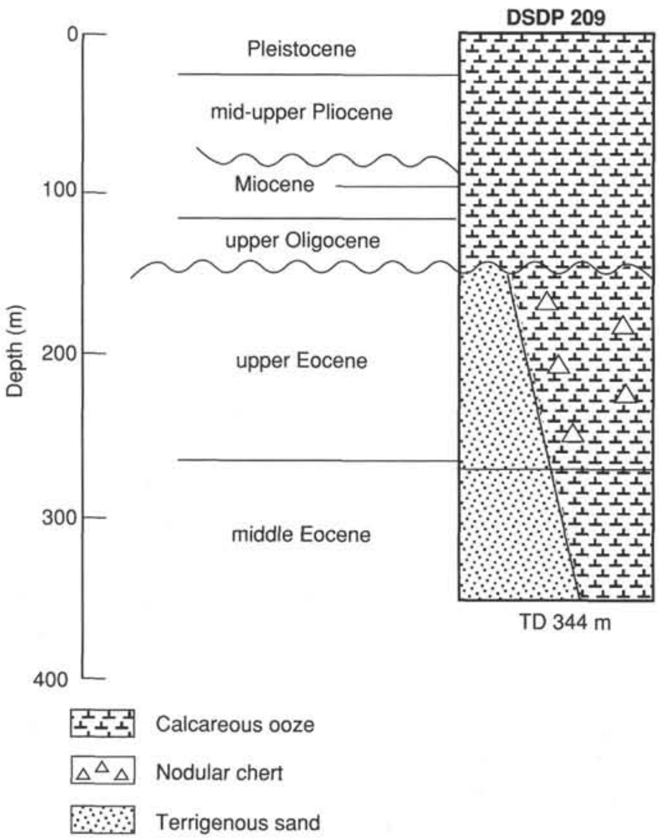

Figure 2. Stratigraphy and facies at Site 209 (Burns, Andrews, et al., 1973).

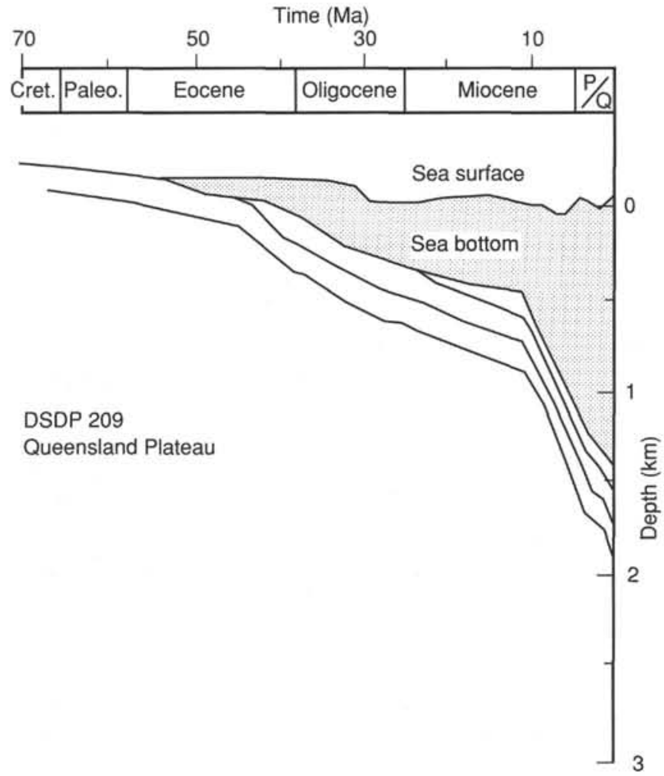

Figure 3. Subsidence history of the Queensland Plateau (Burns, Andrews, et al., 1973).

moonpool wear ring that was caused by wireline wear. The ship moved to the fueling pier at 1515L 8 August. Fueling was completed, and the final line was cast off at 1355L 9 August. The harbor pilot was away at 1423L, and the sea voyage to the northeastern Australian margin began.

Guam to Site 811

Site 811 (proposed Site NEA-8) is located off the northeastern coast of Australia, 2017 nmi southwest of Guam. A magnetometer was streamed at 1800L, shortly after leaving Guam. The new conical side-entry submersible (CSES) was geared up to a 28,000 ft-lb torque, and the releasing wireline packoff was tested. The new vibrapercussive corer (VPC) was assembled, and two drill collars were placed in the RCB for a test; however, the 60-ft length of VPC required that the drill collars be lowered below the ship; thus, we could not conduct the test while the ship was under way.

The entire sea voyage to our first site covered 2017 nmi in 174 hr at an average speed of 11.6 kt. Seas and wind were calm for the first half of the voyage (12.3 kt average), but winds of 35 kt, 8-ft seas, and the loss of two propulsion motors slowed our progress thereafter to an average of 10.9 kt.

Site NEA-8

An 18-nmi pre-site seismic survey was run over Site 811 using optimal GPS positioning. The first beacon (a commandable recall model) was dropped at 0021L 17 August. The beacon drop initiated Hole 811A.

Hole 811A

Our precision depth recorder (PDR) indicated that water depth was 937.5 m from sea level. The ship moved 15 m west of the beacon, and a used 11-7/16-in. Security four-cone tungsten carbide insert bit was run to a water depth of 933.1 m for the first core. Hole 811A was spudded at 0751 hr, 17 August, at 16°30.977′S and 148°9.436′E. From Core 133-811A-1H we recovered 5.55 m of sediment; thus, it was accepted as a mud-line core. The mud-line was estimated by drill-pipe measurement (DPM) at 937.1 m from sea level. Continuous APC cores (Cores 133-811A-1H through -23H) were taken from 0.0 to 214.5 mbsf, with 213.51 m recovered (91.9% recovery). Orientation surveys were taken from Cores 133-811A-4H through -23H.

The pump pressure bled from 2600 to 2000 psi after shooting Core 133-811A-23H. The core barrel stuck and could not be freed even with a core-line pull of as much as 12,500 lb. We discovered that the drill pipe was plugged, which made circulation impossible. The overshot would not release, so we used the Kinley cutter to sever the core line at the core barrel. The drill string stuck again when the bit was at 187.4 mbsf while starting the trip out of the hole. The drill string came free after we worked it for 45 min, using an overpull of as much as 260,000 lb. The bit cleared the seafloor at 2204L 17 August, which ended Hole 811A (NEA-8). The drill collars were broken down and the core barrel removed, but the APC upper section remained stuck in the barrel despite an overpull of up to 150,000 lb. The bottom drill collars were full of nannofossil ooze and reef debris; we think that the back flow through the lockable flapper valve (LFV) filled the drill collar with sufficient material to hinder APC operation and to interfere with the overshot release. The stuck APC upper section indicated that metal debris (possibly a shear pin or mechanical failure) jammed the tool and prevented its removal.

Hole 811B

The ship was moved 30 m east to 16°30.948′S, 148°9.454′E (15 m east of the beacon), and the same six drill-collar

A

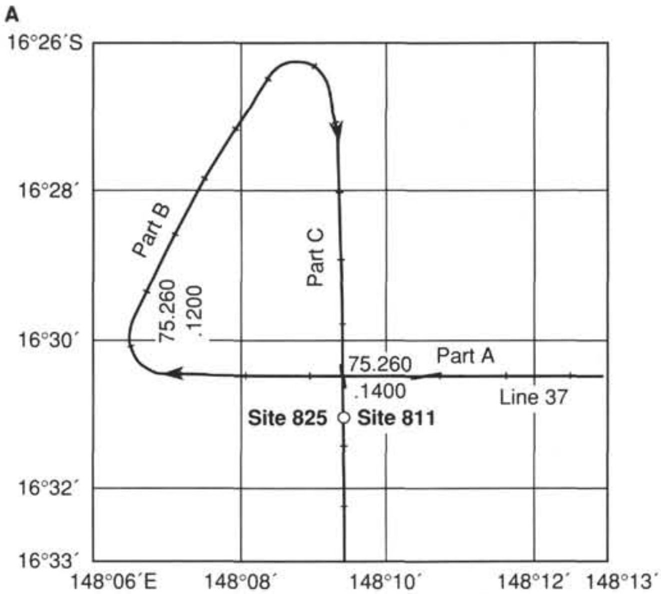

B

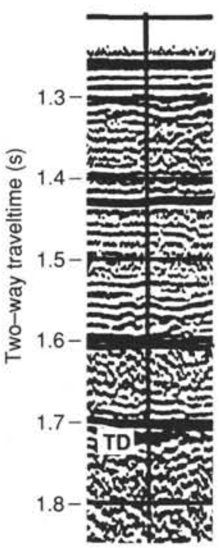

Depth (mbsf)	Age	Velocity (km/s)	Lithology	Paleoenvironment	Sedimentation rate (m/m.y.)	Comments
0	Pliocene to Holocene	1.55	Sand and mud	Pelagic plateau outer margin	21	Periplatform sediments
(62)	latest Miocene to Pliocene	1.6	Sand and mud	As above	8	Periplatform sediments
H4 (138)	late Miocene	1.7	Sand and mud		20	Periplatform sediments
(240)	middle Miocene	1.8	Sand and mud with gravel beds and possible hardgrounds		7	
H6 (292)	latest Oligocene to early Miocene	2.0	Gravel, sand, and mud		5	
H7 / TD (400)	(?) Paleozoic		Low grade metasediment			Basement
500						

Figure 4. Multichannel seismic Line 75/037 (C), showing: A. Site position; B. Pre-drilling interpreted stratigraphy.

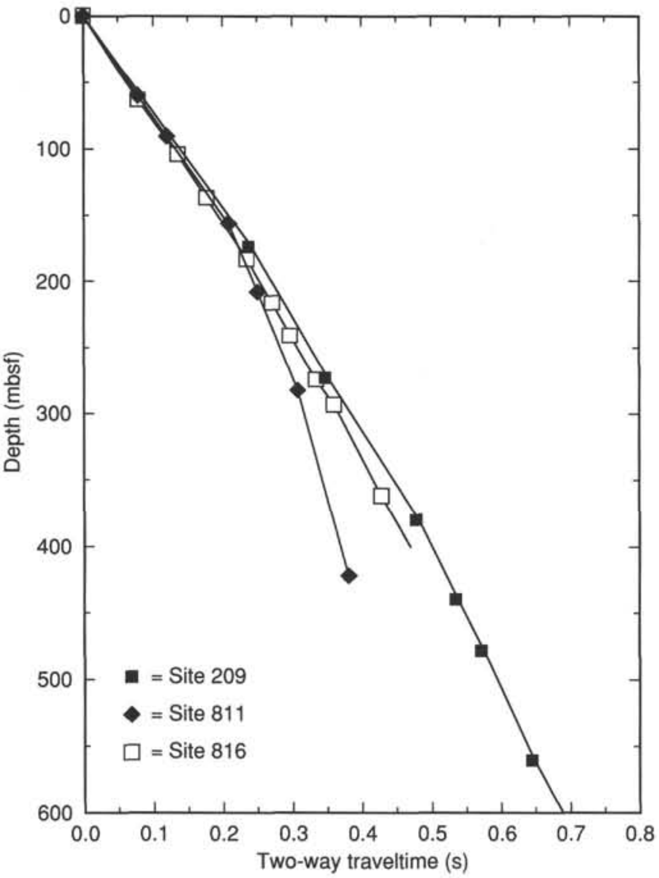

Figure 5. Comparison of reflection time (TWT) vs. depth curves estimated for Site 811 and DSDP Site 209 on the Queensland Plateau.

APC/XCB BHA was run with Hydrolex jars, with three drill collars added as a precaution. The PDR indicated a water depth of 938.4 m from sea level; the hole was spudded and washed to 194.0 m. Continuous XCB cores (Cores 133-811B-1X through -6X) were taken from 193.2 to 250.3 mbsf, with 57.1 m of sediment cored and 0.28 m recovered (0.5% recovery). Recovery was poor to none in soft nannofossil ooze and coarse calcareous sand sequences; therefore, we decided to try the new VPC.

Continuous VPC cores (Cores 133-811B-7V through -10V) were taken from 250.3 to 264.6 mbsf, with 14.3 m cored and 5.89 m recovered. This was the first operational test of the new VPC design. Bit advancement was by recovery on Cores 133-811B-8V through -10V in an effort to get a complete section. Core 133-811B-7V was wireline-deployed, but two shear pins sheared on release. Cores 133-811B-8V through -10V were dropped without shear pins. The heave compensator closed when a pump pressure of 1200 psi was used to lift the BHA hydraulically. Tool vibration was evident in a fluctuation of pressure gauges of ±30 psi. The VPC produced good undisturbed cores with horizontal banding still evident and only minor external fluidization. The VPC test was stopped because of vibration times (±20 min) that yielded slow penetration in coarse calcareous sands.

Continuous XCB cores (Cores 133-811B-11X through -24X) were taken from 264.6 to 392.5 mbsf, with 127.9 m of sediment cored and 7.37 m recovered (5.76% recovery). Verbal approval from ODP/TAMU was obtained to core the hole down to a seismic reflector estimated as between 400 and 430 mbsf (450 mbsf maximum). However, before we reached this objective, the drill string became stuck after coring 7.6 m of Core 133-811B-24X. The pipe was worked up with an overpull of 250,000 lb (280,000-lb string weight), but would not come free. However, the string did come free after two 100,000-lb blows with the Hydrolex jars. These jars were clearly responsible for freeing the string. After regaining circulation and rotation, a 30-bbl-gel hole-cleaning sweep was pumped. The string then was pulled up slightly, and the core barrel was retrieved; however, the XCB shoe, core catchers, and sub had unscrewed and were lost in the hole along with the core. This junk in the hole terminated coring at Hole 811B.

A 30-bbl-gel sweep was circulated to clean the hole at 372 mbsf, and the drill string was run in the hole to condition it for logging. A 30-bbl-gel sweep was circulated on bottom at 388.5 mbsf, and the bit was pulled up to 103.2 mbsf for logging. A go-devil was dropped to open the LFV for logging. This short trip encountered no drag while pulling out of the hole. Thus, indications were that pipe was stuck at the bit by a coarse calcareous sand cave-in and/or by accumulation of cuttings. The coarse sand was unconsolidated, contained little fine-grained material, and washed easily with water; thus, we conducted operations so as to minimize any hydraulic effects.

The DITE/HLDT/sonic/caliper/NGTC/TCC tool string was run in at 1425L 19 August, but tagged a bridge in the BHA at 53 mbsf. The tool string could not be worked or circulated past the obstruction; therefore, we pulled it out at 1500 hr. The less-rigid TCC tool was removed to shorten the tool string, which then was run with the same negative results. We thought it possible that the core catcher from Core 133-811B-24H had fallen off in the BHA and lodged in the BHA upset. When the go-devil was retrieved from above the obstruction, scars on its nose confirmed that it had landed on additional junk in the BHA; therefore, the logging program was terminated.

The APC/XCB BHA was pulled and cleared the seafloor at 0750L 19 August. The liner support ring from Core 133-811B-24H was found wedged in the head sub windows. Twelve hours remained before the departure for Site 812, which had been timed so as to meet a GPS window. We thus decided to reenter the hole to attempt to obtain a less-disturbed mud-line interval. We checked the bit, LFV, APC/XCB BHA, and jars and ran them in the hole.

Hole 811C

Hole 811C was spudded at 0128L 20 August, at 16°30.942′S and 148°9.451′E. Estimated water depth from the PDR was 938.4 m from sea level. The first core (133-811C-1H) was shot while the bit was positioned at 934.9 m below sea level, with 7.73 m of sediment recovered. We accepted this core as a mud-line core and determined that the mud line was at 936.8 mbsf. Continuous APC cores (Cores 133-811C-1H through -6H) were taken from 0.0 to 55.2 mbsf, with 55.2 m of sediment cored and 55.28 m recovered (100.0% recovery). Orientation surveys were taken from Cores 133-811C-3H through -6H. Coring ended when our allotted time ran out, and the BHA then was pulled. The bit cleared the seafloor at 0440L 20 August, the bit cleared the rotary table at 0625L 20 August, and Hole 811C terminated. The coring summary for Site 811 is presented in Table 1.

SITE 825 OPERATIONS

Transit to Site 825

We decided to return to the Site 811 proposed site (NEA-8) to re-attempt penetration of basement rock and the overlying

Table 1. Coring summary, Site 811.

Core no.	Date (Aug. 1990)	Time (UTC)	Depth (mbsf)	Length cored (m)	Length recovered (m)	Recovery (%)
Hole 811A						
1H	16	2155	0–5.6	5.6	5.55	100.0
2H	16	2220	5.5–15.0	9.5	8.93	94.0
3H	16	2240	15.0–24.5	9.5	9.62	101.0
4H	16	2300	24.5–34.0	9.5	9.88	104.0
5H	16	2320	34.0–43.5	9.5	10.19	107.2
6H	16	2350	43.5–53.0	9.5	9.86	104.0
7H	17	0015	53.0–62.5	9.5	9.97	105.0
8H	17	0040	62.5–72.0	9.5	9.81	103.0
9H	17	0105	72.0–81.5	9.5	9.67	102.0
10H	17	0135	81.5–91.0	9.5	7.30	76.8
11H	17	0200	91.0–100.5	9.5	9.62	101.0
12H	17	0225	100.5–110.0	9.5	9.89	104.0
13H	17	0255	110.0–119.5	9.5	9.87	104.0
14H	17	0325	119.5–129.0	9.5	9.58	101.0
15H	17	0355	129.0–138.5	9.5	9.88	104.0
16H	17	0415	138.5–148.0	9.5	10.06	105.9
17H	17	0440	148.0–157.5	9.5	8.77	92.3
18H	17	0505	157.5–167.0	9.5	9.85	103.0
19H	17	0535	167.0–176.5	9.5	9.97	105.0
20H	17	0600	176.5–186.0	9.5	9.59	101.0
21H	17	0630	186.0–195.5	9.5	9.12	96.0
22H	17	0655	195.5–205.0	9.5	9.56	100.0
23H	18	1610	205.0–214.5	9.5	6.86	72.2
Coring totals				214.6	213.40	99.5
Hole 811B						
1X	18	0250	193.2–202.7	9.5	0.00	0.0
2X	18	0320	202.7–212.0	9.3	0.01	0.1
3X	18	0410	212.0–221.7	9.7	0.94	9.7
4X	18	0500	221.7–231.0	9.3	0.01	0.1
5X	18	0530	231.0–240.7	9.7	0.00	0.0
6X	18	0600	240.7–250.3	9.6	0.00	0.0
7V	18	0755	250.3–258.8	8.5	0.26	3.1
8V	18	0915	258.8–263.7	4.9	4.85	99.0
9V	18	1120	263.7–264.1	0.4	0.33	82.0
10V	19	1250	264.1–264.6	0.5	0.50	100.0
11X	19	1400	264.6–269.5	4.9	0.00	0.0
12X	19	1435	269.5–279.1	9.6	0.27	2.8
13X	19	1500	279.1–288.7	9.6	0.00	0.0
14X	19	1535	288.7–298.4	9.7	0.00	0.0
15X	19	1600	298.4–308.0	9.6	0.17	1.8
16X	19	1645	308.0–317.7	9.7	2.76	28.4
17X	19	1725	317.7–327.3	9.6	0.82	8.5
18X	19	1750	327.3–337.0	9.7	2.15	22.1
19X	19	1815	337.0–346.6	9.6	0.45	4.7
20X	19	1845	346.6–356.3	9.7	0.75	7.7
21X	19	1930	356.3–365.9	9.6	1.28	13.3
22X	19	2005	365.9–375.6	9.7	0.00	0.0
23X	19	2040	375.6–384.9	9.3	0.00	0.0
24X	18	2240	384.9–392.5	7.6	0.00	0.0
Coring totals				199.3	15.55	7.8
Hole 811C						
1H	19	1530	0.0–7.7	7.7	7.73	100.0
2H	19	1550	7.7–17.2	9.5	9.42	99.1
3H	19	1625	17.2–26.7	9.5	8.29	87.2
4H	19	1650	26.7–36.2	9.5	9.90	104.0
5H	19	1715	36.2–45.7	9.5	10.01	105.3
6H	19	1745	45.7–55.2	9.5	9.93	104.0
Coring totals				55.2	55.28	100.1

Note: Times are given in Universal Time Coordinated (UTC), which is 10 hr later than local time (L).

sediments. As the time expired since our previous operations at that site was more than a few weeks, a new beacon was required and the site was given a new number: Site 825.

Transit to Site 825 (NEA-8) began at 0430L 6 October and covered 33 nmi in 3.0 hr at an average speed of 11.0 kt. We did not run a seismic survey. A Datasonics beacon was dropped at 0808L 6 October 1990.

Hole 825A

Hole 825A was located at 16°30.961'S, 148°9.457'E; the PDR predicted water depth as 939.8 m from sea level. We lowered the bit to a water depth of 934.4 m from sea level for the first shot. Hole 825A was spudded at 1050L 6 October. The mud line was placed at a water depth of 939.4 m from sea level. A 9-7/8-in. hole was washed from 4.5 to 200.0 mbsf, and WSTP samples were taken at 50.0, 100.0, and 150.0 mbsf. APC coring continued, while Cores 133-825A-5H through -8H were taken from 200.5 to 238.0 mbsf; 38.0 m was cored and 38.3 m was recovered.

Cores 133-825A-9X through 14X were taken from 238.0 to 295.7 mbsf, with 57.7 m cored and 10.87 m recovered (18.8% recovery). Overpull was 20,000 to 40,000 lb on the connections, while 20-bbl-mud sweeps were necessary for each core because of sloughing sediment. After we landed Core 133-825A-15X, the pipe became stuck at 295.7 mbsf. It was pulled up to an overpull of 190,000 lb, the Hydrolex jars hit one blow, and the pipe came free. A 40-bbl-mud sweep was circulated before and after reaming to the bottom.

Despite the bad hole conditions, we decided to continue operations. Cores 133-825A-15X through -23X were taken from 295.7 to 381.5 mbsf, with 85.8 m cored and 0.26 m recovered (0.3% recovery). Poor recovery in the flowing silt made continued coring inadvisable. The bit cleared the rotary table at 1115L October 7.

Hole 825B

The ship moved 25 m west, and an RCB BHA with an MBR was run to a water depth of 933.5 m. Hole 825B was located at 16°30.961'S, 148°9.457'E. The mud line was estimated at a water depth of 939.3 m from sea level. A 9-7/8-in. hole was washed from 0 to 379.5 mbsf, with 0.31 m recovery.

Cores 133-825B-2R through -10R were taken from 379.5 to 466.3 mbsf, with 86.8 m cored and 3.0 m recovered (3.46% recovery). The hole was sloughing in, which caused a drag of 20,000 to 40,000 lb with 3 to 6 m of fill on connections. A 20-bbl-mud sweep was required for each core to avoid stuck pipe. We penetrated hard basement at approximately 453.0 mbsf. The bit was released with the MBR at 465 mbsf. The hole was not conditioned with a short trip to save time, nor was the MBR sleeve shifted. The pipe was pulled to 96.3 mbsf for logging. Logs were run as follows: the induction/sonic/gamma-ray/caliper (DITE/SDT/NGT/MCDG) logging tool was placed in the hole at 1207L 8 October, when we found 18.2 m of fill above total depth. This tool string was out of the hole at 0355L.

The MBR cleared the seafloor at 1450L 8 October and the rotary table at 1857L. A beacon was recalled and recovered at 1880L.

The original port call plans for Leg 133 called for the cruise to end in Townsville. We learned that fuel was unavailable in Townsville, so we developed an alternative plan for departing Hole 825B by 2300L 8 October so that the ship could be fueled in Cairns before finishing the transit to Townsville. However, fuel also was unavailable in Cairns; thus, it was decided to fuel the ship in Gladstone at the beginning of the Leg 134 cruise. A coring summary for Site 825 is presented in Table 2.

SITE GEOPHYSICS

The *JOIDES Resolution* departed Guam about 1400 (JD 221/0400UTC) on 9 August 1990, and after a 7-day transit, arrived at a position of 16°18.8'S and 148°09.96'E, about 12 nmi north of Site 811 (proposed site NEA-8), at 2018L on 16 August 1990 (JD 228/1018UTC). This site (the first drilled during Leg 133) lies on the western margin of the Queensland

Table 2. Coring summary, Site 825.

Core no.	Date (Oct. 1990)	Time (UTC)	Depth (mbsf)	Length cored (m)	Length recovered (m)	Recovery (%)
Hole 825A						
1H	5	0055	0–4.5	4.5	4.50	100.0
2W	6	0100	50.0–100.0	50.0	0.01	(wash core)
3W	6	0306	100.0–150.0	50.0	0.01	(wash core)
4W	6	0456	150.0–200.0	50.0	0.01	(wash core)
5H	6	0700	200.0–209.5	9.5	9.83	103.0
6H	6	0725	209.5–219.0	9.5	9.72	102.0
7H	6	0820	219.0–228.5	9.5	9.69	102.0
8H	6	0925	228.5–238.0	9.5	9.53	100.0
9X	6	1030	238.0–247.5	9.5	0.00	0.0
10X	6	1050	247.5–257.1	9.6	5.81	60.5
11X	6	1115	257.1–266.8	9.7	3.59	37.0
12X	6	1150	266.8–276.4	9.6	1.47	15.3
13X	6	1215	276.4–286.1	9.7	0.00	0.0
14X	6	1240	286.1–295.7	9.6	0.00	0.0
15X	6	1500	295.7–305.4	9.7	0.00	0.0
16X	6	1600	305.4–315.0	9.6	0.26	2.7
17X	6	1650	315.0–324.7	9.7	0.00	0.0
18X	6	1740	324.7–334.3	9.6	0.00	0.0
19X	6	1830	334.3–343.9	9.6	0.00	0.0
20X	6	1925	343.9–353.5	9.6	0.00	0.0
21X	6	2020	353.5–362.9	9.4	0.00	0.0
22X	6	2110	362.9–372.2	9.3	0.00	0.0
23X	6	2210	372.2–381.5	9.3	0.00	0.0
Coring totals				186.0	54.40	29.2
Washing totals				150.0	0.03	
Combined totals				336.0	54.43	
Hole 825B						
1W	7	1215	0–379.5	379.5	0.31	(wash core)
2R	7	1310	379.5–389.1	9.6	0.00	0.0
3R	7	1405	389.1–398.7	9.6	0.00	0.0
4R	7	1500	398.7–408.4	9.7	0.00	0.0
5R	7	1555	408.4–418.0	9.6	0.07	0.7
6R	7	1650	418.0–427.7	9.7	0.54	5.6
7R	7	1745	427.7–437.4	9.7	0.44	4.5
8R	7	1840	437.4–447.0	9.6	0.34	3.5
9R	7	2015	447.0–456.7	9.7	0.48	5.0
10R	7	2325	456.7–466.3	9.6	0.82	8.5
Coring totals				86.8	2.69	3.1
Washing totals				379.5	0.31	
Combined totals				466.3	3.00	

Note that times are given in Universal Time Coordinated or UTC, which is 10 hr later than local time or L.

Plateau, immediately east of Holmes Reef (Fig. 6) and about 250 km east of Cairns.

After changing our course to about 180° and reducing the ship's speed to 5 kt, we deployed single-channel seismic profiling gear at JD 228/1023UTC on 16 August 1990. Seismic recording began at JD 228/2040UTC; during the survey, we collected about 35 km of data. An important requirement of the site location survey was that the seismic records obtained on the *JOIDES Resolution* should be as close as possible in appearance to those collected by the BMR during the 1987 site survey when the vessel *Rig Seismic* was used (Symonds and Davies, 1988; Feary et al., 1990). Our aim was to reduce ambiguity during site definition and when comparing seismic stratigraphy of the two data sets. This necessitated some changes to the *JOIDES Resolution* streamer and 80-in.^{3} water-gun deployment systems to ensure that the frequency content and display parameters of the two data sets were similar.

The site-location survey was designed (1) to give the seismic technicians enough time for testing the seismic system before crossing the drilling site, (2) to develop procedures for locating the Leg 133 sites as efficiently as possible, and (3) to compare the site location determined from the *Rig Seismic* navigation system with the *JOIDES Resolution* global positioning system (GPS). Distribution of regional seismic data in the area around the site is shown in Figure 6, while the tracks of the original *Rig Seismic* site survey and the *JOIDES Resolution* site location survey are shown in Figure 7.The *JOIDES Resolution* initially sailed south across Site 811; after proceeding for another 2 nmi to the south, she headed back across the site on a reciprocal course; finally, she turned about 1 nmi north of the site and headed south on a reciprocal course for the last pass. Signals from four GPS satellites were received during the entire site location survey, and we consider that the ship's track was accurately positioned. On the basis of both the seismic record and the ship's location, a beacon was dropped at 0021L 17 August (JD 228/1421UTC 16 August 1990) at 16°31.0715′S and 148°09.429′E. Excellent correlation was obtained for the site between the *JOIDES Resolution* single-channel seismic data and the *Rig Seismic* multichannel seismic profile (Fig. 8),as well as the vessels' respective GPS positions. Seismic data also were recorded over the site on the final pass after dropping the beacon, after which data acquisition stopped, and seismic equipment was retrieved at JD 228/1430.

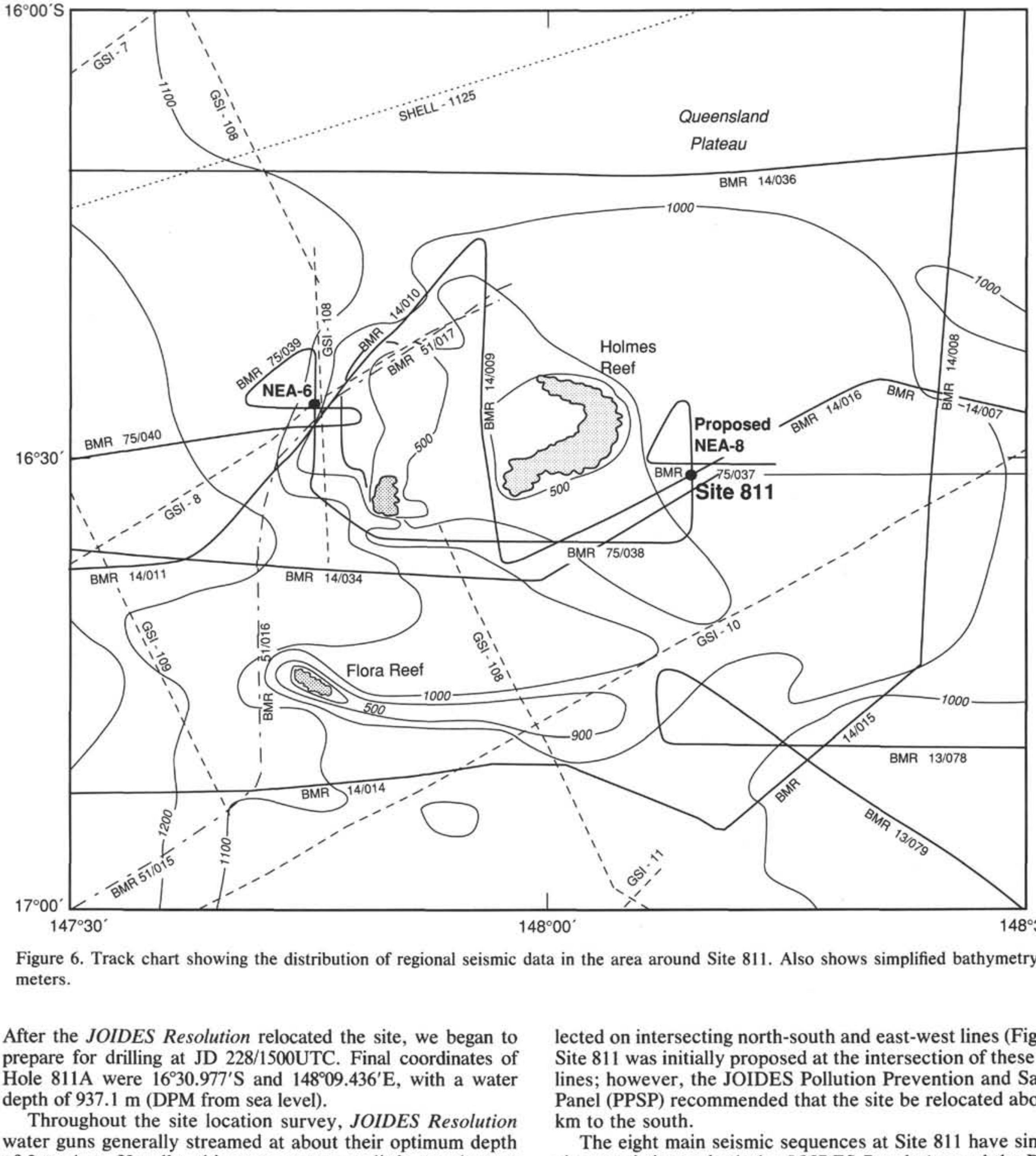

Figure 6. Track chart showing the distribution of regional seismic data in the area around Site 811. Also shows simplified bathymetry in meters.

After the *JOIDES Resolution* relocated the site, we began to prepare for drilling at JD 228/1500UTC. Final coordinates of Hole 811A were 16°30.977′S and 148°09.436′E, with a water depth of 937.1 m (DPM from sea level).

Throughout the site location survey, *JOIDES Resolution* water guns generally streamed at about their optimum depth of 3 to 4 m. Usually, this streamer was a little too deep at about 8 to 9 m, and it went even deeper during the northward leg with a following sea. The affects of this can be seen on the seismic record by a reduction in the high-frequency component of the signal (Figs. 8 and 9). In general, the quality of single-channel data was good, although some noise was introduced by the 25- to 30-kt southeasterly winds and related force 6 (Beaufort Scale) sea, and the 3- to 4-m swells that occurred throughout the survey period.

The original position of Site 811 (proposed site NEA-8) was based on the 1987 *Rig Seismic* site survey, during which about 40 km of 24-channel, 80-in^3 water-gun data were collected on intersecting north-south and east-west lines (Fig. 7). Site 811 was initially proposed at the intersection of these two lines; however, the JOIDES Pollution Prevention and Safety Panel (PPSP) recommended that the site be relocated about 1 km to the south.

The eight main seismic sequences at Site 811 have similar characteristics on both the *JOIDES Resolution* and the BMR *Rig Seismic* seismic profiles (Fig. 10). Figure 10 also shows the pre-drilling prognosis of the age, lithology, and depositional environment of these sequences, as modified from Feary et al. (1990). In the *Resolution* data, basement at the site is about 0.45 s two-way traveltime (TWT) below seafloor. This basement is overlain by a thin sequence (S7, 0.03 s TWT thick) and then by a nonreflecting zone (S6) about 0.07 s TWT thick. The next sequence (S5), which is about 0.06 s TWT thick, is a strongly reflecting unit having a flat base and an irregular upper surface: it is the most prominent sequence in the vicinity of the site. This sequence is onlapped by a

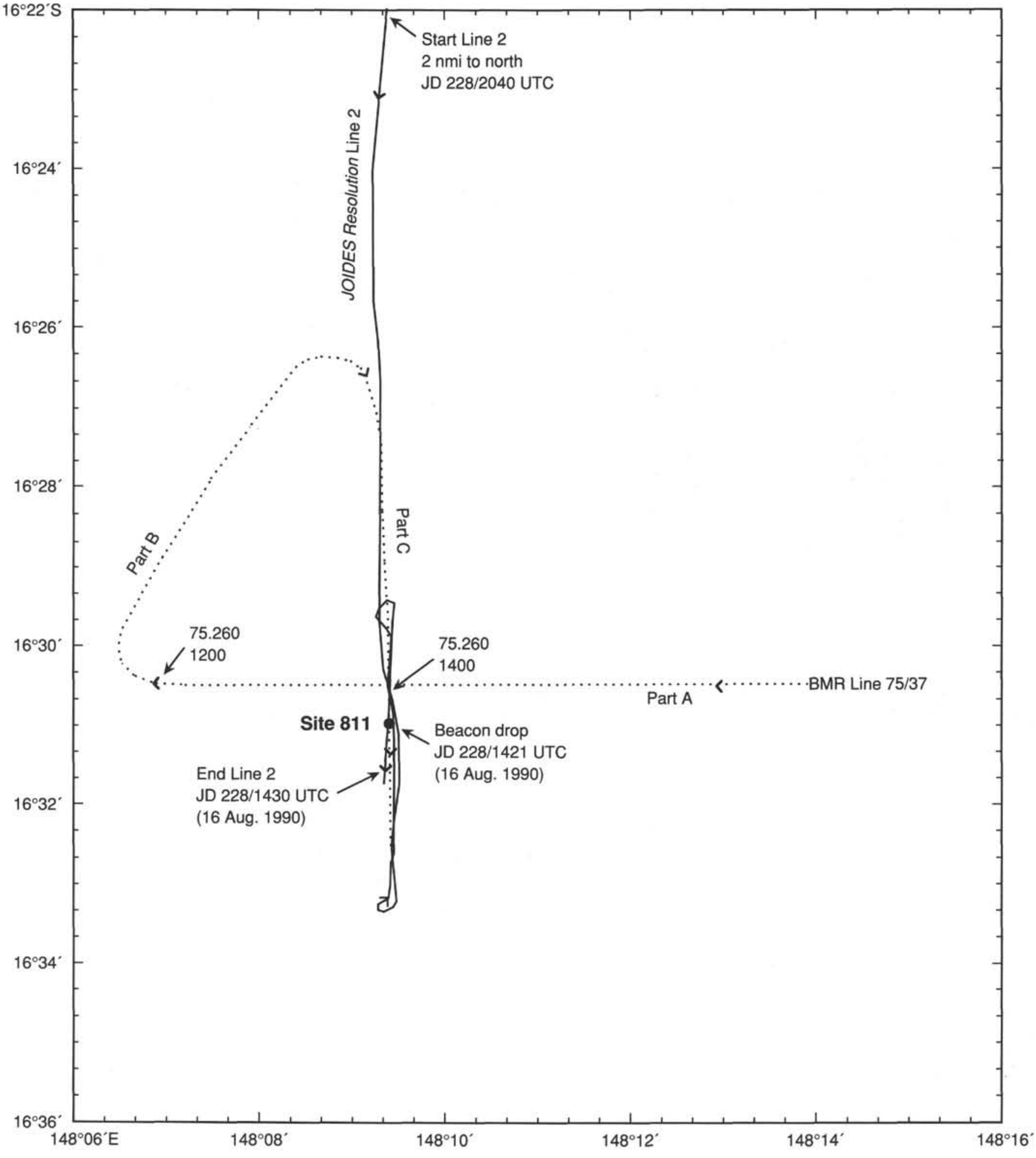

Figure 7. *JOIDES Resolution* Leg 133 site-location tracks (solid line) and *Rig Seismic* 1987 site-survey tracks (dotted line) around Site 811.

0.12-s-TWT-thick sequence (S4) that contains subparallel, low-amplitude reflectors, which in turn appear to be truncated at the base of the overlying 0.03-s-TWT-thick zone of strong parallel reflectors (S3). Sequence S2 consists of about 0.08 s TWT of low-amplitude, parallel reflectors and is overlain by the uppermost sequence (S1; 0.06 s TWT thick), which is hummocky and appears to have an irregular base. The pre-drilling interpretation (Fig. 10), which was based on regional considerations, including results from DSDP Site 209, suggested that sequences S1 through are Holocene to upper Miocene carbonate sand and mud of periplatform origin; S5 is middle Miocene carbonate sand and mud with gravel beds and possible hardgrounds; S6 is upper Oligocene to lower Miocene gravel, sand, and mud with an increasing terrigenous compo-

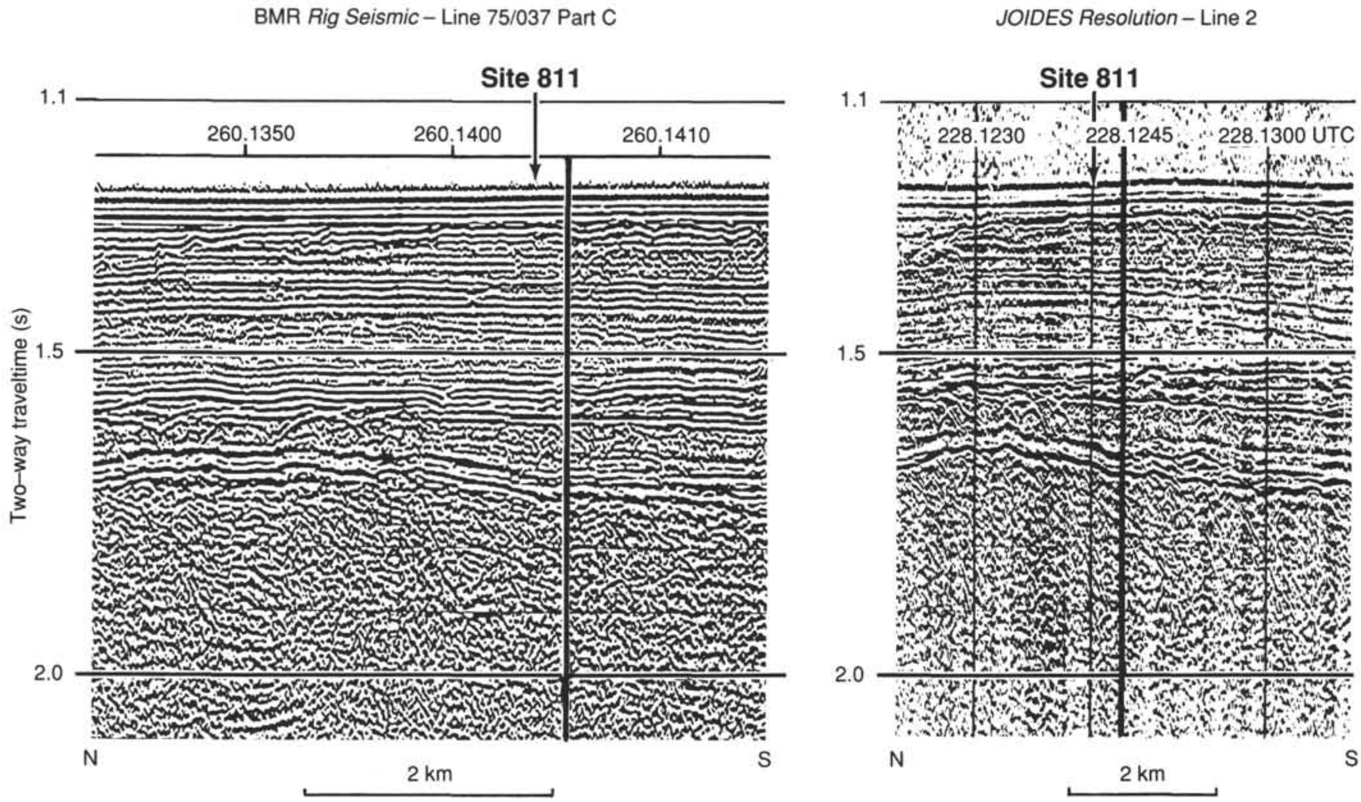

Figure 8. Comparison of *JOIDES Resolution* with *Rig Seismic* 80-in.^{3} water-gun seismic profiles across Site 811.

nent toward its base; S7 is a sand and gravel unit that contains a large amount of terrigenous material derived locally from the underlying basement; and basement is composed of low-grade (?)Paleozoic metasediments.

To provide some predictive capability during the drilling at Site 811, we estimated the reflection time (TWT)/depth relationship below the seafloor and thus the depth of the various sequence boundaries, using stacking-derived interval velocities from the BMR site survey. This estimate showed reasonable agreement, at least to 200 mbsf (Fig. 5), with estimates based on sonobuoy and physical property results from DSDP Site 209 (Burns, Andrews, et al., 1973; Andrews, 1973).

SITE 811 LITHOSTRATIGRAPHY

Lithologic Units

Site 811 is located 9 km southeast of Holmes Reef at a water depth of 937 m. A 385-m-thick sedimentary carbonate-rich sequence, extending from Quaternary to lower Oligocene (possibly Eocene), was cored with APC, XCB, and VPC in combined Holes 811A, 811B, and 811C (Fig. 11). Because Site 811 was drilled in close proximity to the shallow carbonate platform of Holmes Reef, its calcareous sedimentary record consists of a series of mixed pelagic and bank-derived carbonate intervals separated by a pure pelagic carbonate unit. The latter has been interpreted to represent time intervals during which productivity on Holmes Reef was "turned off."

The top two-thirds of the sedimentary sequence at Site 811 are dominated by a series of periplatform and pelagic oozes and chalks that were deposited in water depths ranging from 600 to 1000 m (middle bathyal environment) and can be differentiated on the basis of their variable content of bank-derived carbonate sediments. These intercalated shallow-water carbonate sediments were exported into the basin either (1) during distinct gravity-flow events recorded as calciturbidite layers and debris-flow deposits, or (2) as fine-grained, bank-derived carbonate particles, admixed into the pelagic sediments (mostly foraminifers and coccoliths) by direct settling from the water column and/or by low-density flows. The bottom one-third of the Site 811 sedimentary sequence consists mostly of neritic calcareous sand-rich sediments deposited in the vicinity of a shallow-water carbonate platform. This platform might well be the ancestor of the modern and smaller Holmes Reef carbonate bank. The lowermost part of the section at Site 811 consists of a more open-marine pelagic sedimentary package directly overlying a hard horizon having poor recovery, except for a small pebble of Eocene pelagic limestone.

The variable proportion of bank-derived carbonate material added to the pelagic components and the water depth variations from middle bathyal-to-neritic depositional environments form the basis for dividing Site 811 into five (possibly six) lithologic units: Units I, II, III, IV, V, and VI (Figs. 11 and 12). The two uppermost units, Units I and II, are further subdivided into three (Subunits IA, IB, and IC) and two subunits (Subunits IIA and IIB), respectively. The stratigraphic distribution of the units and subunits is summarized in Figure 11, while each is discussed in detail next.

Unit I (Core 133-811A-1H to Section 133-811A-4H-6, 115 cm; depth, 0–33.15 mbsf; and Core 133-811C-1H to Section 133-811C-4H-4, 117 cm; depth, 0–32.37 mbsf; age, late Pleistocene to late Pliocene)

The main lithologies of Unit I in Holes 811A and 811C range from foraminifer oozes with nannofossils to nannofossil oozes with foraminifers. Together, these oozes have been intercalated with redeposited shallow-water carbonate sediments that include lithologies ranging from unlithified bioclastic packstones with nannofossils to lithoclastic rudstones that

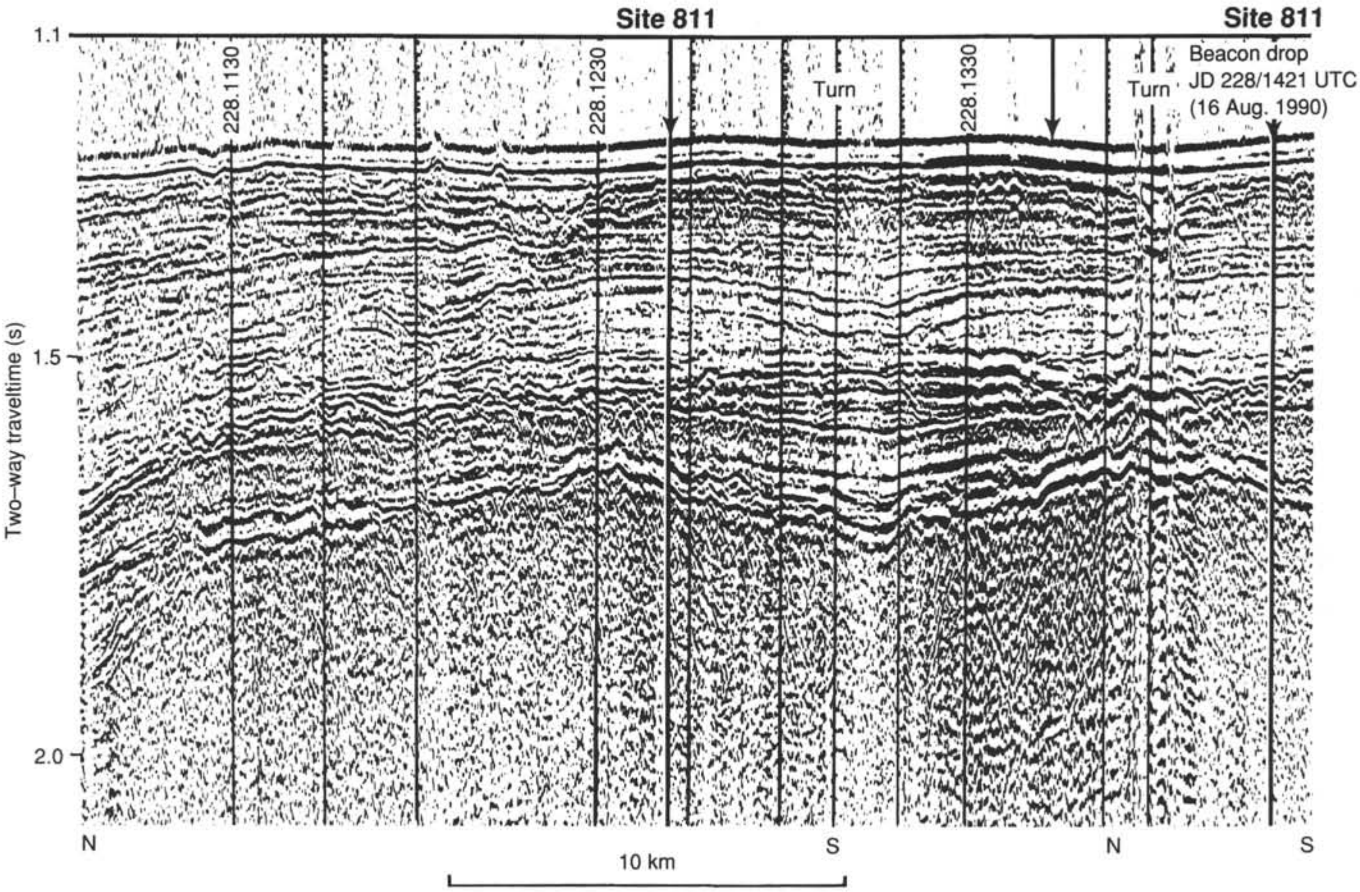

Figure 9. *JOIDES Resolution* shipboard analog single-channel seismic profile collected during Site 811 site-location survey using two 80-in.^{3} water guns.

have been interpreted as turbidite layers and debris-flow deposits. Most of the fine-grained carbonate fraction (70% to 80%) consists of nonidentifiable calcareous particles that have been interpreted as of shallow-water origin. The occurrence of metastable aragonite in Unit I, in addition to that accounted for by pteropod tests, also provides good evidence that the sediments of Unit I are a mixture of pelagic and bank-derived calcareous sediments called periplatform oozes (Schlager and James, 1978). Carbonate content values for bulk samples of this sediment range between 90% and 98%. The bundling of the turbidite layers within the top one-third of Unit I and the occurrence of two debris-flow deposits within its bottom one-third contrast with the absence of turbidite layers in the middle part of Unit I. We subdivided Unit I into three subunits on the basis of the uneven distribution of turbidite layers and debris-flow deposits. Because of the high degree of disturbance induced by coring and core-splitting in Holes 811A and 811C, the boundaries between Subunits IA, IB, and IC remain approximate. The lithologic characteristics of the subunits are described in detail below.

Subunit IA (Core 133-811A-1H to Section 133-811A-2H-2, 85 cm; depth, 0–7.85 mbsf; and Core 133-811C-1H-CC, 23 cm, depth, 0–7.7 mbsf; age, late Pleistocene)

Subunit IA consists of nannofossil foraminifer (and foraminifer nannofossil) oozes with pteropods that have been intercalated with a series of 10- to 15-cm-thick unlithified foraminifer bioclastic packstone layers that we interpreted as calciturbidite layers. The color of these oozes grades from light gray and very pale brown to white. Because of the high degree of core disturbance caused by drilling and core splitting (amplified in the top 10 mbsf of Holes 811A and 811C because of high water contents), the calciturbidite layers are not always obvious. We estimate that these constitute up to 20% of Subunit IA. Although values of bulk carbonate content range between 90% and 95% in Subunit IA, in Subunit IB, they are the lowest of the values measured in Holes 811A and 811B (see "Inorganic Geochemistry" section, this chapter) and correspond to the Quaternary. The carbonate phase consists of calcite and aragonite; magnesian calcite is absent. The aragonite values (as high as 38%) have been attributed to the presence of pteropod tests and fine-grained bank-derived particles in the sediments of Subunit IA. Magnesian calcite, the other metastable carbonate phase, usually occurs in association with aragonite in periplatform sediments of the Bahamas, the Nicaragua Rise, and the Maldives (Droxler et al., 1988: Droxler et al., 1990; Glaser and Droxler, 1991) in water depths similar to that of Site 811 (937 m). This absence of magnesian calcite at relatively shallow water depth is probably an indication of the high degree of corrosiveness of the waters over the Queensland Plateau with respect to metastable carbonate phases.

Subunit IB (Sections 133-811A-2H-2, 85 cm, to -3H-2, 150 cm; depth, 7.85–18.00 mbsf, and Sections 133-811C-1H-CC, 23 cm, to -2H-CC, 17 cm; depth, 7.7–17.2 mbsf; age, approximately middle Pleistocene)

The major lithologies of Subunit IB vary between white nannofossil foraminifer oozes and foraminifer oozes with nannofossils. The absence of turbidite layers, the absence of whole pteropods tests and fragments in the coarse fraction,

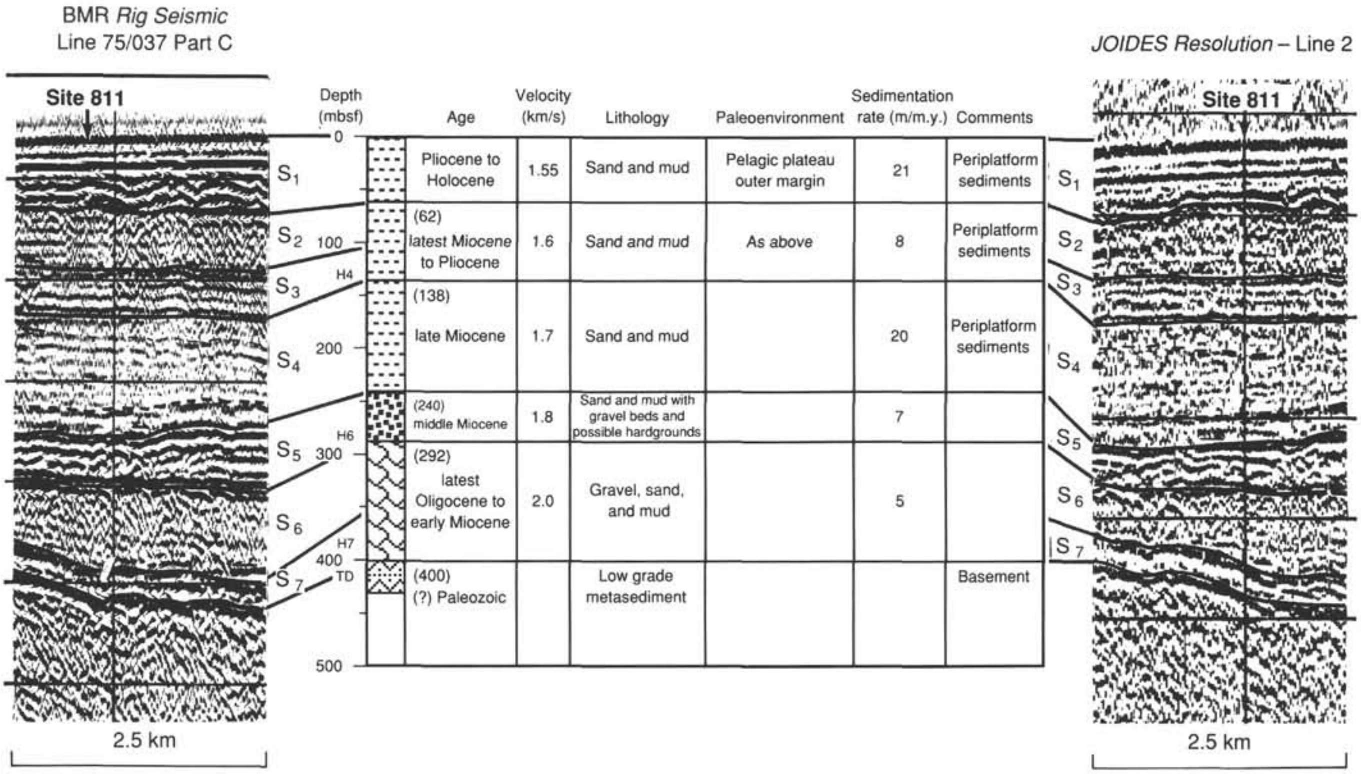

Figure 10. Seismic sequence characteristics for *JOIDES Resolution* and *Rig Seismic* water-gun seismic profiles across Site 811. Also shown is the pre-drilling prognosis.

and the nondetection of aragonite in the bulk carbonate sediments (see "Inorganic Geochemistry" section, this chapter) are the main characteristics of Subunit IB. In addition, nannofossils account for only 25% of the fine fraction. The other 75% consists of nonrecognizable carbonate (calcite) particles and has been interpreted as having been derived from carbonate platforms of Holmes Reefs. Because of the large proportion of fine bank-derived particles, these sediments are called periplatform oozes. The carbonate content ranges between 90% and 94%, similar to that in Subunit IA.

Subunit IC (Sections 133-811A-3H-2, 150 cm, to -4H-6, 133 cm, depth, 18.00–33.15 mbsf, and Sections 133-811C-2H-CC, 17 cm, to -4H-4, 117 cm, depth, 17.2–32.37 mbsf; age, late Pliocene, 1.8–2.5 Ma)

The occurrence of two distinct debris-flow deposits between 18 and 33 mbsf in both Holes 811A and 811C that consist of a mixture of unlithified bioclastic packstones with nannofossils and unlithified lithoclastic rudstones and floatstones distinguishes the lower part of Unit I as a distinct subunit. A 7-m-thick white to light gray nannofossil foraminifer ooze separates the upper from the lower debris-flow packages. Several shallow-water carbonate lithoclasts having well-developed moldic porosity are scattered in the upper debris-flow deposit package (Fig. 13). Part of the lower debris-flow package consists of thick layers of normally graded calcareous gravels and sands (Fig. 14). Values for bulk carbonate contents in Subunit IC, which range from 95% to 99%, are higher than those in the overlying sediments of Subunits IA and IB and are less than those in the underlying sediments of the upper part of Unit II. Aragonite, which is absent in Subunit IB, is preserved in small amounts within the debris-flow deposits (see "Inorganic Geochemistry" section, this chapter).

The two debris-flow deposit packages are well recorded in the GRAPE density data and are characterized by overall high-density values (1.8–2.0 g/cm^3) that exceed the average density values of underlying and overlying sediments by 0.2 to 0.3 g/cm^3 (see "Physical Properties" section, this chapter). Nannofossil dates from core-catcher samples above and below the debris-flow deposits suggest that these deposits are late Pliocene in age. The lower debris flow occurred between 1.8 and 2.4 Ma, and the upper one is younger than 1.8 Ma, possibly also Pliocene. The timing of their emplacement should then correspond to the initiation of global, late Pleistocene-type high-amplitude fluctuations in sea level caused by the initiation of Northern Hemisphere glaciations at 2.4 Ma (Shackleton and Hall, 1989). The moldic porosity in the shallow-water carbonate lithoclasts scattered within the floatstones signifies meteoric diagenesis, which probably occurred when the Holmes Reef carbonate bank was exposed during lowerings in sea level. The timing of meteoric diagenesis remains uncertain.

Unit II (Sections 133-811A-4H-6, 115 cm, to -16H-6, 150 cm, depth, 33.15–147.5 mbsf, and partially in Sections 133-811C-4H-4, 117 cm, to -6H-CC; age, late Pliocene to late Miocene, 2.5–8.75 Ma)

Unit II corresponds to a long interval (late Pliocene to late Miocene, or more than 6 m.y.) characterized by the absence of gravity-flow deposits in a homogeneous, 115-m-thick, mostly white ooze that ranges from nannofossil ooze with foraminifers to foraminifer ooze with nannofossils. The upper boundary of this zone is defined by the base of the lower debris-flow deposit of Subunit IC, and its lower boundary is marked by the reappearance of gravity-flow deposits in Core 133-811A-16H. Variations in the fine fraction of nannofossils and unidentifiable calcareous (bank-derived?) particles is the

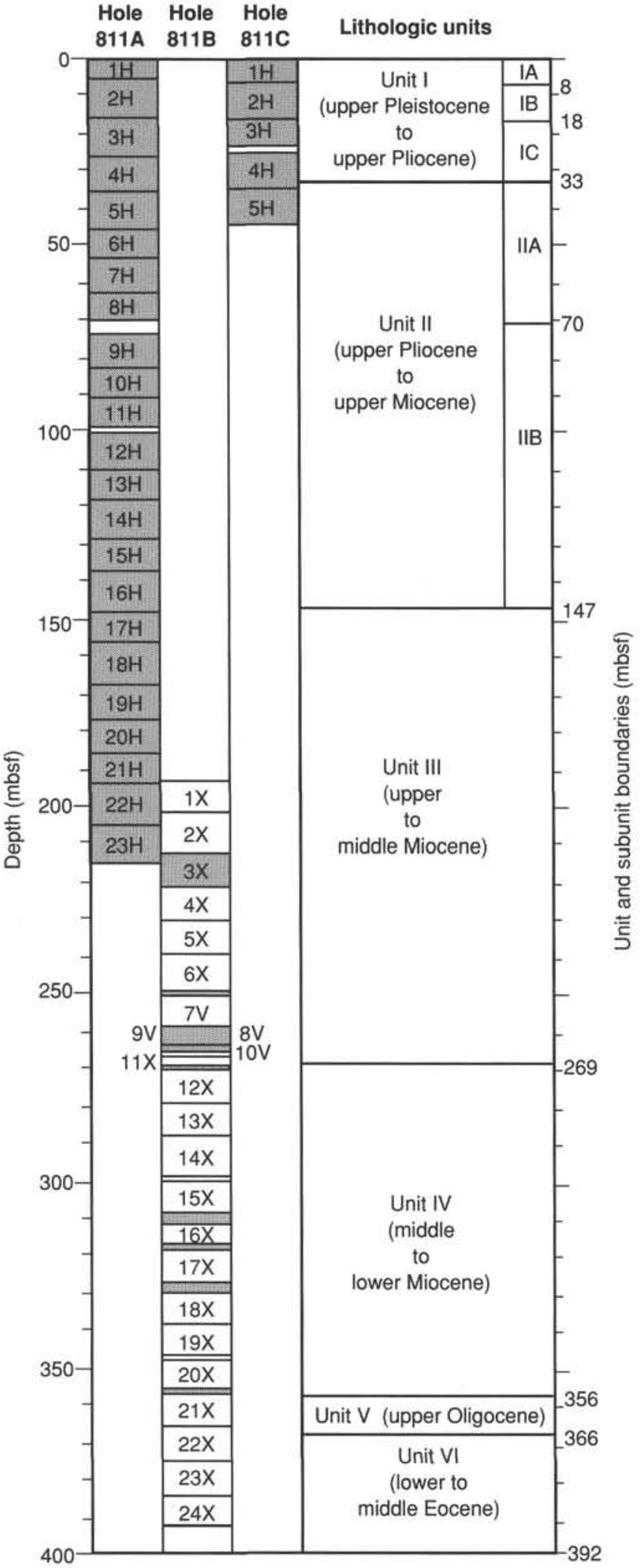

Figure 11. Summary of lithologic units for Holes 811A, 811B, and 811C. Shading indicates well-recovered cores.

basis on which Unit II has been divided into Subunits IIA and IIB. In the fine calcareous fraction of Subunit IIA, nannofossil proportions range between 25% and 75%, whereas in Subunit IIB, nannofossil proportions are always higher than 75%. The uppermost chalk occurs in Subunit IIA at 68.5 mbsf, and at 88 mbsf, one-third of the core lithology has been described as chalk. The proportion of chalk decreases farther downward in Subunit IIB, and the sediments are totally unlithified at the base of Unit II in Cores 133-811A-15H and -16H, from 130 to 150 mbsf.

Subunit IIA (Sections 133-811A-4H-6, 115 cm, to -8H-7, 70 cm, depth, 33.15–70.00 mbsf; and partially in Sections 133-811C-4H-4, 117 cm, to -6H-CC; age, early late Pliocene, 2.5–3.75 Ma)

Despite the absence of gravity-flow deposits, the sediment in Subunit IIA is a mixture of pelagic and bank-derived fine calcareous particles and *sensu lato* can be called a periplatform ooze, although calcite, rather than aragonite, is the only carbonate mineral present, exclusive of a small percentage of dolomite. The proportions of bank-derived fine particles steadily decrease downward within Subunit IIA, from 75% at the top to 25% at the bottom. The admixture of bank-derived fine calcareous particles into the pelagic sediments can be seen clearly in the average values of sedimentation rates (30 m/m.y.) for Subunit IIA. These values are twice as high as those of average sedimentation rates (15 m/m.y.) for the purely pelagic sequence in Subunit IIB. White nannofossil micritic ooze with foraminifers and having faint purplish and brownish banding occurs at the top of Subunit IIA. This lithology changes gradually downward into a white nannofossil ooze with foraminifers that has scattered brown to black burrows in Subunit IIA. Values of bulk carbonate content, which are highly variable through Subunit IIA, range between 93% and 98%. The uppermost chalk horizon occurs at the bottom of Subunit IIA. The average GRAPE density value for Subunit IIA is 1.78 (g/cm^3), which is higher than the average density value (1.75 g/cm^3) for the underlying pelagic sediments at the top of Subunit IIB. The higher values for the periplatform ooze in Subunit IIA suggest that these sediments originally contained more metastable bank-derived aragonite and magnesian calcite, which subsequently dissolved or recrystallized as calcite in the oozes of Subunit IIA.

Subunit IIB (Sections 133-811A-8H-7, 70 cm, to -16H-6, 150 cm, depth, 70–147.5 mbsf; age, early Pliocene to late Miocene, 3.75–8.75 Ma).

The 78-m-thick sediment sequence of Subunit IIB consists of mostly white pelagic unconsolidated to weakly lithified sediments that range between nannofossil oozes with foraminifers and foraminifer oozes with nannofossils. Nannofossils in Subunit IIB make up more than 75% of the fine fraction (see "Biostratigraphy" section, this chapter), and Subunit IIB is devoid of calciturbidite layers. Surprisingly, the upper part of Subunit IIB is more chalky (up to 30% chalk at 88 mbsf) than the lower part, which is totally unlithified in Cores 133-811A-15H and -16H. This reversed trend in abundance of chalk is incompatible with the GRAPE density values, which gradually increase from average values of 1.75 g/cm^3 at the top of Subunit IIB to 1.80 g/cm^3 at the bottom. The abrupt increase of GRAPE density values at 140 mbsf (the lowermost part of Subunit IIB) to 1.85 g/cm^3 does not coincide exactly with the selected depth for the boundary between Units II and III. Values of bulk carbonates vary slightly, but gradually increase through Subunit IIB from 94% to 96%. The boundary between Units II and III corresponds to an abrupt 2% increase in the

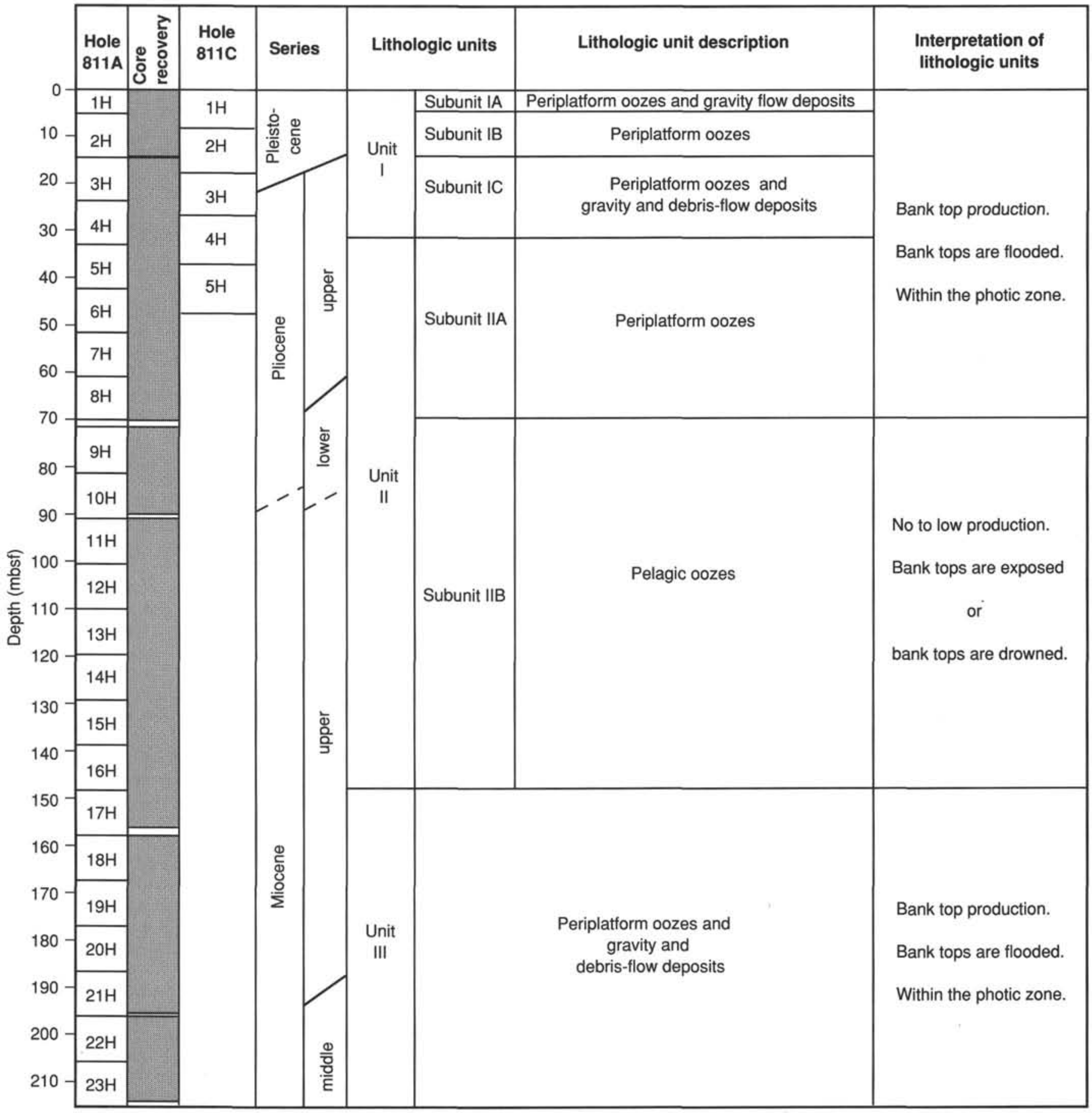

Figure 12. Summary of lithologic units and interpretation for well-recovered sections in Holes 811A and 811C. Shading in recovery column indicates recovered intervals.

carbonate content (see "Inorganic Geochemistry" section, this chapter).

Unit III (Section 133-811A-16H-6, 150 cm, to Core 133-811B-11X, depth, 147.5–269.5 mbsf; age, late-to-middle Miocene, 8.75–12.5 Ma).

The upper 60 m of Unit III was cored using the APC, with 94% recovery. Recovery was poor in the underlying 30 m using XCB coring (<5%), whereas recovery improved (25%) in the bottom 20 m by coring an 8.5-m-interval using the VPC, with 5.5 m recovered. White nannofossil oozes with micrite gradually change through the top 60 m of Unit III into nannofossil foraminifer and foraminifer nannofossil oozes with micrite, then into micritic foraminifer ooze with bioclasts. In the fine fraction, nannofossil abundance rapidly decreases through Unit III from 30% to less than 10% (see "Biostratigraphy" section, this chapter). The oozes alternate with numerous 10- to 70-cm-thick, usually upward-fining, light gray bioclastic foraminifer wackestone, packstone, lithoclast floatstone, and rudstone layers interpreted as calciturbidites and debris-flow deposits. These redeposited calcareous layers account for 4% to 29% (average 16%) of periplat-

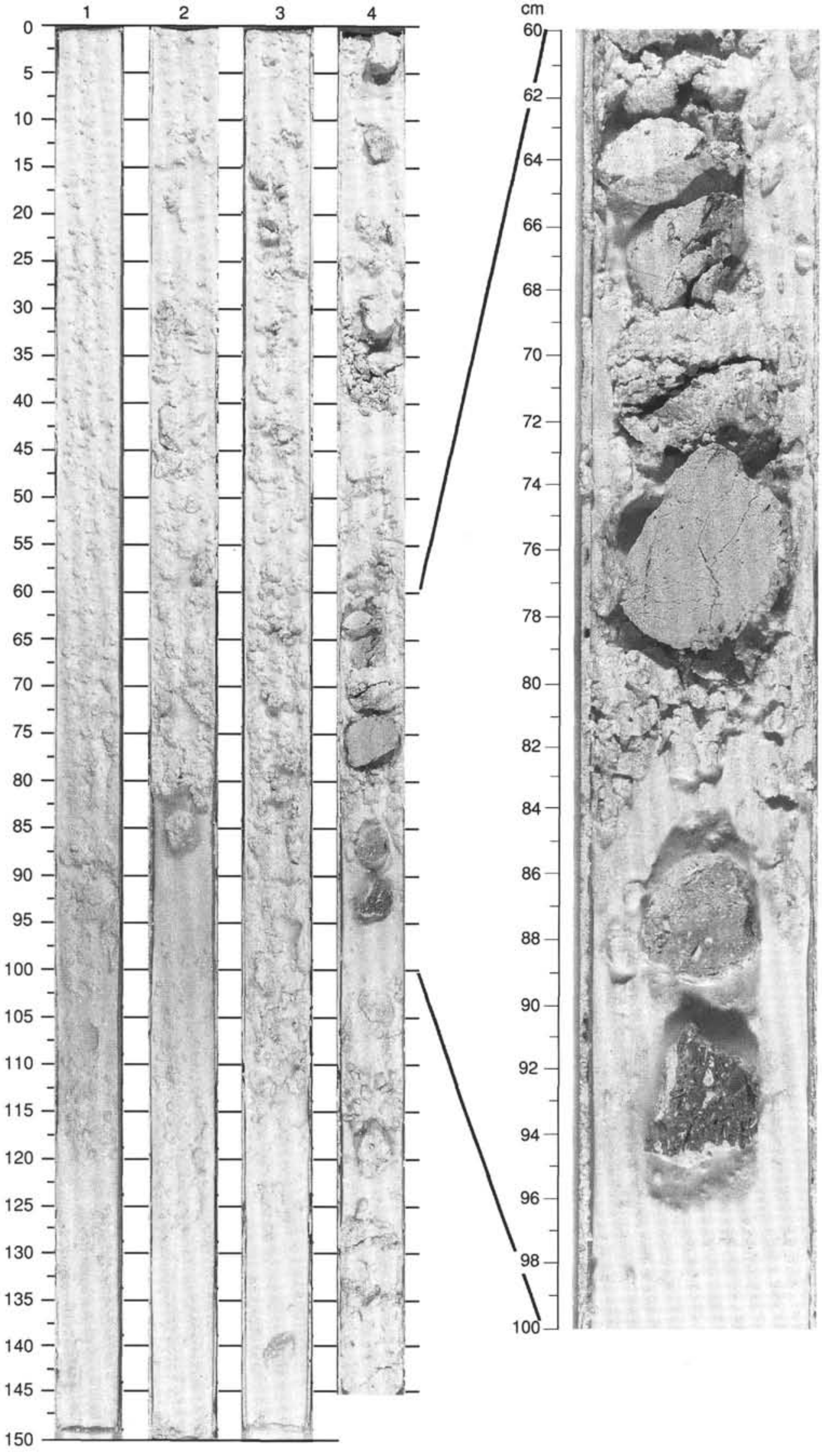

Figure 13. Upper debris-flow package (Core 133-811C-3H). Details of lithoclasts at the base of the package display moldic porosity (Section 133-811C-3H-4, 60–100 cm).

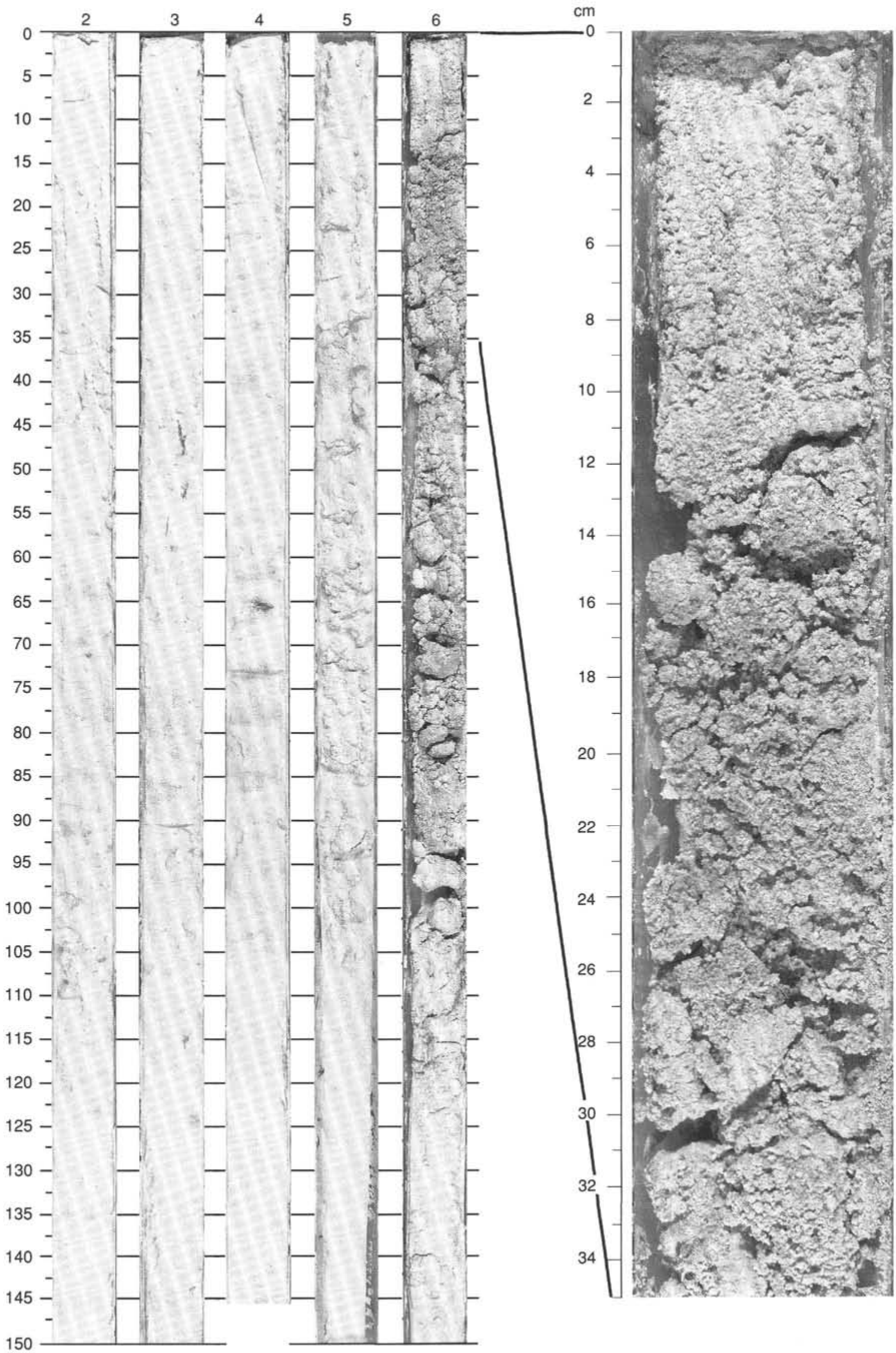

Figure 14. Lower debris-flow package (Core 133-811A-4H). Details of coarse sands and gravels at the base of the package (Section 133-811A-4H-6, 0–35 cm).

form sediments in the top 60 m of Unit III, or 28 single turbidite layers in 3.75 m.y., a frequency of one event per 130 k.y., which is two orders of magnitude lower than was recorded in the Tongue of the Ocean (the Bahamas) during the late Pleistocene (Droxler and Schlager, 1985). The sediments in the upper part of Unit III are usually oozes, with a few partially chalky layers. These oozes become more chalky downward, but oozes with chalky horizons are most common in the lowermost APC core (Core 133-811A-23H). Recovery was poor in the lower 50 m of Unit III using the XCB, thus difficult to describe. Based upon the 5.5 m of core recovered by the VPC between 250 and 265 mbsf, the sediments are a suite of white bioclastic nannofossil oozes/chalks and bioclastic-to-micritic chalks with foraminifers, which are similar to the sediments cored in the upper part of Unit III using the APC. However, these sediments are generally more lithified. Because of the generally poor recovery, we had trouble identifying the ooze/chalk boundary in the lower part of Unit III. It might be conservatively placed at the top of VPC Core 133-811B-8V, which corresponds to 259 mbsf.

Unit IV (Cores 133-811B-11X to 133-811B-20X, depth, 269.5–356.3 mbsf; age, middle-to-early Miocene, 12.5–[?] Ma).

Unit IV consists of an 87-m-thick sequence of very white, mostly unlithified bioclastic or skeletal packstones, grainstones, and rudstones. This lithology contrasts with the overlying periplatform chalks characteristic of the bottom of Unit III. Because of the poor XCB recovery (10%) at the base of Hole 811B, one cannot locate precisely the transition from middle bathyal periplatform chalks at the bottom of Unit III to neritic (shelf, inner platform, or fore-reef?) bioclastic sands and gravels of Unit IV. The presence of a hiatus between the two units is probable. The top of Core 133-811B-12X was selected as the boundary between Unit III and Unit IV on the basis of the unlithified bioclastic packstone in Section 133-811B-12X-CC, which contrasts with the periplatform chalks in Section 133-811B-10V-CC. Unit IV is a thick reworked sand and rubble package with mostly skeletal grains as coral debris, alcyonarian spicules, mollusk fragments, small and larger benthic foraminifers (amphisteginids, miliolids, textularians), echinoids, crustaceans, bryozoans, and red algae. The depositional environment for Unit IV has been interpreted as shallow (possibly a water depth of 50 m, becoming even more shallow toward its base) and to represent a fore- or back-reef environment. On the basis of a few badly preserved planktonic foraminifers, we think that Unit IV was deposited in the late-to-early Miocene.

Unit V (Cores 133-811B-20X to 133-811B-21X; depth, 356.3–365.9 mbsf; age, late Oligocene)

Unit V consists of a 10-m-thick, unlithified to well-cemented, fine-grained skeletal packstone sequence with abundant planktonic foraminifers in a micritic matrix composed of silt-size bioclastic particles. The occurrence of planktonic foraminifers, which yield a late Oligocene age and suggest a cold-water environment, contrasts with the lack of open-water fauna in the overlying Unit IV.

Unit VI (Section 133-811B-22X-CC to Core 133-811B-24X; depth, 365.9–392.5 mbsf; age, early-to-middle Eocene)

Only a small pebble was recovered in the core catcher of Core 133-811B-22X. A trace amount of calcareous sediment was recovered in Core 133-811B-23X, and Core 133-811B-24X came back on deck empty. The planktonic foraminifers observed in this small pelagic limestone pebble yield an early-to-middle Eocene age. This pebble may represent the cover of the hard seismic basement.

SITE 825 LITHOSTRATIGRAPHY

Lithologic Units

Site 825 reoccupied Site 811. Two holes were drilled at Site 825 to recover by rotary drilling the seismic basement of the Queensland Plateau and to improve the poor core recovery in the lower part of Site 811 (below 200 mbsf). In Hole 825A, after recovering a 4.5-m-long APC mud-line core and washing down to 200 mbsf, 4 APC and 19 XCB cores were retrieved to a depth of 381.5 mbsf. In Hole 825B, after washing down to 379.5 m, 10 rotary drilled cores were retrieved to a depth of 466.3 mbsf.

The sedimentary sequence cored at Site 811 was divided into five, possibly six, lithostratigraphic units on the basis of the variable proportion of bank-derived carbonate material added to the pelagic components and variations in water depth of the depositional environments from middle bathyal to neritic (see "Site 811 Lithostratigraphy" section, this chapter). The 4.5-m-long mud-line core of Hole 825A corresponds to the upper part of Subunit IA in Holes 811A and 811C, whereas the sediments cored using APC and XCB in Hole 825A (between 200 and 269 mbsf) correspond to the lower part of Unit III, where recovery was poor using XCB drilling in Hole 811B. Only 33 cm of sediment was recovered using the XCB in the lower 112.5 m of Hole 825A, between 269 and 381.5 mbsf, a depth interval corresponding in Hole 811B to Units IV (269–356 mbsf), Unit V (356–366 mbsf), and to a questionable Unit VI, in the lowermost part of Hole 811B.

The sedimentary material recovered in Hole 825B between 408.4 and 453 mbsf, a deeper penetration than at Hole 811B (TD = 392.5 mbsf), was significantly different from the Site 811 sediments of Unit V and the questionable Unit VI, which was defined by a single pebble. Seismic basement (Unit VII) was recovered in the lower two Cores 133-825B-9R and -10R. A lithostratigraphic comparison of Site 811 with Site 825 is illustrated in Figure 15. The following lithologic description includes only the intervals cored and recovered at Site 825. These were placed in the corresponding lithologic units defined and described in the "Site 811 Lithostratigraphy" section (this chapter).

Subunit IA (Core 133-825A-1H; depth, 0–4.5 mbsf; late Pleistocene in age) Sediments in mud-line Core 133-825A-1H consist of light gray, pinkish, and brownish white, slightly bioturbated micrite nannofossil foraminifer ooze alternating in Section 133-825A-1H-3 with four 8- to 10-cm-thick foraminifer pteropod packstone layers, which were interpreted as calciturbidites. The lithology of this core is characteristic of Subunit IA, late Pleistocene in age, defined as periplatform ooze with gravity-flow deposits in Holes 811A and 811C.

Unit III (Core 133-825A-5H to Section 133-825A-12X-1; depth, 200–268.27 mbsf; age, middle Miocene)

Sediments in Cores 133-825A-5H, -6H, -7H, and -8H, fully recovered by APC drilling, consist of white micritic ooze and chalk with nannofossils and foraminifers alternating with white unlithified to partially lithified bioclastic packstones and floatstones. The bioclastic packstone intervals occur as a few centimeters-thick to several tens of centimeters-thick layers in Cores 133-825A-5H and -6H, 1.5-m-thick bed in Core 133-825A-7H, whereas Core 133-825A-8H consists only of unlithified and partially lithified bioclastic packstone. Several intervals of 20-cm- to 1.5-m-thick unlithified floatstones with a calcareous ooze matrix are also present. Chalk levels appear either as discrete beds or intervals of scattered lumps and account for up to 50% of the sediments. Core recovery substantially dropped further down with Cores 133-825A-9X,

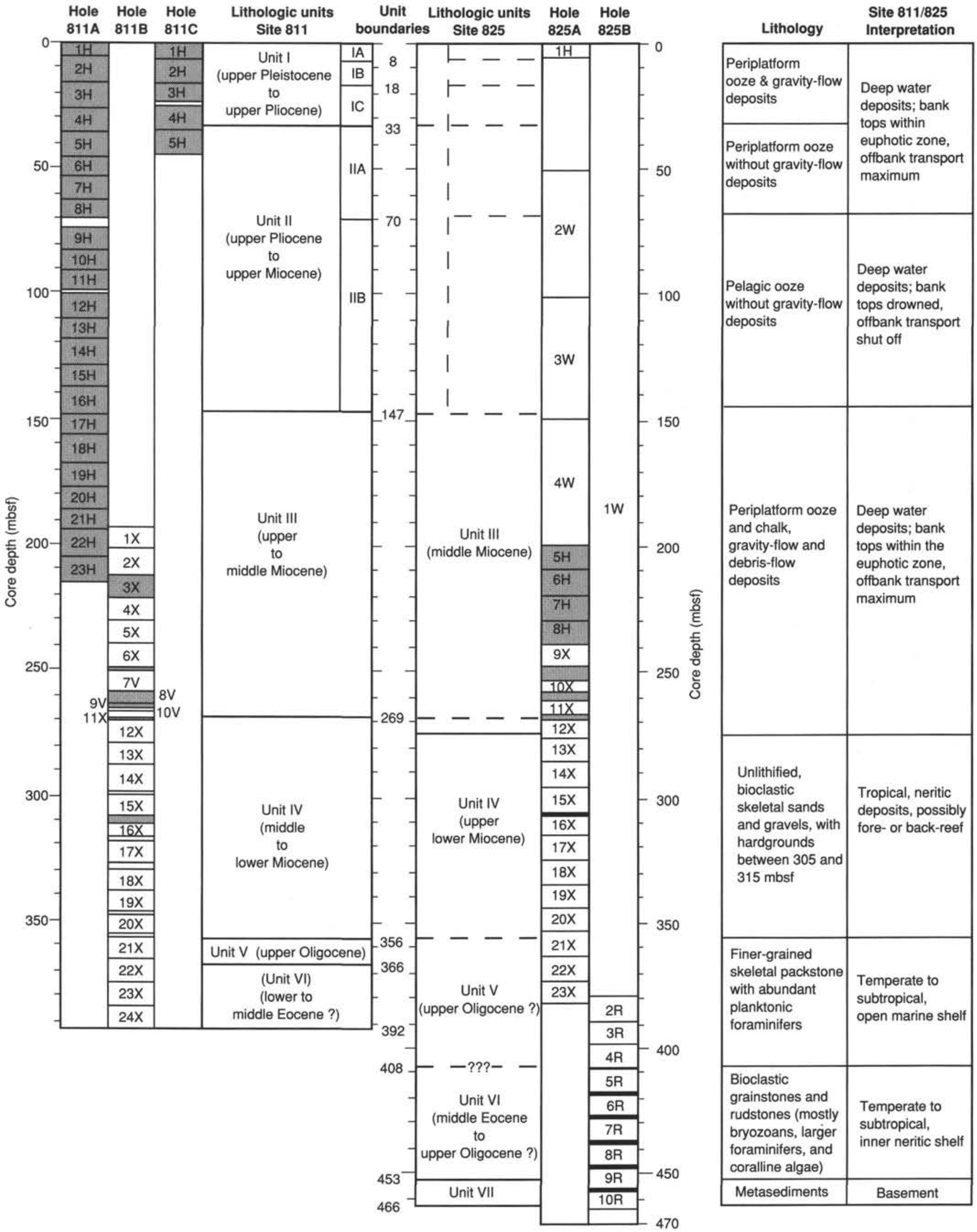

Figure 15. Comparison of lithologic units for Sites 825 and 811. Tentative interpretation of depositional environment is also shown. Shading indicates well-recovered cores.

-10X, -11X, and -12X, with an average of only 35%. No sediments were recovered in Core 133-825A-9X. Sediments in Cores 133-825A-10X, -11X and -12X consist of either white calcareous ooze (50%) and chalks (50%) with foraminifers, foraminifer ooze and chalk, and micritic ooze and chalk in the same proportions. A 1-m-thick layer of unlithified, white, foraminifer packstone also was observed at the base of Core 133-825A-11X.

The lithologies recovered in Cores 133-815A-5H to -12X are identical to the sediments in Unit III at similar depths in the lower half of Hole 811B that had poor recovery and that have been interpreted to represent a series of deep-water periplatform ooze and chalk alternating with several gravity-flow and debris-flow deposits. The lower boundary of Unit III, estimated to be at 269 mbsf in Hole 811B, was not better defined in Hole 825B because no material was recovered from Cores 133-825A-13X and -14X.

Unit IV (Sections 133-825A-15X-CC and -16X-CC; depth, 305.4–315.0 mbsf; age, late early Miocene)

Unit IV is represented in Hole 825A by only a few pebbles of white, lithified, bioclastic packstone with foraminifers in Section 133-825A-15X-CC and in 33 cm of angular, pale yellow-to-yellow, well-lithified bioclastic rudstone with larger benthic foraminifers, coralline algae, and coral molds. The same hard lithologic level was also partially recovered in Cores 133-811B-15X and -16X and was encountered at the same level during the drilling of Hole 825B, as well as partially recovered in the wash Core 133-825B-1W. This level represents a local hardground within Unit IV that consists mostly of unlithified bioclastic or skeletal packstones, grainstones, and rudstones. These sediments were difficult to recover using XCB drilling. The depositional environment for Unit IV has been interpreted as shallow (possibly 50 m of water depth or even shallower), which represents a tropical fore- or back-reef environment.

Unit V, consisting of Cores 133-811B-20X and -21X and representing a late Oligocene temperate-to-subtropical, more open-water setting than the overlying Unit IV, was not recovered in Hole 825A. The questionable Unit VI, defined on the basis of a single, small pebble recovered in Section 133-133-811B-22X-CC and dated by planktonic foraminifers as early-to-middle Eocene in age, was not recovered either in the lowermost part of Hole 825A or in the uppermost part of Hole 825B. Because the definition of Unit VI was based only on a small pebble in Hole 811B, Unit VI has been redefined on the basis of the material recovered in Cores 133-825B-5R, -6R, -7R, -8R and the upper 6 m of -9R.

Unit VI (Cores 133-825B-5R, -6R, -7R, -8R, and the upper 6 m of -9R; depth, 408.4–453 mbsf; age, middle Eocene to early Miocene, but probably late Oligocene)

The upper limit depth (408.4 mbsf) of Unit VI was arbitrarily selected as the top of Core 133-825B-5R, because no material was recovered in the overlying Cores 133-825B-2R, -3R, and -4R. These latter cores were incorporated as the base of Unit V, defined in Hole 811B. The lower limit of Unit VI has been defined as the top of the metamorphic basement and was estimated as within Core 133-825B-9R at 453 mbsf on the basis of the drilling operations. At that level, drilling rates became much slower because of the hardness of the metamorphic basement. Unit VI consists of white, pale yellow-to-yellow, alternating with more pinkish levels, well-lithified, bioclastic grainstone and rudstone. The grains are usually well-sorted and range in size from coarse sands to granules. The dominant components are branching and colonial bryozoans and larger foraminifers, with coralline algae, echinoids, mollusks, and small branching corals as secondary components (see Fig. 16). Coral fragments become rare and seem to disappear toward the base of Unit IV. Pinkish levels represent the same facies as the yellowish intervals, but appear more recrystallized. Primary intergranular porosity is well preserved, with only minimum moldic porosity (see Fig. 16). Glauconitic grains can be observed in Section 133-825B-8R-1. A dark brown metamorphic sandstone pebble, evidence for active erosion of the metamorphic basement during that interval, is intercalated in Section 133-825B-8R-1, at 25 cm.

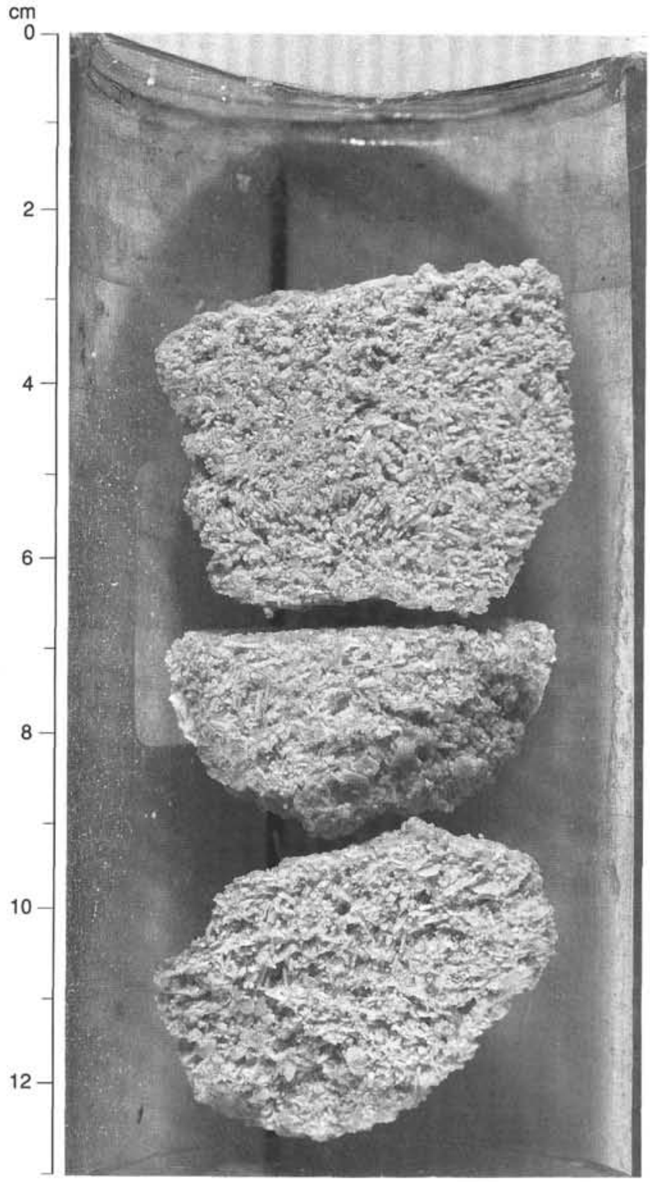

Figure 16. Well-lithified bioclastic grainstone and rudstone (Section 133-825B-8R-1, 0–13 cm). Dominant components are branching and colonial bryozoans and larger benthic foraminifers, with coralline algae, echinoids, mollusks, and small branching corals as secondary components. Primary intergranular porosity is well preserved, whereas moldic porosity is minimum.

Unit VI in Hole 825B is almost identical to Unit VI cored in Hole 824C on the western slope of Holmes Reef, overlying the metamorphic basement (as in Hole 825B). The lithologies of Unit VI in Holes 825B and 824C represent a temperate-to-subtropical depositional environment on an inner neritic shelf and may be the first sedimentary facies transgressing the metamorphic basement in the northwest corner of the Queensland Plateau. The single age for Unit VI, based on nannofossil stratigraphy in Hole 825B, comes from the geopetal mud-infilling of a cavity in Section 133-825B-8X-1 at 20 cm, which yields an age younger than middle Eocene, but older than middle Miocene. Because of the proximity of Sites 824 and 825, the similar bryozoan and larger foraminifer-rich facies of Unit VI in both sites, and their similar position on top of the metamorphic basement, a late Oligocene to early Miocene age, tentatively estimated at least for the top of Unit VI in Hole 824C, may be given to Unit VI in Hole 825B. The occurrence of numerous larger foraminifers in Unit VI and their identification during shore-based research should help to determine a more precise age for Unit VI.

Unit VII (Cores 133-825B-9R and -10R; depth, 453–466.3 mbsf; age, unknown)

The seismic basement in Hole 825B consists of fine-grained, dark gray, poorly foliated, well-lithified, quartz-feldspar-mafic (?) metasediment or metavolcanic rock that contains more coarsely crystalline zones of quartz and feldspar. Thin, discontinuous quartz or feldspar veinlets are present, and disseminated pyrite is common (see Fig. 17).

The drilling of Site 825 added new information about the general evolution of the northwest corner of Queensland Plateau, especially regarding the lithologic nature of its basement and the first transgressive sedimentary facies. As at Site 824, the seismic basement (Unit VII) comprises metamorphic sediments, is covered by Unit VI, and consists of temperate-to-subtropical, possibly upper Oligocene bryozoan and larger foraminifer-rich grainstone and rudstone deposited in an inner neritic shelf. The overlying Unit V consists of more fine-grained skeletal, upper Oligocene packstones with abundant planktonic foraminifers and represents a temperate-to-subtropical more open outer-shelf depositional environment. The upper-to-lower Miocene to possibly lower-middle Miocene fauna and flora, included in the overlying unlithified, or partially lithified, bioclastic sands and gravels of Unit IV, represent a tropical, inner neritic deposit, possibly a fore- to back-reef environment. The overlying 270 m (Units III, II, and I) contain middle bathyal sediments. The sediments in Unit III consist of lower-to-upper Miocene periplatform ooze and chalks alternating with gravity-flow and debris-flow deposits, supporting the idea that some shallow carbonate banks existed in close vicinity and were shedding material toward the deeper surroundings. The overlying Subunit IIB consists of upper Miocene to lower Pliocene, purely pelagic oozes devoid of gravity-flow deposits and of any bank-derived material. The absence of bank-derived material in the sediments deposited in the basin during the deposition of Subunit IIB has been interpreted by a systematic drowning below the euphotic zone of the nearby shallow carbonate banks during the late Miocene and early Pliocene. Production on the shallow carbonate banks and off-bank transport of bank-derived sediments toward their surrounding deep basins was re-initiated in the early late Pliocene, first as influx of fine material added to pelagic sediments by settling through the water column (Subunit IIA) and finally as gravity- and debris-flow deposits. These are in addition to the fine-grained mixture of pelagic and bank-derived sediments during the late Pliocene and the Pleistocene (Unit I).

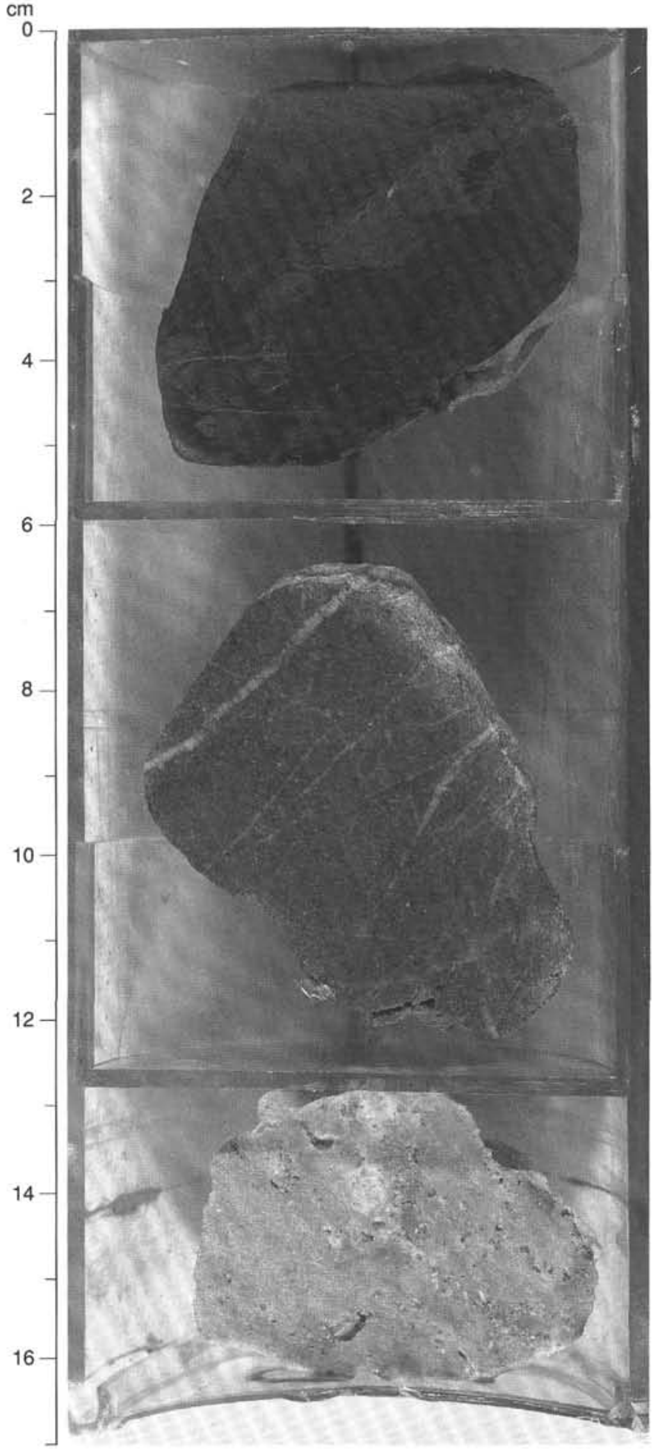

Figure 17. Seismic basement in Hole 825B consists of fine-grained, dark gray, poorly foliated, well-lithified, quartz-feldspar-mafic (?) metasediment or metavolcanic rock that contains more coarsely crystalline zones of quartz and feldspar. Thin, discontinuous quartz or feldspar veinlets are present; disseminated pyrite is common (Section 133-825B-9R-1, 0–17 cm).

SITE 811 BIOSTRATIGRAPHY

Biostratigraphy and Paleoenvironment Synthesis

Nannofossils and planktonic, benthic, and larger foraminifers were examined from the core-catcher samples at Site 811. Additional nannofossil samples from within selected cores also were studied. Biostratigraphic results and zonal assignments are summarized in Figures 18 and 19.

Core-catcher samples from Hole 811A contain generally well-preserved calcareous microfossils in the upper part of the section, while preservation deteriorates downhole. Calcite overgrowths are apparent in planktonic and benthic foraminifers in and below Core 133-811A-11H-CC. Despite these overgrowths, benthic foraminiferal morphology is well preserved in Hole 811A, while planktonic foraminiferal preservation is poor to moderate.

Benthic foraminiferal assemblages indicate that deposition in most of Hole 811A and in Hole 811B above Section 133-811B-11X-CC occurred in the middle bathyal zone (600–1000 m). Several benthic foraminiferal species suggest further refinement of this paleobathymetric estimate to the lower middle bathyal zone. Neritic deposits are indicated by the occurrence of larger foraminifers in the lower Miocene section at Hole 811B. Core-catcher samples below lithologic Unit IV yield poorly preserved planktonic and smaller benthic foraminifers. No depth-diagnostic benthic foraminiferal species could be identified in this section.

Calcareous Nannofossils

Site 811 yielded abundant calcareous nannofossils in the upper part of the section, decreasing downward as a progressively larger proportion of the sediments–all carbonate–becomes detrital, until finally, only trace numbers of nannofossils are present. Preservation also deteriorates downward as fossils become increasingly more overgrown, and the few specimens present are difficult or impossible to identify to the species level.

Hole 811A

Hole 811A extends from 0 to 214.5 mbsf. Sedimentation rates are moderately variable. Because samples are relatively far apart (generally 9.5 m), one cannot always be sure whether the section is complete or whether significant hiatuses are present. Following is a brief description of the nannofossil biohorizons identified in the core-catcher samples, except for Core 133-811A-11H, in which several samples were examined.

Surface sediments (sediment/water interface) were not examined. Sample 133-811A-1H-CC (5.6 mbsf) contains abundant *Gephyrocapsa caribbeanica* and other upper Pleistocene species, but lacks *Emiliania huxleyi* and *Pseudoemiliania lacunosa*, which constrain this level to an age of 275 to 450 k.y. Sample 133-811A-2H-CC yielded *Pseudoemiliania lacunosa* (large, circular variants) with abundant *Gephyrocapsa* spp., an assemblage of late Pleistocene aspect although older than 450 k.y. The next lower sample (133-811A-3H-CC) yielded *Discoaster brouweri*, which places the Pliocene/Pleistocene boundary within Core 133-811A-3H. Several lower Pleistocene biohorizons were not identified, which suggests that the middle and lower Pleistocene is greatly attenuated. Alternatively, one or several hiatuses may be present within Core 133-811A-3H.

The next lower biohorizon recognized is the highest occurrence of *Discoaster pentaradiatus* in Sample 133-811A-4H-CC, followed by *Discoaster tamalis* in Sample 133-811A-5H-CC. The upper Pliocene extends downward through Core

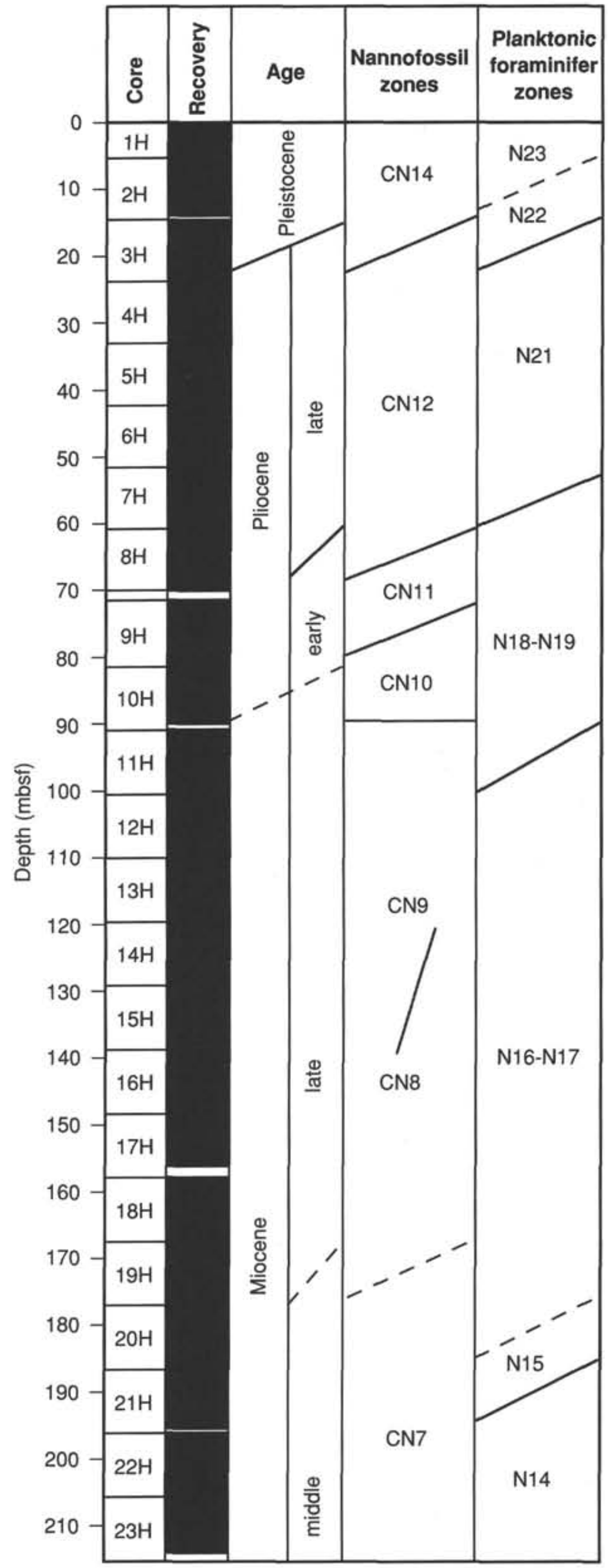

Figure 18. Summary of planktonic microfossil data from Hole 811A.

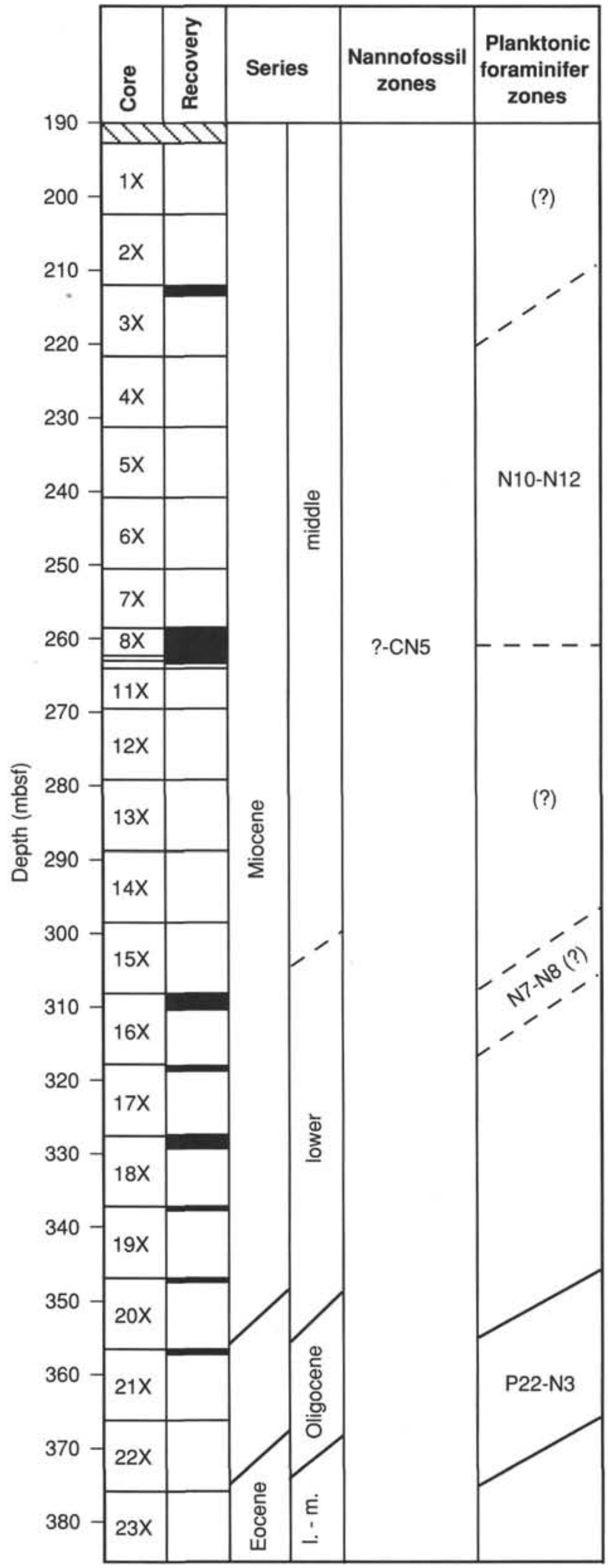

Figure 19. Summary of planktonic microfossil data from Hole 811B.

133-811A-8H; Sample 133-811A-8H-CC yielded *Sphenolithus abies*, which suggests a relatively narrow age range from 3.45 to 3.51 Ma (mid-Pliocene). Sample 133-811A-9H-CC contains *Reticulofenestra pseudoumbilica*, *Discoaster asymmetricus*, and *Amaurolithus tricorniculatus*, a lower Pliocene assemblage older than 4.24 Ma.

Ceratolithus armatus was recorded in Sample 133-811A-10H-CC, and the highest occurrence of *Discoaster quinqueramus* is between Sample 133-811A-10H-CC and -11H-CC, at 55 cm. Therefore, the Miocene/Pliocene boundary is within Core 133-811A-10H, because neither of these two species occurs in the post-Messinian (i.e., post-Miocene) sediments of the Mediterranean. Sample 133-811A-11H-CC yielded *Amaurolithus amplificus*, a short-lived late Miocene species with an age range of 5.6 to 5.9 Ma. Ceratoliths of the genus *Amaurolithus* occur in Sample 811A-12H-CC, indicating an age younger than 6.74 Ma for this sample.

The next lower marker, the highest occurrence of *Discoaster neohamatus*, in Sample 133-811A-14H-CC is not reliable because specimens that are similar (perhaps identical) to this species are scattered higher in the section. It is possible that (1) these specimens have been redeposited, (2) they are overgrown *Discoaster brouweri*, or (3) *Discoaster neohamatus* survived much longer in this tropical sea than in more temperate regions, where it may be a more reliable marker. Heavily overgrown *Catinaster calyculus* occurs in Samples 133-811A-16H-CC and -17H-CC, and *Discoaster neohamatus* occurs down to Sample 133-811A-18H-CC. *Discoaster hamatus* was found in Sample 133-811A-19H-CC; the highest occurrence of this species approximates the upper Miocene/middle Miocene boundary, which was projected as being within Core 133-811A-19H. Below Core 133-811A-19H, the abundance of nannofossils is greatly reduced (see Fig. 18), and preservation is poor. *Cyclicargolithus floridanus* was recorded in Sample 133-811A-23X-CC, but these specimens are not typical of the species.

Hole 811B

The recovered interval in Hole 811B extends from 193.5 to about 385 mbsf. Core recovery was poor throughout the hole, and nannofossils are few-to-rare and heavily overgrown. *Cyclicargolithus floridanus* was recovered from several core-catcher samples (e.g., Cores 133-811B-4X, -8V, -9V, -16X, -17X, -18X, -20X, and -21X). Sample 133-811B-8V-CC contains *Calcidiscus premacintyrei*, the range of which has been correlated with magnetostratigraphy in the North Atlantic at 12.3 to 14.1 Ma (i.e., middle Miocene). Sediments below this level can be assigned only a mid-Cenozoic age, based on the uncertain occurrence of *Cyclicargolithus floridanus*.

No samples were examined from Hole 811C.

Planktonic Foraminifers

All core-catcher samples from Hole 811A were examined for their contents of planktonic foraminifers. From core-catcher Sample 133-811A-11H-CC (100.5 mbsf) to the top of the section, planktonic foraminifers are abundant and well preserved.

Pleistocene Zones N22 and N23 are present in Sections 133-811A-1H-CC and 133-811A-2H-CC, as exemplified by the presence of *Globorotalia truncatulinoides*. The boundary between N22 and N23 was difficult to place because the zonal marker *Globigerinella calida* is not present in this hole. To approximate this boundary, we used the first occurrence of *Globigerina ruber* pink and *Globigerinella adamsi*.

The first occurrence of *Globorotalia tosaensis* is in Sample 133-811A-6H-CC (53 mbsf), indicating the N21/N19 boundary. Co-occurring species in Zone N21 are *Globigerinoides* *obliquus extremus*, *Globigerinoides fistulosus*, *Globorotalia limbata*, and in the lower part of the zone (Sample 133-811A-6H-CC, 53 mbsf), the last appearance of *Globoquadrina altispira* was found.

The boundary between Zones N18 and N19 was not delineated because both the first occurrence of *Sphaeroidinella dehiscens* and the last occurrence of *Globorotalia tumida tumida* specimens were present in Sample 133-811A-11H-CC (100.5 mbsf), while below this level *G. tumida tumida* disappeared from the record, marking the top of Zone N16-N17.

From this level downward, the preservation of the planktonic foraminifers deteriorates as a result of calcite overgrowth of the specimens. Zone N16-N17 is characterized by the presence of *Globorotalia tumida plesiotumida* and co-occurring *Neogloboquadrina acostaensis* specimens. The first occurrence of the latter in Sample 133-811A-19H-CC (176.5 mbsf) indicates the upper limit of Zone N15. However, it may well be that this zone does not exist in this area. Perhaps the small four- to five-chambered *N. acostaensis* specimens are present in the <125 μm size fraction. The top of *Globorotalia siakensis* was found in Sample 133-811A-21H-CC (195.5 mbsf), delineating the upper limit of Zone N14.

In contrast to Hole 811A, Hole 811B yielded few planktonic foraminifers, and these were not preserved well. The upper part of the section was barren.

Samples 133-811B-3X-CC through -9X-CC (221.7–264.1 mbsf) contained some poorly preserved specimens, which possibly are of the *Globorotalia fohsi* series or *Globorotalia praemenardii*, indicating the presence of Zones N10 through N12. Below the latter level, samples were barren, except for Samples 133-811B-15X-CC (308.0 mbsf) and the lowermost part of the section (Samples 133-811B-20X-CC through -22X-CC). Sample 133-811B-15X-CC contains sparse *Praeorbulina sicana*, *Globoquadrina dehiscens*, and possibly some *Globorotalia birnageae* specimens, designating Zones N7 and N8. We assigned Samples 133-811B-20X-CC and -21X-CC to the late Oligocene Zone P22-N3, as indicated by the presence of abundant *Globigerina ciperoensis* and *Globigerina angulisuturalis* specimens. Preliminary results of a thin section made from Sample 133-811B-22X-CC revealed one planktonic foraminifer and one benthic foraminifer in a micritic matrix. We estimated the age of this sample at early to middle Eocene, based on the presence of *Morozovella* sp.

Benthic Foraminifers

Core-catcher samples from Hole 811A contain well-preserved, diverse benthic foraminifer assemblages, while Hole 811B yielded poorly preserved foraminifers having calcite overgrowths that sometimes obscured test morphology. Benthic foraminiferal assemblages indicate a middle bathyal (600–1000 m) paleodepth for Hole 811A and above Unit IV in Hole 811B. Most of the core-catcher benthic foraminiferal assemblages examined from Hole 811A contain rare occurrences of shallow-water contaminants, such as *Amphistegina* spp., *Asterigerina* spp., *Discorbinella* spp., *Discorbis* spp., and *Planorbulina* spp., indicating a minor amount of downslope transport from a reefal source area. In contrast, the faunas at Hole 811B contain a large displaced component. As a result of shipboard time constraints, approximately one out every four core-catcher samples was examined for qualitative contents of benthic foraminifers to estimate paleobathymetry.

Hole 811A benthic foraminifer assemblages contain the typical bathyal species *Cibicidoides bradyi*, *Cibicidoides mundulus*, *Cibicidoides subhaidingerii*, *Eggerella bradyi*, *Globocassidulina subglobosa*, *Hoeglundina elegans*, *Laticarinina pauperata*, *Lenticulina* spp., *Sigmoilopsis schlumbergeri*, *Sphaeroidina bulloides*, *Uvigerina hispida*, *Uvigerina pigmaea*, and *Uvigerina proboscidea* (van Morkhoven et al., 1986). Several taxa typical of the middle bathyal zone or deeper (>600 m) are present, including *Anomalinoides globulosus*, *Cibicidoides robertsonianus*, and *Pyrgo murrhina* (van Morkhoven et al., 1986). Benthic foraminifer species that restrict the depth estimate for Hole 811A to shallower than 1000 m are *Hanzawaia mantaensis*, *Melonis pompilioides* (van Morkhoven et al., 1986), and *Uvigerina hornibrooki* (<1200 m) (Boersma, 1984). These species associations indicate a middle bathyal paleodepth for most of Hole 811A. The abundance of *P. wuellerstorfi* in many of the core-catcher samples examined suggests that the paleodepth was in the deeper end of this range. A lower middle bathyal paleobathymetric estimate (800–1000 m) for Hole 811A is further supported by the presence of both *Melonis pompilioides* and forms that are transitional to its deeper-water morphotype, *M. sphaeroides*.

An exception to the lower middle bathyal paleobathymetric estimate may be Sample 133-811A-10H-CC, which contains shallower benthic foraminiferal elements. In addition to the bathyal species listed above, this sample contains *Cibicidoides guazamalensis*, which is usually found at upper bathyal depths (200–600 m). Notably, *P. wuellerstorfi* is absent from this sample, while the generally upper-to-middle bathyal *P. dohertyi* is present. The presence of *Anomalinoides globulosus* (>600 m) in this sample suggests that it is probably transitional between the upper bathyal and middle bathyal zones.

While most of the Hole 811A benthic foraminiferal faunas were primarily *in situ*, Sample 133-811A-5H-CC contained abundant, well-preserved shallow-water contaminants and well-preserved, reworked older foraminifers. Shallow-water taxa include *Amphistegina* sp., *Asterigerina* spp., *Discorbinella* sp., *Discorbis* sp., *Elphidium* spp., and *Planorbulina* sp. Reworked, older specimens in this sample include *Anomalinoides pseudogrosserugosus*, *Cibicidina walli*, *Cibicidoides micrus*, and *Planulina renzi*.

Poor preservation and dilution by shallow-water contaminants characterize the benthic foraminiferal assemblages in Hole 811B core-catcher samples. Despite this, a middle bathyal paleodepth (600–1000 m) was estimated for the section above Unit IV. We based this on faunal components that were found throughout the section, but not in each sample, including *Cibicidoides mundulus*, *Laticarinina pauperata*, *Sphaeroidina bulloides*, *Planulina wuellerstorfi*, *Uvigerina carapitana*, and *Uvigerina pigmaea*. *Uvigerina hornbrooki* (<1200 m) (Boersma, 1984), *Hanzawaia mantaensis* (100–1000 m), and *Rectuvigerina striata* (200–1000 m) (van Morkhoven et al., 1986) further restrict the paleobathymetric estimate to upper to middle bathyal. *Cibicidoides havanensis* (generally >800 m) in Sample 133-811B-4X-CC and abundant *Planulina wuellerstorfi* in Sample 133-811B-3X-CC suggest that the paleodepth in this part of the section may have been lower middle bathyal.

Core-catcher samples in and below Unit IV yield poorly preserved benthic foraminifers. No depth-diagnostic species could be identified in this section.

Larger Foraminifers

Larger benthic foraminifers were analyzed from Samples 133-811B-2X-CC and -16X-CC. In Sample 133-811B-2X-CC, reworking and redeposition of shallower-water deposits are indicated by the occurrences of *Gypsina* sp., *Operculina* sp., *Lepidocyclina* sp., and *Cycloclypeus* sp. Sample 133-811B-16X-CC contains *Nephrolepidina* sp., *Eulepidina* sp. (possibly reworked), *Heterostegina* sp., and *Cycloclypeus* (transitional form of *C. eidae* to *C. carpenteri*), assigning it to Chaproniere's (1981) Larger Foraminiferal Assemblage 5 or 6 (upper Te or lower Tf; see Adams, 1970).

SITE 825 BIOSTRATIGRAPHY

Core recovery at Site 825 was poor, and biostratigraphic resolution is limited (see Fig. 20). Calcareous nannofossil and planktonic foraminiferal data suggest that Cores 133-825A-5H through -12X (200–270 mbsf) are middle Miocene in age. Core 133-825A-15X is of early Miocene age on the basis of planktonic foraminiferal data. The oldest sediment recovered from the site is in Core 133-825B-9R. The age of this sample cannot be determined precisely; the sparse coccoliths indicate a possible age range of middle Eocene to early Miocene.

Core-catcher samples examined yielded assemblages of bathyal benthic foraminifers with abundant shallow-water fauna. Larger benthic foraminifers are common in the lower sedimentary sequence.

Calcareous Nannofossils

Calcareous nannofossils are few to rare and poorly preserved in all the core-catcher samples from Site 825, except for Sample 133-825A-1H-CC. Biostratigraphic resolution is poor owing to a low species diversity; usually only two or three species are represented. In Figure 20, we present a summary of the biostratigraphic results.

Sample 133-825A-1H-CC yielded a Pleistocene nannofossil assemblage, which includes abundant *Gephyrocapsa caribbeanica*. Both *Emiliania huxleyi* and *Pseudoemiliania lacunosa* are absent. This suggests an age of Subzone CN14b (0.275–0.465 Ma).

Specimens of *Sphenolithus* are present from Sample 133-825A-5H-CC through -12X-CC. This indicates that these samples are older than 3.45 Ma (Zone CN11). *Calcidiscus premacintyrei* occurs in Sample 133-825A-11X-CC. The presence of this species constrains the sample to an age range of 12.2-14.1 Ma (CN4–CN5). Consequently, the interval from Samples 133-825A-5H-CC through -10H-CC can be assigned to a combined Zone CN5–CN11.

Samples below 270 mbsf (including those from Hole 825B) contain virtually no age-diagnostic taxa. The presence of *Cyclicargolithus floridanus* in the upper part of Core 133-825B-9R (immediately above the metamorphic basement rock) suggests a broad age range of middle Eocene to early Miocene.

Planktonic Foraminifers

Core-catcher Samples 133-825A-5H-CC through -12X-CC from Hole 825A contain abundant, moderately preserved planktonic foraminifers. The presence of abundant *Globorotalia siakensis* indicates that this interval can be assigned to middle Miocene combined Zones N10 to N14. Below Core 133-825A-12X no planktonic foraminifers were present, except for Sample 133-825A-15X-CC, in which a meager fauna that included the late early Miocene species *Globorotalia birnageae* (N7–N8) was found.

Benthic Foraminifers

Benthic foraminifers from Hole 825A core-catcher samples are characterized by poor preservation and calcite overgrowths. Samples examined from Hole 825A contain abundant shallow-water contaminants, such as *Amphistegina* spp., *Asterigerina* spp., *Buliminella elegantissima*, *Cibicides lobatulus*, *Discorbinella* spp., *Discorbis* spp., *Elphidium* spp., and *Planorbulina* spp. *In-situ* benthic foraminifers include the upper-to-middle bathyal (200–1000 m) species association of *Cibicidoides mundulus*, *Cibicidoides pachyderma*, *Globocas-*

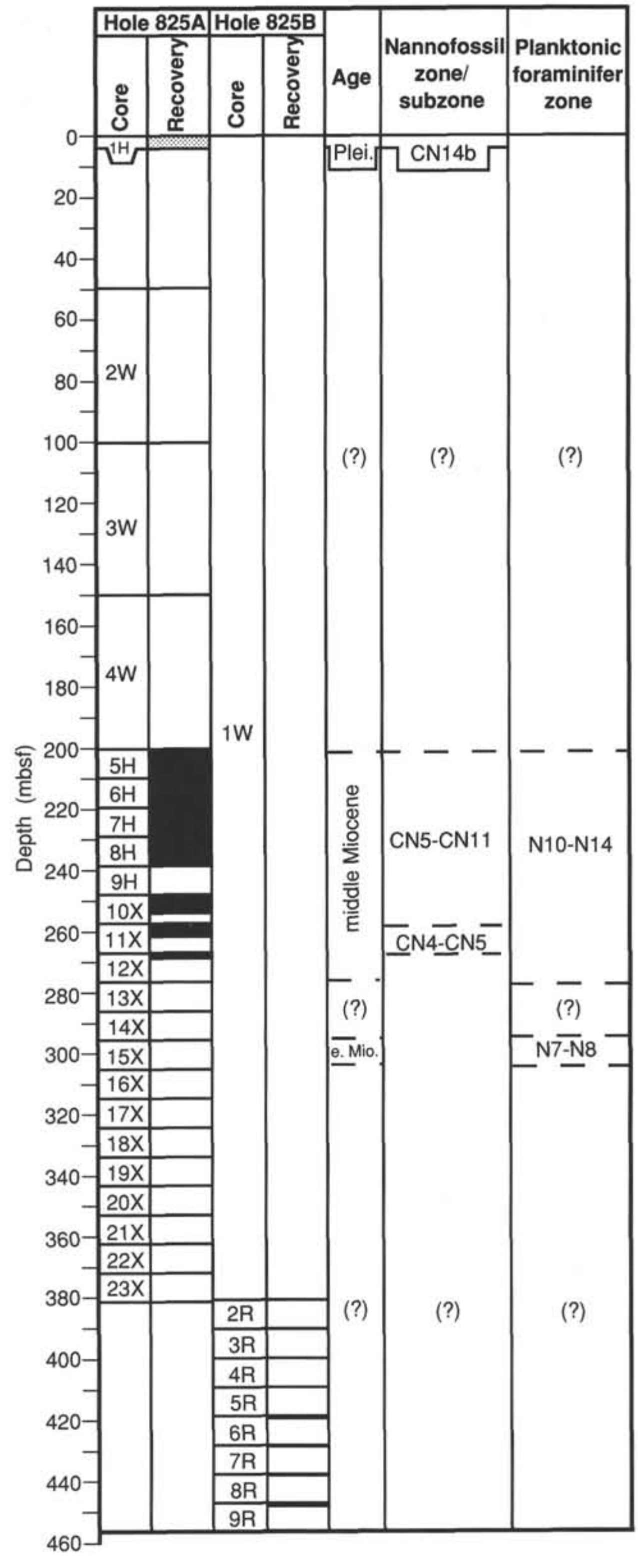

Figure 20. Summary of planktonic microfossil data from Site 825.

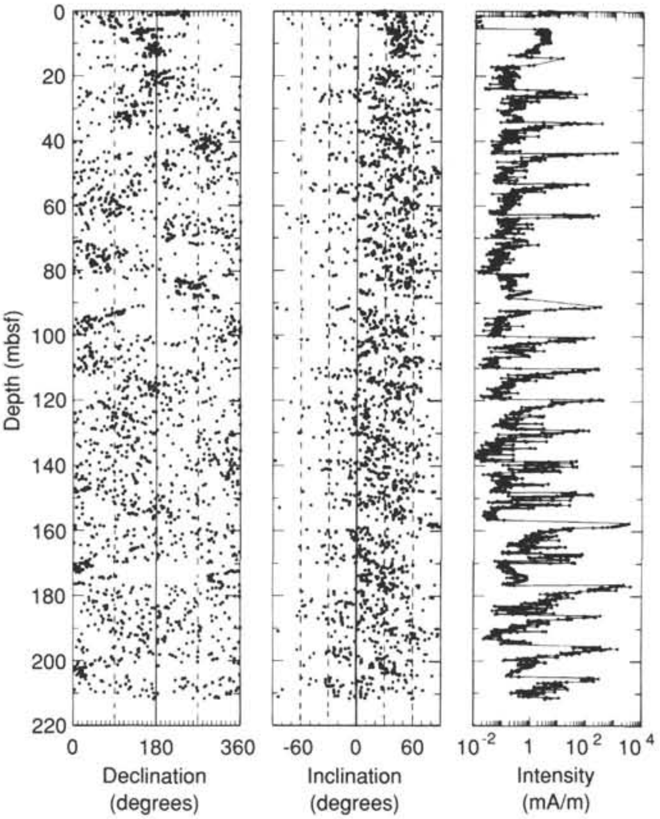

Figure 21. Depth profiles of Hole 811A showing declination, inclination, and intensity at AF 15-mT level. Note the strong intensity excursion at regularly spaced depth intervals. This intensity spike is attributed to intraliner contamination with metallic debris from the drill pipe. Contaminated zones show scattered normal and reverse inclinations consistent with loose magnetic grains in the annular space between the sediment and core liner.

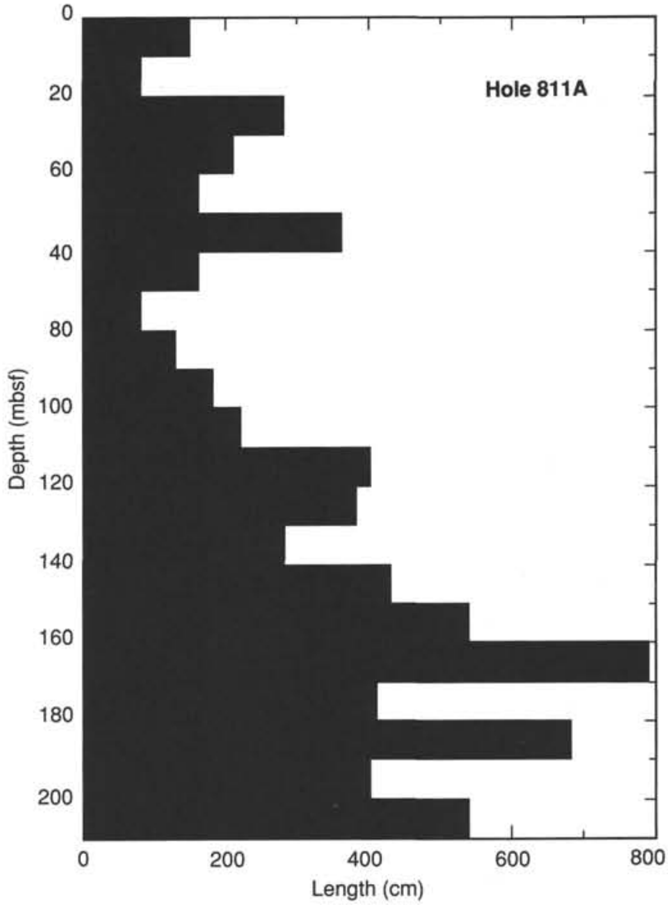

Figure 22. Summary of core contamination as determined from zones of high NRM intensity (> 5 mA/m) plotted as total length per 10-m interval below seafloor in Hole 811A. Note the general trend of increasing contamination with depth, perhaps as additional lengths of pipe were added to the drill string.

sidulina subglobosa, *Laticarinina pauperata*, *Rectuvigerina striata*, *Sigmoilopsis schlumbergeri*, *Uvigerina hispida*, and *Uvigerina proboscidea* (van Morkhoven et al., 1986). Samples in and below 133-825A-12R-CC contained no depth-diagnostic species.

Larger Benthic Foraminifers

Larger benthic foraminifers occur in all cores of Site 825. The middle Miocene interval is characterized by the occurrence of frequent *Nephrolepidina*, rare-to-frequent *Cycloclypeus* and rare to frequent *Operculina*. In addition, Sample 133-825A-12X-CC contains abundant *Miogypsina*.

In Hole 825B, frequent-to-abundant operculinid foraminifers occur, clearly dominating the larger benthic foraminifer associations. A further interpretation of this interval will rely on shore-based thin-section analysis.

SITE 811 PALEOMAGNETISM

Shipboard paleomagnetic measurements conducted at Site 811 failed to resolve magnetic polarity reversals that could be correlated to the geomagnetic polarity time scale (GPTS). The establishment of a magnetostratigraphic pattern correlative with the GPTS was hindered by a combination of core disturbance, downcore contamination with drill-string rust (?) particles, and perhaps a soft, viscous drill-string magnetization. Physical disturbance resulting from drilling and a high sediment-water content precluded whole-core measurements in several of the upper core sections (e.g., Sections 2 through 7 of Core 133-811-1H-1). The split cores showed evidence of fluidized sediment flow between the round sediment core and the plastic liner. This intraliner annular flow was also suspected as having contributed to downcore contamination from metallic particles. An inner-liner contamination was suggested by the intensity spikes (often >50 mA/m and sometimes >300 mA/m) near the top of each core section (Fig. 21). These spikes decrease uniformly downward for 2 m below the core top, but in some cases, they extend down more than 3 m. Whole-core alternating-field (AF) demagnetization at 15 mT had no effect on the high-intensity spikes. Therefore, we suspect that the high-coercivity phase originated from rust(?) particles inside the drill stem that became dislodged during core retrieval and drilling and fell into the bottom of the hole. The contamination recorded in the intensity logs appears to become progressively worse downward. Vertical plots of the cumulative length of the contaminated interval (marked by >5 mA/m intensity at NRM and AF 15 mT levels) are shown in Figure 22. The "rust" problem may have been significantly greater at this first site because the drill casing had not been used for several weeks (or months) before being used at this site. Finally, we suspect that the section is overprinted with a drill-string (viscous) magnetization. Plotted vs. depth, the inclination angles nearly always (excluding the rust-contaminated zones) exhibit a steep and upward direction (normal in

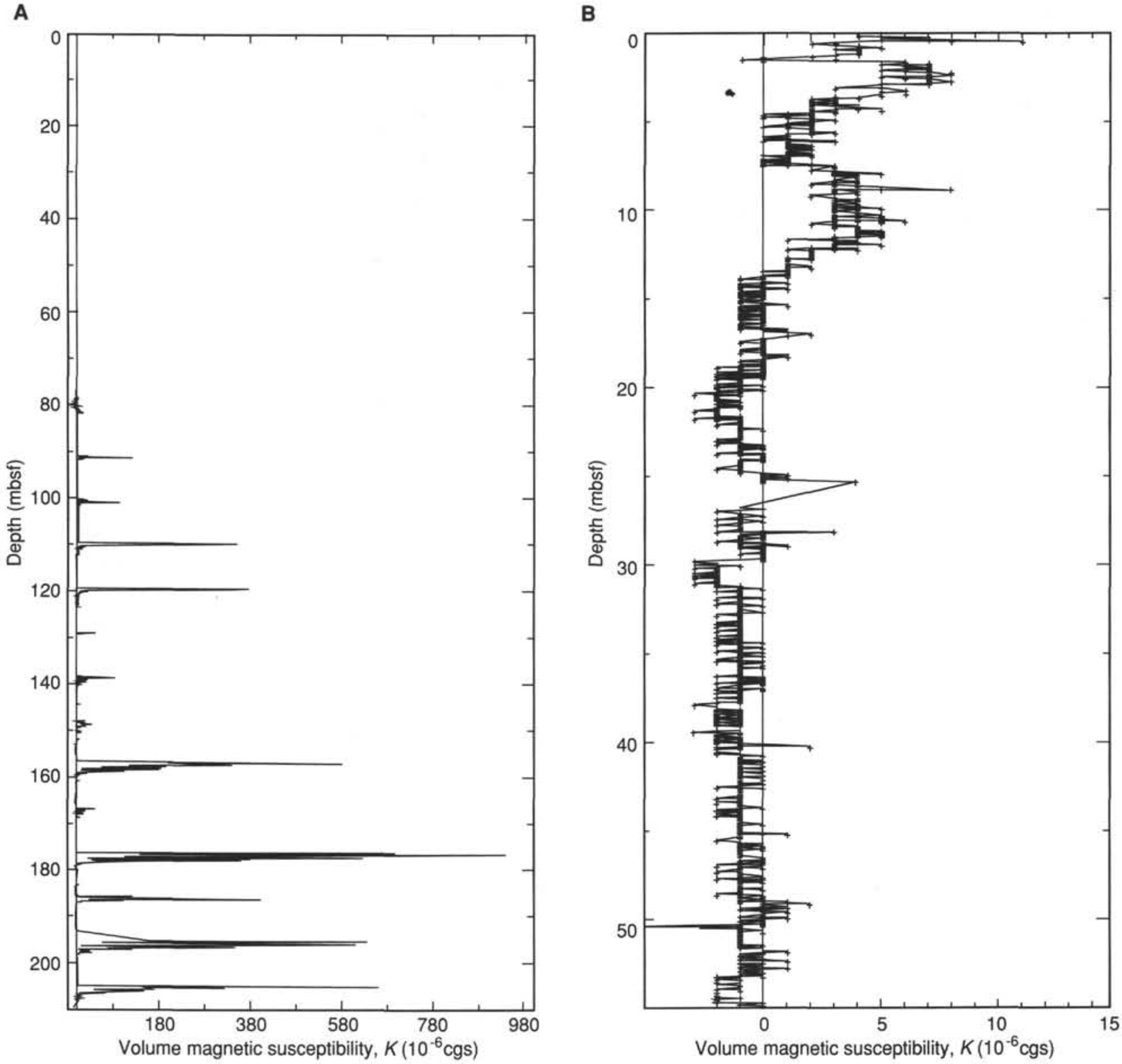

Figure 23. Summary of whole-core susceptibility values for part of (**A**) Hole 811A and (**B**) the upper 55 m of Hole 811C. The strong susceptibility excursions in the lower part of the hole correlate with zones of metallic (rust?) contamination seen in the whole-core magnetic intensity record. The low baseline susceptibility suggests that significant quantities of magnetite are absent from these cores, except in the uppermost 15 m, where a slight positive susceptibility occurs.

the Southern Hemisphere and plotted as positive during Leg 133). This overprint dominates the NRM directions, but is considerably "softer" relative to the rust-contaminated zones and starts to respond to AF demagnetization at 15 mT. A higher AF demagnetization level will thus be used during shore-based studies to remove completely this overprint and to determine if a reliable remanence direction is present.

Cores 133-811A-1H to -23H were measured for susceptibility using the pass-through "loop" sensor of the shipboard Bartington susceptibility bridge before they were split. The automated susceptibility system measured the recovered core every 10 cm down to 205 mbsf, except for Cores 133-811A-1H through -10H because the system was temporarily inoperative. The susceptibility record from Hole 811C (Cores 133-811C-1H to -6H, 0–55.2 mbsf) partially fills in this missing interval. This upper part of the section is characterized by a slightly positive susceptibility from 0 to 12.5 mbsf (Fig. 23). This upper zone may reflect either a change in the magnetic mineral influx (detrital or biogenic) or a progressive diagenetic destruction of the ferrimagnetic grains. Below 12.5 mbsf, the susceptibility is generally less than zero, indicating an absence of ferrimagnetic grains (mainly magnetite).

The volume susceptibility log (Fig. 23) generally is low downcore, except for strong peaks that are correlative with the pervasive core-top contamination zones. Thus, a low susceptibility suggests that relatively little magnetite is present in the sediments. This low susceptibility value is consistent with the highly oxidized nature of the pelagic ooze, which would tend to destroy any original biogenic or detrital magnetite grains.

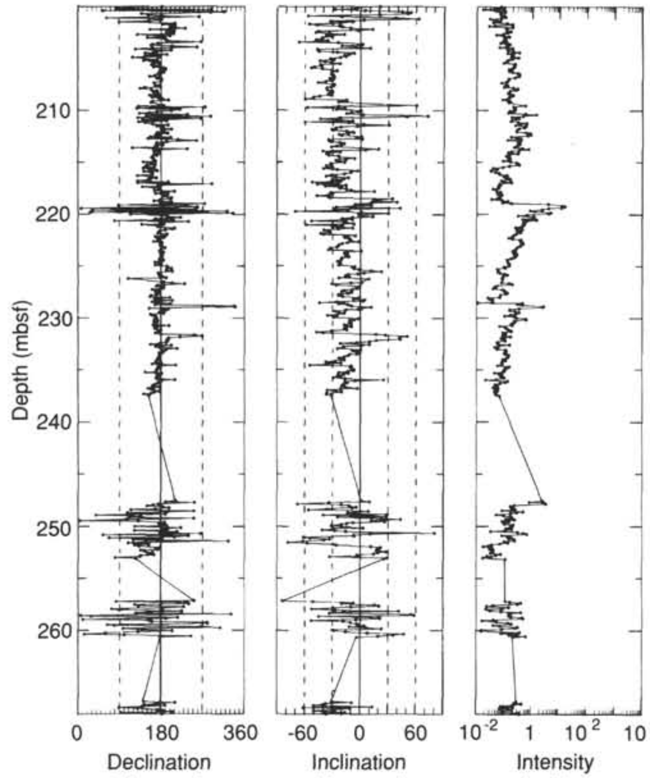

Figure 24. Paleomagnetic data from Hole 825A showing a predominantly reversed polarity.

SITE 825 PALEOMAGNETISM

From Hole 825A (a reoccupation of Site 811), we recovered seven cores between 219 and 276 mbsf that were analyzed using the cryogenic magnetometer. These cores were measured for NRM and remeasured after AF demagnetization at 15 mT. The section between 219 and 238 mbsf had a reversed polarity at the NRM and AF measurement steps, although the inclination record contains considerable scatter (Fig. 24). Magnetic intensity at NRM is between 0.1 and 1 mA/m and between 0.06 and 0.5 mA/m after AF demagnetization. Several large intensity excursions are present at some of the core tops, suggesting a contamination component that contributed to the remanence.

The reversed component could not be correlated with the GPTS given the limited recovery and the absence of refined biostratigraphy within the middle Miocene section. The lower three cores (133-825A-10X to 12X) contained scattered inclinations, thus an uncertain polarity.

SITE 811 SEDIMENTATION RATES

Sediment accumulation for Site 811 is represented in the age-depth plot in Figure 25. All biohorizons that are internally consistent (occurring in the recognized order of biohorizon succession) were used in the plot. All were derived from calcareous nannofossils and planktonic foraminifers. The error bar on the depth axis represents sample spacing. Highest occurrences are plotted midway between the highest observed occurrence and the next superjacent sample in which the species was not recorded; lowest occurrences are plotted midway between the lowest sample in which the species was recorded and the next subjacent sample in which the species was not recorded. With few exceptions, the ages assigned to the various biohorizons were taken from Berggren et al. (1985).

The sample spacing of one sample per core allows for only a general interpretation of sedimentation rates. This sample spacing does not allow one to identify hiatuses, although some may be found in this section. The sedimentation rate was approximately 3 cm/k.y. from 20 to 80 mbsf (much of the Pliocene). The lowermost Pliocene section (90–120 mbsf) has a sedimentation rate of about 1.5 cm/k.y. The section from approximately 180 to 270 mbsf (lower to lower middle Miocene) has a sedimentation rate of about 2 cm/k.y.

It is instructive at this point to consider the changes in the proportion of pelagic and detrital influx to the sediment (Fig. 25). While coccoliths constitute only 20% to 30% of the sediment in the Pleistocene and upper Pliocene sequences, they may make up in excess of 70% of the sediment in the lower Pliocene and upper part of the upper Miocene record. From the lower part of the upper Miocene downward, nannofossils are a few percent to less than 1% of the sediment.

When the sedimentation rate is assessed alongside an abundance plot of pelagic influx to the sediment, one notices that dilution by nonpelagic carbonates–the only other component in the sediment–may have increased sedimentation rate over the upper Pliocene interval to perhaps twice the rate normal for the area. However, this did not greatly alter sediment accumulation in the lowermost upper Miocene and middle Miocene sections from the pelagic carbonate accumulation rate characteristic for this area. Given that the benthic foraminifers do not indicate a significant change of water depth at this time, the high upper Pliocene sediment accumulation may be interpreted as having been enhanced by bank-derived detritus. For the lowermost upper Miocene and the middle Miocene, a reasonable explanation is that the detrital carbonate that makes up the bulk of the sediment may be only the residue of bank-derived carbonate detritus that was periodically swept through this area, which carried away with it the pelagic sediment that had accumulated at Site 811 and left behind mainly much coarser detritus.

SITE 811 INORGANIC GEOCHEMISTRY

Interstitial Waters

Interstitial-water samples were taken from the first 11 cores of Hole 811A and every third core thereafter down to Core 133-811A-20H. One sample was also taken in Hole 811B at Core 133-811B-8V. Squeezed samples were analyzed according to procedures outlined in the "Explanatory Notes" chapter (this volume).

Calcium, Magnesium, and Strontium

Concentrations of calcium and strontium increase rapidly within the first two to three cores of Hole 811A (Table 3 and Fig. 26) to concentrations of 16.7 mM and 240 μM, respectively. The concentration of these elements remains at these values throughout the remainder of Hole 811A. Magnesium concentrations decrease slightly from their surface-water values to between 48 and 50 mM.

Alkalinity, Sulfate, pH, and Phosphate

The highest alkalinity at this site is exhibited in Core 133-811A-1H. The value of 3.11 mM in Core 133-811A-1H is accompanied by a small reduction in sulfate from 29.1 to 28.8 mM (Table 3 and Fig. 26). Concentrations of phosphate remained below detection throughout Holes 811A and 811B. The apparent absence of sulfate reduction, the absence of phosphate, and the low alkalinity reflect the low concentration

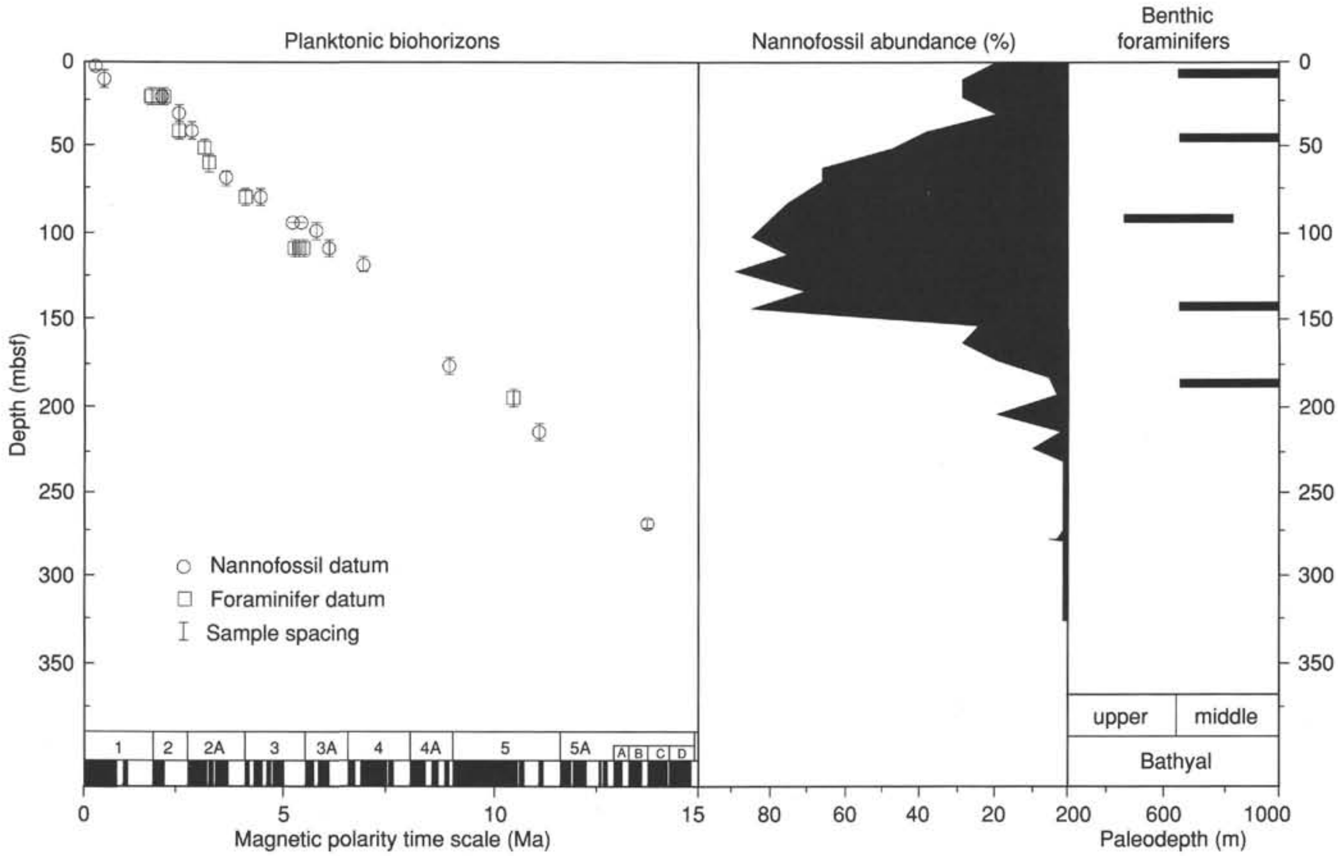

Figure 25. Age vs. depth plot for Hole 811A. All biohorizons are derived from calcareous nannofossils and planktonic foraminifers. Benthic foraminifer paleobathymetric estimates are from selected qualitative core-catcher samples.

Table 3. Interstitial-water data, Site 811.

Core, section, interval (cm)	Depth (mbsf)	pH	Alk. (mM)	Sal. (g/kg)	Cl^- (mM)	Mg^{2+} (mM)	Ca^{2+} (mM)	SO_4^{2-} (mM)	Si (μM)	Sr^{2+} (μM)
Surface seawater		8.34	2.789	35.5	533	53.64	10.40	29.09		88
133-811A-										
1H-3, 145–150	4.45	7.57	3.106	36.0	543	49.80	13.80	28.80	77	149
2H-5, 145–150	12.95	7.13	3.104	36.3	551	47.68	16.06	28.46	88	167
3H-5, 145–150	22.45	7.31	2.920	35.9	555	48.78	16.32	28.25	97	240
4H-4, 145–150	30.45	7.19	2.673	36.0	555	48.38	16.43	29.21	102	119
5H-4, 145–150	39.95	7.14	2.547	36.0	557	48.40	16.42	28.86	106	114
6H-5, 145–150	50.95	7.10	2.546	36.1	552	48.42	16.56	29.42	196	115
7H-5, 145–150	60.45	7.09	2.489	36.0	556	48.72	16.26	28.92	124	117
8H-4, 145–150	69.95	7.19	2.549	36.0	551	49.07	16.70	29.71	117	114
9H-4, 145–150	79.45	7.13	2.549	36.0	557	48.82	16.56	29.51	133	115
10H-4, 145–150	87.45	7.14	2.531	35.9	555	48.01	16.57	29.38	124	112
11H-4, 145–150	98.45	7.12	2.605	36.0	557	48.66	16.24	29.50	140	119
14H-4, 145–150	126.95	7.36	2.483	35.8	555	49.09	16.38	29.20	305	99
17H-4, 145–150	153.95	7.40	2.395	36.0	542	50.39	16.40	29.72	238	112
20H-4, 145–150	183.95	7.43	2.505	36.0	547	48.18	16.66	29.27	162	111
133-811B-										
8V-2, 145–150	354.05	7.45	3.219	36.0	557	48.88	16.71			

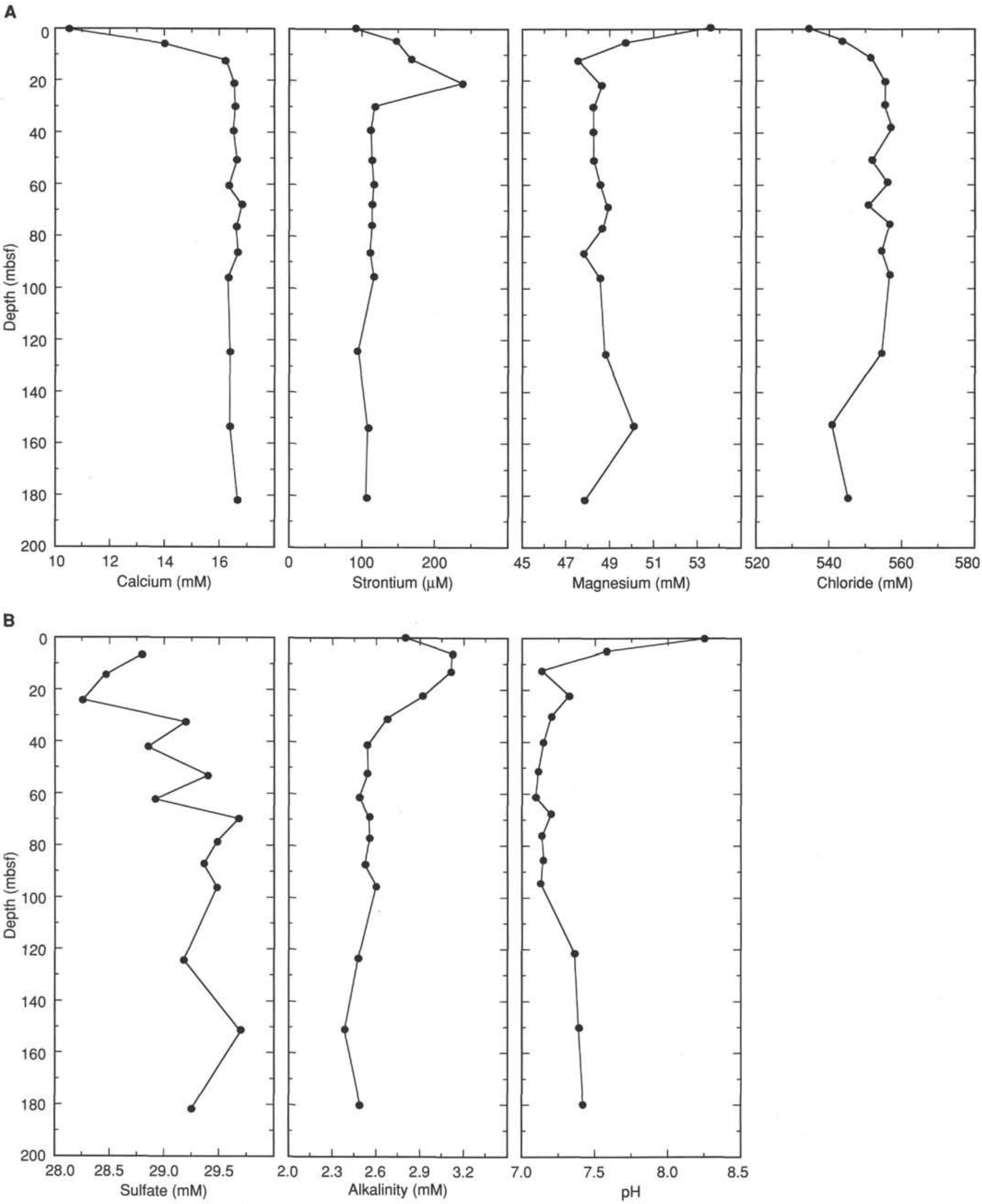

Figure 26. **A.** Concentrations of Ca^{2+}, Sr^{2+}, Mg^{2+}, and Cl^- as a function of depth in Site 811. **B.** Concentrations of SO_4^{2-}, alkalinity, and pH as a function of depth at Site 811.

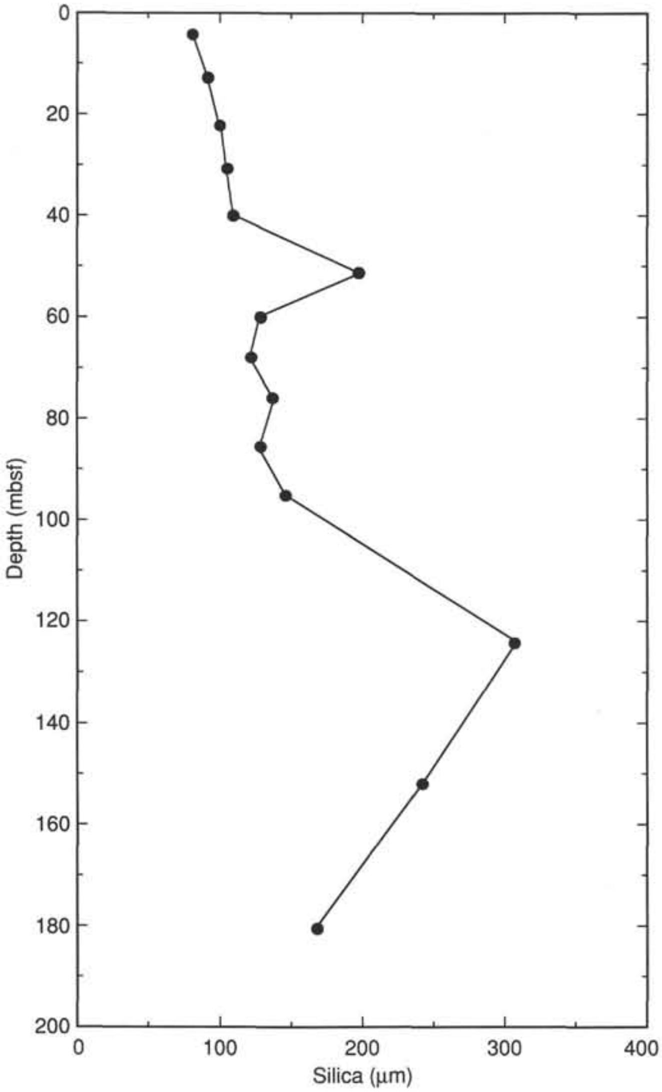

Figure 27. Concentrations of Si as a function of depth at Site 811.

Table 4. Mineralogy data, Site 811.

Core, section, interval (cm)	Depth (mbsf)	Calcite (%)	Aragonite (%)	Quartz (%)	Dolomite (%)
133-811A-					
1H-1, 97–98	0.97	90.0	7.5	2.4	0.0
1H-2, 86–87	2.36	83.4	15.4	0.4	0.8
1H-3, 85–86	3.85	90.6	1.7	5.8	1.9
1H-3, 145–150	4.45	61.1	36.7	1.5	0.7
1H-4, 26–27	4.76	56.9	37.6	5.5	0.0
2H-1, 67–68	5.22	97.1	0.0	2.9	0.0
2H-2, 67–68	7.67	100.0	0.0	0.0	0.0
2H-3, 67–68	9.17	98.3	0.0	0.5	1.2
2H-5, 145–150	12.95	100.0	0.0	0.0	0.0
3H-1, 102–103	16.02	94.0	0.0	6.0	0.0
3H-4, 66–67	20.16	97.3	0.0	2.7	0.0
3H-5, 145–150	22.45	100.0	0.0	0.0	0.0
4H-1, 67–68	25.17	99.9	0.0	0.0	0.1
4H-3, 67–68	28.17	98.5	0.0	0.0	1.5
4H-4, 145–150	30.45	96.4	0.0	0.9	2.7
5H-1, 137–138	35.37	98.3	0.0	0.0	1.7
5H-2, 140–141	36.9	96.0	0.0	2.3	1.7
5H-3, 127–128	38.77	99.9	0.0	0.0	0.1
5H-4, 145–150	39.95	98.1	0.0	0.0	1.9
6H-2, 133–134	46.33	97.2	0.0	2.6	0.1
6H-5, 145–150	50.95	91.7	0.0	4.7	3.5
7H-5, 145–150	60.45	97.6	0.0	0.0	2.4
8H-1, 136–137	63.86	98.6	0.0	0.0	1.4
8H-5, 145–150	69.95	96.3	1.7	0.0	2.0
9H-5, 145–150	79.45	96.8	0.0	1.7	1.4
10H-4, 145–150	87.45	98.8	0.0	0.0	1.2
11H-5, 145–150	98.45	100.0	0.0	0.0	0.0
14H-5, 145–150	126.95	98.6	0.0	0.0	1.4
17H-4, 145–150	153.95	99.0	0.0	1.0	0.0
18H-2, 58–59	159.58	98.7	0.0	0.9	0.4
18H-2, 98–99	159.98	98.6	0.0	0.0	1.4
20H-5, 145–150	183.95	98.3	0.0	0.5	1.3
133-811B-					
15H-CC, 11–12	261.67	95.0	0.0	5.0	0.0
8V-2, 137–138	298.51	100.0	0.0	0.0	0.0
16X-2, 71–72	310.21	97.5	0.8	1.6	0.0
16X-5, 92–93	314.92	99.0	0.0	0.8	0.1
17X-1, 40–41	318.1	98.1	0.0	0.0	1.9
18X-1, 49–50	327.79	96.7	0.0	3.3	0.0
18X-1, 59–60	327.89	100.0	0.0	0.0	0.0
19X-1, 7–8	337.07	100.0	0.0	0.0	0.0
20X-2, 68–69	348.78	99.5	0.0	0.0	0.5
20X-5, 145–150	354.05	97.8	0.0	0.0	2.2
21H-1, 70–71	357	97.5	0.0	2.5	0.0

of organic material in these sediments (See "Organic Geochemistry" section, this chapter). The increase in alkalinity seen in Cores 133-811-1H and -2H is consistent with the dissolution of aragonite over this interval. As a consequence of the low concentration of phosphate, no measurement of ammonia was performed at Site 811.

Silica

Concentrations of silica increased to 305 μM by 300 mbsf (Fig. 27), reflecting the dissolution of biogenic silica and the small amount of detrital quartz present in the sediments.

Carbonate Content and X-Ray Mineralogy

Samples for X-ray diffraction (XRD) analyses were taken from the sediment squeezed for interstitial water (IW) and selected physical property (PP) samples. These samples were scanned between 20° and 45° 2θ (Cu K_a) to identify major mineral constituents and then were subjected to quantitative analysis, as outlined in the "Explanatory Notes" chapter (this volume).

Coulometric and XRD analyses indicate that the sediments of Site 811 are predominantly calcium carbonate (Tables 4 and 5, and Figs. 28 and 29). The carbonate content averages more than 95% throughout both Holes 811A and 811B (Table 5 and Fig. 29). Results of the quantitative analyses indicate that aragonite is absent below 10 mbsf, although traces of this mineral were detected to depths of 30 mbsf. Small concentrations of dolomite and quartz persist in certain units throughout the remainder of Hole 811A. The percentage of carbonate content (Fig. 29) shows distinct variations that correlate with the major sedimentological units recognizable in the core (See "Site 811 Lithostratigraphy" section, this chapter). Unit I (0–33.15 mbsf; Pleistocene to upper Pliocene) is characterized by carbonate contents of between 90% and 98%, with progressively higher concentrations toward the base of the unit. The bulk of the nonacid soluble fraction is composed of quartz. In comparison to other units at Site 811, Unit I possesses the lowest carbonate content. Unit II (upper Pliocene–upper Miocene), between 33.15 and 147.5 mbsf, has a relatively constant carbonate content of 94% and lower concentrations of quartz and dolomite, reflecting the absence of gravity flows that might contain detrital quartz. Unit III (upper Miocene to middle Miocene) has an average carbonate content of 97%, with little or no quartz or dolomite. Units IV and V are characterized by poor recovery, but generally trend to high carbonate contents toward the base of Unit V.

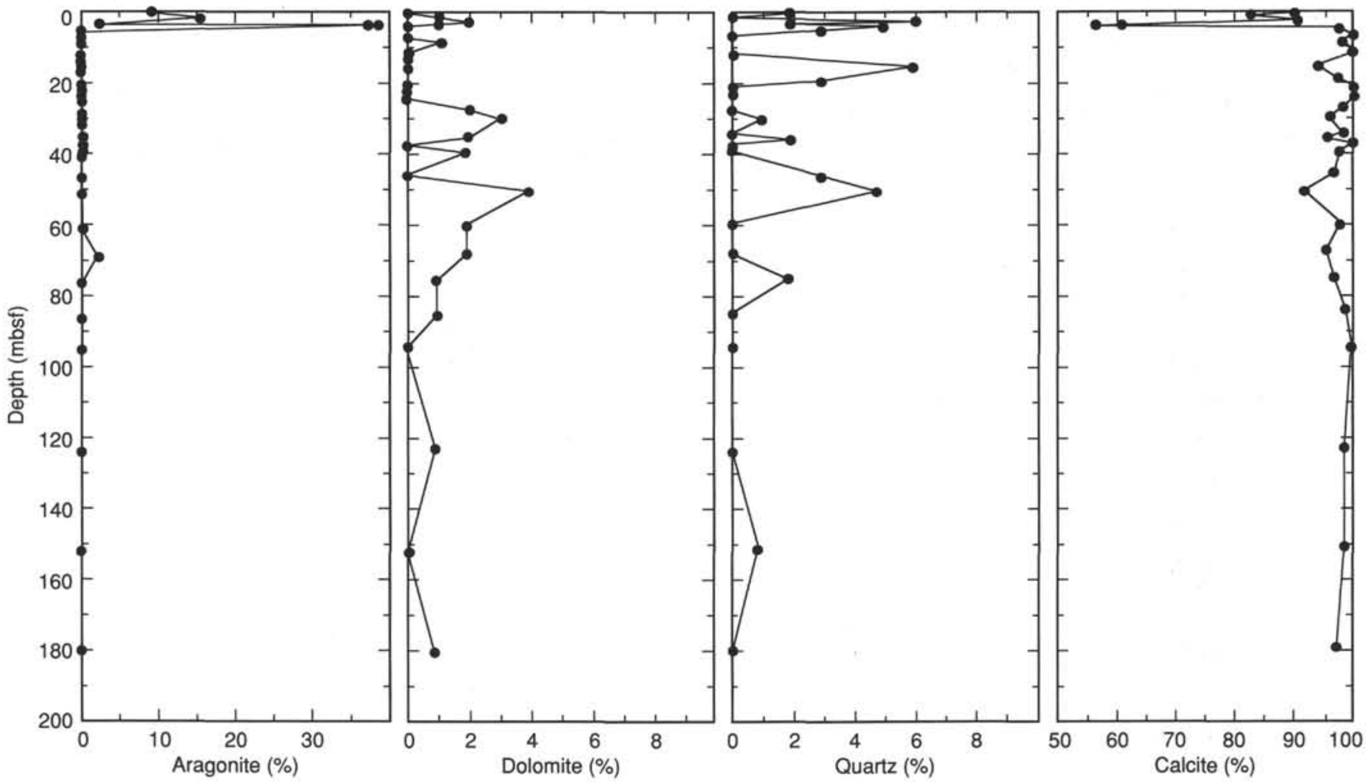

Figure 28. Percentage mineralogy as a function of depth for Site 811.

SITE 825 INORGANIC GEOCHEMISTRY

Interstitial Waters

Site 825 is a reoccupation of Site 811 and for this reason, data from this site have been plotted with data from Site 811 for comparison. Three samples were selected using the WSTP sampler, and three sections from Cores 133-825A-5H, -8H and -10X were squeezed. Samples were analyzed according to procedures outlined in the "Explanatory Notes" chapter (this volume), and data are presented in Table 6 and in Figure 30.

The concentrations of Ca^{2+}, Sr^{2+}, and Mg^{2+} are essentially identical to those from Site 811 (see "Site 811 Inorganic Geochemistry" section, this chapter). As postulated for Site 812 (see "Inorganic Geochemistry" section, "Site 812" chapter, this volume), the nature of the profiles at Sites 811/825 suggests that water moved out of the sediments. This interpretation gains further credence by the higher geothermal gradient at Site 825. The temperature gradient over the upper 150 mbsf was approximately 8°/100 m, compared with approximately 5°C/100 m at Sites 817, 822, and 823.

Carbonate Content and X-Ray Mineralogy

Two samples from Site 825 were analyzed using X-ray diffraction (133-825A-8H, 145–150 cm, and -10X, 145–150 cm). Both were composed of only low-Mg calcite (Table 7 and Fig. 31). The carbonate content of the sediments analyzed from Site 825 between 201 and 267.8 mbsf ranged from 95% to 100% $CaCO_3$. Although the absolute carbonate concentrations of the sediments appear to be slightly higher than at Site 811, a direct comparison with Site 811 is not feasible because the majority of the samples for carbonate analysis from Site 825 were recovered over a depth interval which had little or no recovery in Site 811.

SITE 811 ORGANIC GEOCHEMISTRY

In addition to safety monitoring for hydrocarbons, the main purpose of the shipboard organic geochemistry studies at Site 811 was to assess the amount and type of organic matter preserved in the Holocene to upper Oligocene sediments of the Queensland Plateau.

We determined the amount of total inorganic carbon for 144 samples and also analyzed for physical properties, using a Coulometrics 5011 coulometer equipped with a System 140 carbonate/carbon analyzer. We determined the total nitrogen, sulfur, carbon, and organic carbon contents of 29 additional samples collected for chromatographic analyses of volatile hydrocarbons (headspace samples) using a NA 1500 Carlo Erba NCS analyzer. Detailed descriptions of these methods are outlined in our "Explanatory Notes" chapter (this volume).

Volatile Hydrocarbons

Light hydrocarbon gases (C_1–C_3) in sediments were analyzed routinely as part of the ODP safety and pollution-prevention monitoring program, using the headspace technique and the Carle gas chromatograph. The results of 29 analyses from Holes 811A and 811B are presented in Table 8.

The sediments at Site 811 contained low concentrations of hydrocarbon gases. The concentrations of methane in the headspace gas ranged from 2 to 5 ppm, while only traces of ethane (in Section 133-811B-18X-2) were detected.

Organic Carbon Contents

The total organic carbon (TOC) contents recorded in Holes 811A and 811B are presented in Table 9. We observed low to very low TOC values in the carbonate-rich sediments encountered at Site 811. These values ranged from 0.1% to 0.45%

Table 5. Carbonate content data, Site 811.

Core, section, interval (cm)	Depth (mbsf)	Carbon (%)	$CaCO_3$ (%)
133-811A-			
1H-1, 97–98	0.97	10.8	89.7
1H-2, 86–87	2.36	10.8	89.7
1H-3, 85–86	3.85	10.8	89.7
1H-4, 26–27	4.76	11.3	94.3
2H-1, 67–68	6.17	11.4	95.0
2H-2, 67–68	7.67	11.0	91.8
2H-3, 67–68	9.17	11.5	95.4
2H-4, 67–68	10.67	11.2	93.4
2H-5, 67–68	12.17	11.4	94.7
2H-6, 67–68	13.67	10.8	90.0
3H-1, 102–104	16.02	11.3	94.1
3H-2, 66–68	17.16	11.6	96.7
3H-3, 66–68	18.66	11.9	99.0
3H-4, 66–68	20.16	11.9	98.9
3H-5, 66–68	21.66	11.8	98.6
3H-6, 66–68	23.16	11.8	98.5
4H-1, 67–69	25.17	11.5	96.0
4H-2, 67–69	26.67	11.3	93.8
4H-3, 67–69	28.17	11.4	94.9
4H-4, 67–69	29.67	11.4	95.0
4H-5, 67–69	31.17	11.2	93.1
4H-6, 67–69	32.67	11.8	98.1
5H-1, 137–140	35.37	11.5	95.7
5H-2, 140–142	36.90	11.4	95.1
5H-3, 127–130	38.27	11.8	97.9
5H-4, 130–132	39.80	11.6	96.7
5H-5, 130–133	41.30	11.3	94.0
5H-6, 130–133	42.80	11.3	94.4
6H-1, 133–138	44.83	11.3	94.0
6H-2, 133–138	46.28	11.6	96.7
6H-3, 134–137	47.79	11.3	94.5
6H-4, 134–138	49.29	11.4	95.0
6H-5, 135–138	50.80	11.3	94.0
6H-6, 134–137	52.29	11.2	93.0
7H-1, 137–139	54.37	11.3	94.1
7H-2, 135–138	55.85	11.2	93.5
7H-3, 136–138	57.36	11.4	95.1
7H-4, 136–138	58.86	11.4	94.9
7H-5, 99–101	59.99	11.4	95.1
7H-6, 133–135	61.83	11.5	95.6
8H-1, 95–97	63.45	11.5	95.5
8H-2, 95–97	64.95	11.2	93.5
8H-3, 95–97	66.45	11.5	95.7
8H-4, 76–78	67.76	11.3	94.3
8H-5, 107–109	69.57	11.6	96.3
8H-6, 105–107	71.05	11.6	96.5
8H-7, 34–36	71.84	11.6	96.2
9H-1, 101–104	73.01	11.4	95.0
9H-2, 101–104	74.51	11.4	94.5
9H-3, 101–104	76.01	11.4	95.0
9H-4, 101–104	77.51	11.4	95.0
9H-5, 101–104	79.01	11.3	94.3
9H-6, 101–104	80.51	11.5	95.7
10H-1, 81–84	82.31	11.3	94.2
10H-2, 81–84	83.81	11.4	95.2
10H-3, 67–70	85.17	11.3	94.4
10H-4, 77–80	86.77	11.4	95.2
10H-5, 77–80	88.27	11.3	93.7
11H-1, 104–107	92.04	11.6	96.4
11H-2, 104–107	93.54	11.5	95.4
11H-3, 105–108	95.05	11.4	95.0
11H-4, 105–108	96.55	11.5	95.4
11H-5, 105–108	98.05	11.4	94.8
11H-6, 105–108	99.55	11.4	95.1
12H-1, 82–85	101.32	11.4	95.0
12H-2, 82–85	102.82	11.5	95.8
12H-3, 82–85	104.32	11.6	96.5
12H-4, 96–99	105.96	11.6	96.6
12H-5, 102–105	107.52	11.7	97.2
12H-6, 102–105	109.02	11.2	93.3
13H-1, 101–104	111.01	11.4	94.7
13H-2, 101–104	112.51	11.5	95.4
13H-3, 101–104	114.01	11.6	96.2
13H-4, 101–104	115.51	11.6	96.4
13H-5, 101–104	117.01	11.4	95.0

Table 5 (continued).

Core, section, interval (cm)	Depth (mbsf)	Carbon (%)	$CaCO_3$ (%)
13H-6, 101–104	118.51	11.5	96.1
14H-1, 101–104	120.51	11.5	96.1
14H-2, 101–104	122.01	11.7	97.0
14H-3, 101–104	123.51	11.5	95.7
14H-4, 101–104	125.01	11.5	95.8
14H-5, 101–104	126.51	11.5	95.4
14H-6, 101–104	128.01	11.7	97.1
15H-1, 100–102	130.00	11.5	95.9
15H-2, 100–102	131.50	11.5	95.5
15H-3, 100–102	133.00	11.6	96.2
15H-4, 100–102	134.50	11.6	96.4
15H-5, 100–102	136.00	11.6	96.3
15H-6, 100–102	137.50	11.6	96.5
16X-1, 101–103	139.51	11.5	96.0
16X-2, 101–103	141.01	11.5	95.5
16X-3, 101–103	142.51	11.6	96.6
16X-4, 101–103	144.01	11.6	96.7
16X-5, 101–103	145.51	11.6	96.3
17X-1, 101–101	149.00	11.5	95.5
17X-2, 101–101	150.50	11.5	96.1
17X-3, 101–101	152.00	11.4	95.2
17X-4, 101–101	153.50	11.7	97.1
17X-5, 101–101	155.00	11.7	97.4
17X-6, 101–101	156.50	11.6	97.0
18X-1, 101–104	158.51	11.7	97.4
18X-2, 101–104	160.01	11.7	97.3
18X-3, 101–104	161.51	11.7	97.6
18X-4, 101–104	163.01	11.7	97.8
18X-5, 101–104	164.51	11.7	97.3
18X-6, 101–104	166.01	11.8	98.0
19X-1, 137–140	168.37	11.7	97.2
19X-2, 137–140	169.87	11.7	97.1
19X-3, 137–140	171.37	11.7	97.0
19X-4, 137–140	172.87	11.6	96.9
19X-5, 137–140	174.37	11.4	94.6
19X-6, 137–140	175.87	11.7	97.5
20X-2, 130–133	179.30	11.8	98.4
20X-3, 130–133	180.80	11.9	98.9
20X-4, 130–133	182.30	11.9	98.7
20X-5, 130–133	183.80	11.8	98.6
20X-6, 130–133	185.30	11.7	97.7
21X-1, 96–99	186.96	11.7	97.8
21X-2, 96–99	188.46	11.7	97.4
21X-3, 96–99	189.96	11.7	97.3
21X-4, 96–99	191.21	11.7	97.3
21X-5, 96–99	192.71	11.7	97.3
21X-6, 94–97	194.19	11.7	97.5
22X-1, 125–127	196.75	11.3	94.0
22X-2, 125–127	198.25	11.6	96.4
22X-3, 125–127	199.75	11.6	96.2
22X-5, 125–127	202.75	11.6	96.6
22X-6, 125–127	204.25	11.8	98.1
23X-1, 131–133	206.31	11.7	97.2
23X-2, 131–133	207.77	11.8	97.9
23X-3, 131–133	209.27	11.8	98.0
23X-4, 80–82	210.26	11.8	98.1
23X-5, 73–75	211.52	11.7	97.7
133-811B-			
8V-1, 136–139	260.16	11.8	98.5
8V-1, 137–139	261.67	11.8	98.4
8V-3, 137–139	263.17	11.6	96.7
15X, 11–12	298.51	11.8	98.4
16X-1, 92–93	308.92	11.8	98.6
16X-2, 71–72	310.21	11.9	99.0
17X-1, 40–41	318.10	11.8	98.5
18X-1, 59–60	327.89	11.9	98.9
18X-2, 68–69	329.05	11.8	98.5
19X-1, 7–8	337.07	11.9	99.3
20X-1, 49–50	347.09	11.9	99.0
21X-1, 70–71	357.00	11.9	99.5

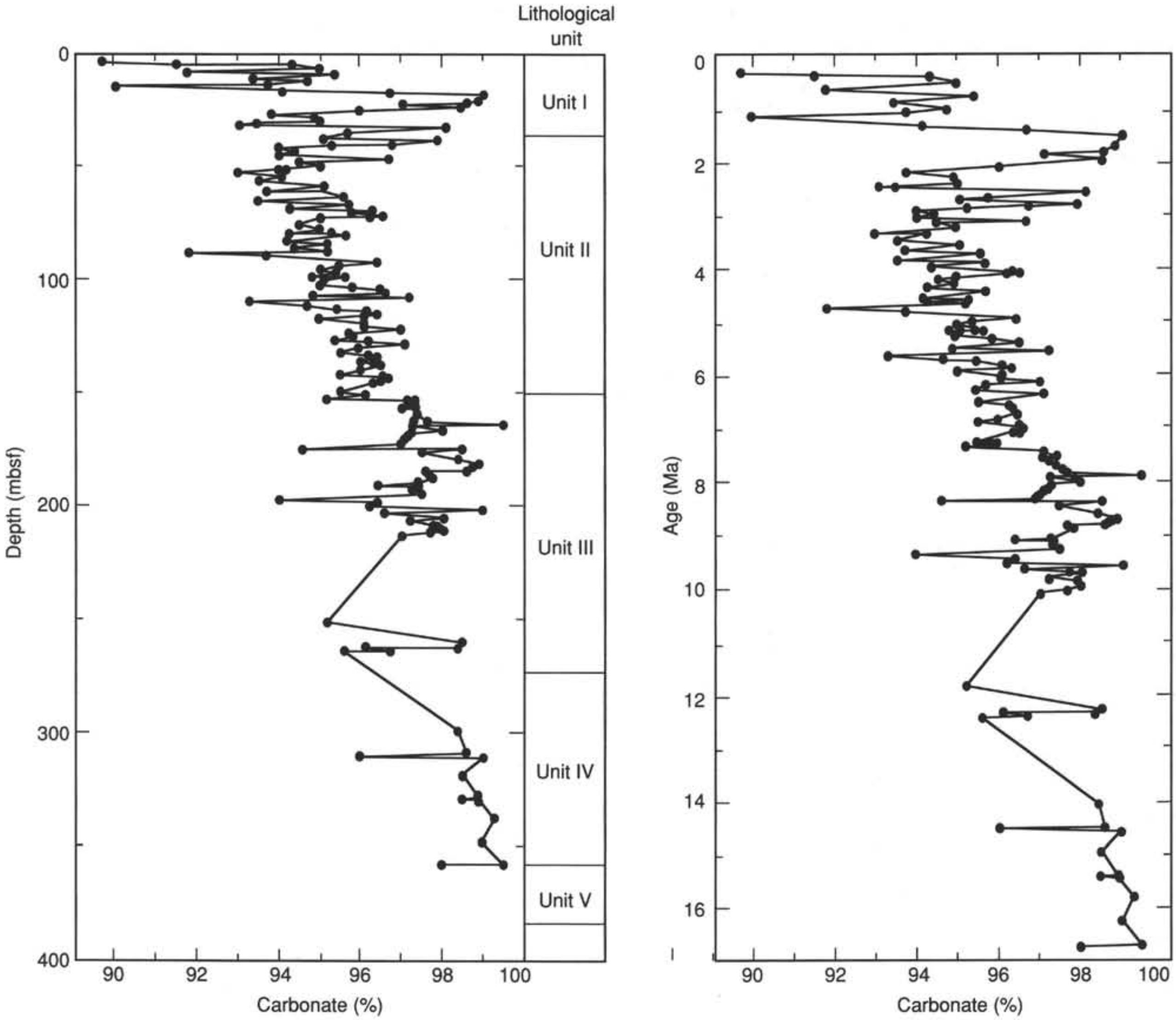

Figure 29. Carbonate content for Site 811 as a function of depth and age.

Table 6. Interstitial-water chemistry data, Site 825.

Core, section, interval (cm)	Depth (mbsf)	pH	Alkalinity (mM)	Salinity (g/kg)	Cl^- (mM)	Mg^{2+} (mM)	Ca^{2+} (mM)	SO_4^{2-} (mM)	Sr^{2+} (μM)
Seawater		7.95	2.487	35.2	549.67	53.40	10.57	28.90	96
133-825A-									
2W-1, 0–7	50.00	7.65	2.593	36.0	560.29	48.14	16.68	30.16	115
3W-1, 0–7	100.00	7.43	2.818	36.0	558.36	48.33	16.65	30.17	116
4W-1, 0–7	150.00	7.63	2.634	35.8	556.43	48.35	16.63	30.27	118
5H-5, 145–150	207.45	7.44	2.591	35.8	561.26	47.82	16.68	29.22	113
8H-5, 140–150	235.95	7.44	2.300	36.0	561.26	48.02	16.57	30.16	110
10X-2, 140–150	250.45	7.45	2.950	35.8	561.26	48.45	16.54	30.38	111

(Fig. 32), while the total nitrogen and sulfur concentrations were below the detection limits of the NCS analyzer.

As a result of such low organic contents, we were unable to conduct detailed geochemical characterization of kerogen types using the Rock-Eval pyrolysis method, as originally planned.

SITE 825 ORGANIC GEOCHEMISTRY

Samples

Five samples were collected from Hole 825A at 10-m intervals over the depth range from 207 to 266 mbsf. The

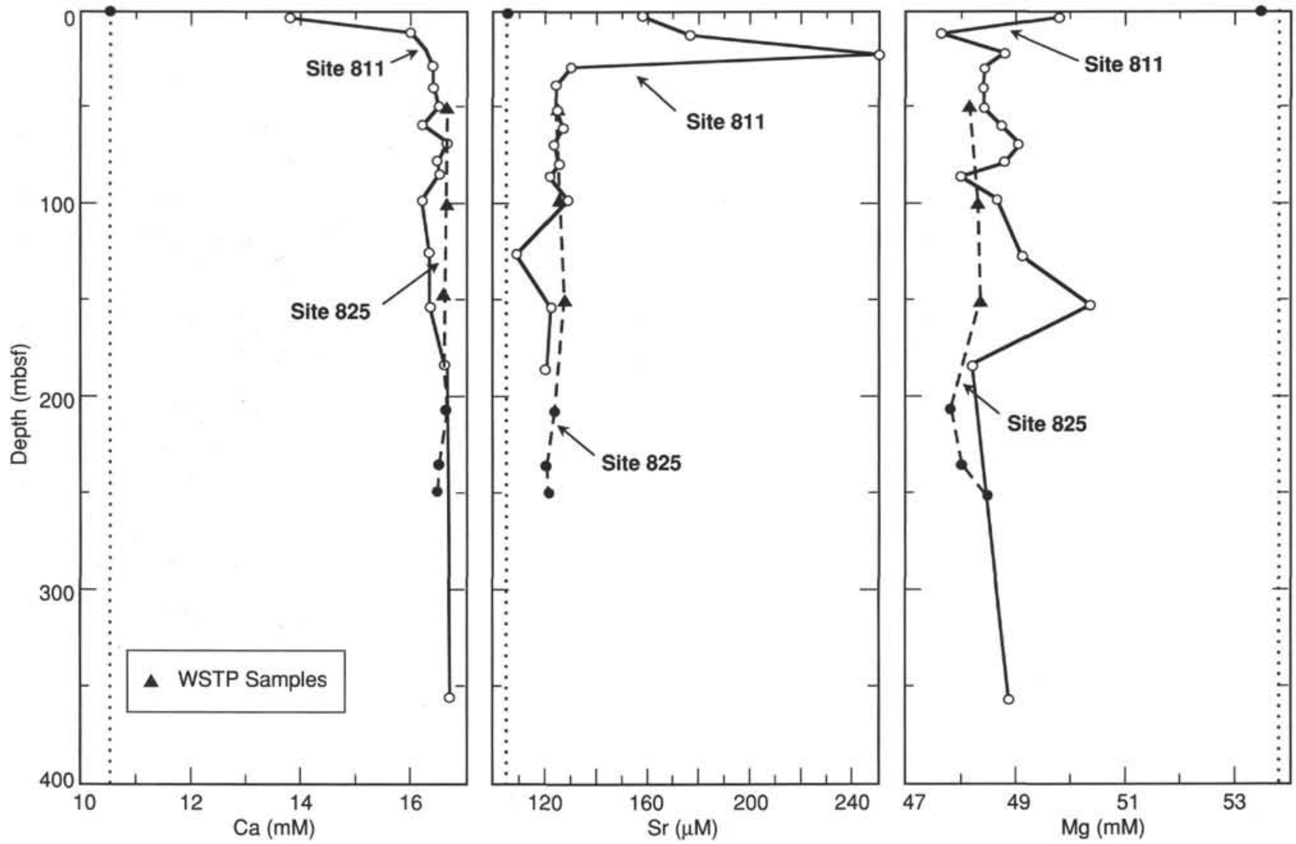

Figure 30. Comparison of data from Site 825 with data from Site 811. The WSTP samples are shown in the solid triangles. Data from these samples compare reasonably well with the squeezed data from both Sites 811 and 825. The dotted line indicates the composition of seawater.

sediments were analyzed for their composition of light hydrocarbons (C_1–C_3) using headspace analyses.

Seven samples were analyzed for total nitrogen, sulfur, and carbon, using a NA 1500 Carlo Erba NCS analyzer. Detailed descriptions of methods are outlined in the "Explanatory Notes" chapter (this volume).

Volatile Hydrocarbons

Hydrocarbon gases in sediments were analyzed as part of the ODP safety and pollution-prevention monitoring program, using the headspace technique and the Carle gas chromatograph (for determining C_1–C_3 concentrations). The results of five headspace analyses from Site 825 are presented in Table 10.

The sediments contained low concentrations of methane (2 ppm), which represented no safety and/or pollution hazards. Ethane and propane were not detected.

Organic Carbon Contents

The TOC contents, together with total nitrogen and sulfur concentrations recorded in Site 825, are presented in Table 11.

The amount of organic carbon was low in these carbonate-rich sediments, $\leq$ 0.27% TOC. The total nitrogen and sulfur concentrations were below the detection limits of the NCS analyzer.

As a consequence of the low organic contents, we were unable to conduct detailed geochemical characterization of kerogen types using the Rock-Eval pyrolysis method, as originally planned. More detailed shore-based studies (elemental analysis and optical investigations of extracted kerogens) will permit characterization of the organic matter preserved in the sediments encountered at Site 825.

SITE 811 PHYSICAL PROPERTIES

Physical properties analyzed for whole cores from this site included bulk density, *P*-wave velocity, and magnetic susceptibility. Discrete measurements of *P*-wave velocity, electrical resistivity formation factor, shear strength, and index properties (including bulk density, grain density, water content, porosity, and void ratio) were performed using split cores. The methods used are described in detail in the "Explanatory Notes" chapter (this volume).

Bulk Density

Bulk density values exhibit a first-order trend that increases downward with several major excursions (see Table 12 and Figs. 33 through 36). As illustrated in Figure 33, the GRAPE-derived bulk densities at Holes 811A and 811C exhibit an interval of high-density values between about 19 and 25 mbsf. This high-density interval also can be clearly seen in the bulk densities determined using a pycnometer (Fig. 34B), and preliminary discussions among the shipboard scientists suggest that this interval may correspond to a unit containing one or more debris flows.

P-Wave Velocity

The *P*-wave velocities exhibit a first-order increase with depth, with sharp excursions between 24 and 30 mbsf and an interval having low-velocity values between 50 and 100 mbsf, indicated by the MST logger (see Fig. 33). The Hamilton Frame velocities also suggest a low-velocity zone in the vicinity of 100 mbsf, but a great deal of variability exists in the Hamilton Frame velocities (Table 13 and Fig. 34C). Data in Figure 36 and the accompanying Table 14 were extracted from

Table 7. Carbonate content data, Site 825.

Core, section, interval (cm)	Depth (mbsf)	Carbonate (%)
133-825A-		
5H-1, 100–103	201.00	95.90
5H-2, 100–103	202.50	97.70
5H-3, 100–103	204.00	99.80
5H-4, 100–103	205.50	98.40
5H-5, 100–103	207.00	97.60
5H-6, 100–103	208.50	97.40
6H-1, 100–103	210.50	95.90
6H-2, 100–103	212.00	96.80
6H-3, 100–103	213.50	98.80
6H-4, 100–103	215.00	97.40
6H-5, 100–103	216.50	98.40
6H-6, 100–103	218.00	99.30
7H-1, 100–103	220.00	99.30
7H-2, 100–103	221.50	100.00
7H-3, 100–103	223.00	99.50
7H-4, 100–103	224.50	97.70
7H-5, 100–103	226.00	98.00
7H-6, 100–103	227.50	98.80
8H-1, 100–103	229.50	95.90
8H-2, 100–103	231.00	97.80
8H-3, 100–103	232.50	99.60
8H-4, 100–103	234.00	96.20
8H-5, 100–103	235.50	98.20
8H-5, 140–145	235.90	98.50
8H-6, 100–103	237.00	97.80
10H-1, 100–103	248.50	99.10
10H-2, 100–103	250.00	98.70
10H-2, 140–145	250.40	98.80
10H-3, 100–103	251.50	98.20
10H-4, 100–103	253.00	98.10
11H-1, 100–103	258.10	99.30
11H-2, 100–103	259.60	98.80
12H-1, 100–103	267.80	99.00

the computer archive data set by ignoring all data values of less than 1400 m/s. We think that these low values result from unsaturated sediment.

Electrical Resistivity Formation Factor

We measured the formation factor at three intervals in each section from Hole 811A (see Table 15 and Fig. 34E). We were concerned about the validity of these measurements in that the measured electrical resistance was obviously a function of submerged probe length as well as the conductivity of pore waters. The electrical resistance of the standard varies as the water level of the standard varies with time. The electrical resistance of the core also varies, depending on how full the half-round core liner is. We were also concerned because the probes are so long that they are not equipotential surfaces and, therefore, do not truly represent formation resistance. Making the probes shorter will exacerbate the problem of uniform probe penetration in the split core. Should the variation in probe penetration be of the order of a few millimeters, a proportionately greater difference would exist for a 3-mm probe than for a 20-mm probe.

Shear Strength

Shear strengths exhibited a great deal of variability, although most values ranged from 1 to 10 kPa (see Table 14 and Fig. 34D).

Porosity

Porosity was one of the index properties determined from pycnometer measurements. A graph of porosity vs. depth is shown in Figure 34F; water content also is shown (Fig. 34G).

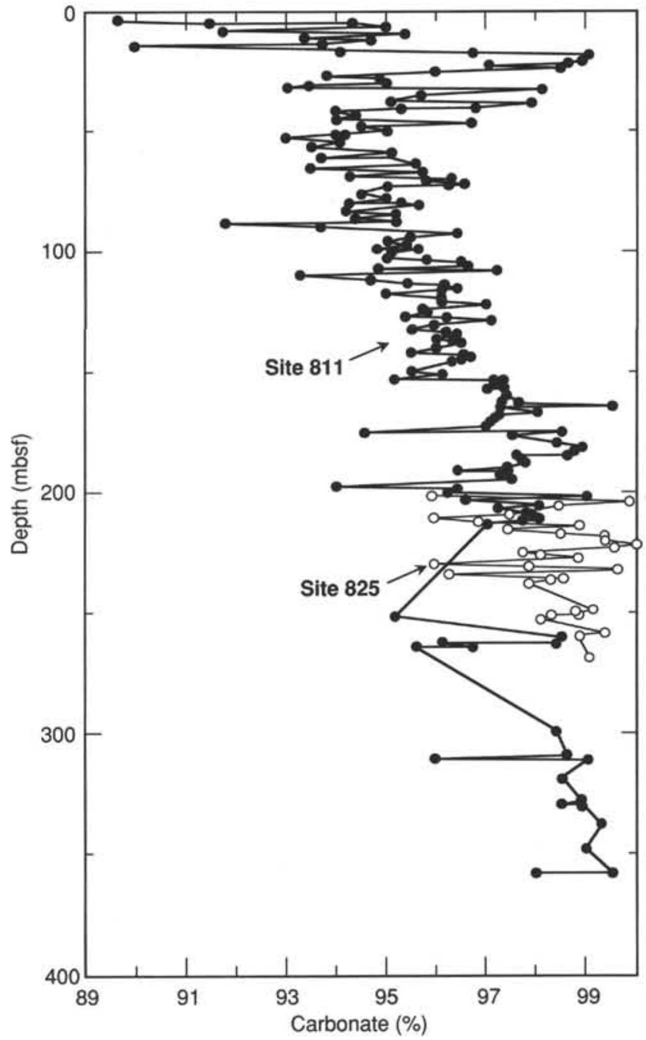

Figure 31. A comparison of carbonates analyzed from Sites 811 and 825. Most of the data from Site 825 fall in an interval from Site 811 from which few carbonate analyses were made.

Anomalously low porosities and water contents can be observed in the same interval (from about 19 to 25 mbsf) as high velocities and high formation factors. A plot of porosity vs. bulk density is shown in Figure 35.

SITE 825 PHYSICAL PROPERTIES

Soft sediments were recovered between 200 and 270 mbsf at Site 825. Physical properties data from this site appear in Tables 16 through 18 and have been plotted vs. depth in Figure 36. These average values are as follows:

Bulk density: 1.88 ± 0.06 g/cm^3
Grain density: 2.68 ± 0.03 g/cm^3
Porosity: $52.4 \pm 3.8\%$
Water content: $40.3 \pm 5\%$
P-wave velocity 1.68 ± 0.02 km/s
Vane shear strength 3.1 ± 0.97 kPa

Because of time constraints, we were unable to interpret these data during the cruise.

Table 8. Volatile hydrocarbon data from headspace analysis at Site 811.

Core, section, interval (cm)	Depth (mbsf)	Sample	Volume (mL)	Gas chromato.	C_1 (ppm)	C_2 (ppm)	C_3 (ppm)	C_1/C_2
133-811A-								
1H-3, 143–150	4.43	Headspace	5	Carle 132	2	0	0	0
2H-5, 143–145	12.93	Headspace	5	Carle 132	2	0	0	0
3H-5, 143–145	22.43	Headspace	5	Carle 132	2	0	0	0
4H-4, 143–145	30.43	Headspace	5	Carle 132	2	0	0	0
5H-4, 143–145	39.93	Headspace	5	Carle 132	2	0	0	0
6H-5, 143–145	50.88	Headspace	5	Carle 132	2	0	0	0
7H-5, 143–145	60.43	Headspace	5	Carle 132	2	0	0	0
8H-5, 143–145	69.93	Headspace	5	Carle 132	2	0	0	0
9H-5, 143–145	79.43	Headspace	5	Carle 132	2	0	0	0
10H-4, 143–145	87.43	Headspace	5	Carle 132	2	0	0	0
11H-5, 143–145	98.43	Headspace	5	Carle 132	2	0	0	0
12H-5, 0–2	106.5	Headspace	5	Carle 132	2	0	0	0
13H-4, 149–150	115.99	Headspace	5	Carle 132	2	0	0	0
14H-6, 0–2	127	Headspace	5	Carle 132	2	0	0	0
15H-5, 0–2	135	Headspace	5	Carle 132	2	0	0	0
16H-5, 0–2	144.5	Headspace	5	Carle 132	2	0	0	0
17H-5, 143–145	155.43	Headspace	5	Carle 132	2	0	0	0
18H-4, 0–2	162	Headspace	5	Carle 132	2	0	0	0
19H-6, 0–2	174.5	Headspace	5	Carle 132	2	0	0	0
20H-6, 0–2	184	Headspace	5	Carle 132	2	0	0	0
21H-4, 0–2	190.25	Headspace	5	Carle 132	2	0	0	0
22H-5, 0–2	201.5	Headspace	5	Carle 132	2	0	0	0
133-811B-								
3X-1, 61–63	212.61	Headspace	5	Carle 132	2	0	0	0
7V-1, 13–14	250.43	Headspace	5	Carle 132	2	0	0	0
8V-3, 0–2	261.75	Headspace	5	Carle 132	2	0	0	0
9V-1, 0–2	263.7	Headspace	5	Carle 132	2	0	0	0
16X-1, 148–150	309.48	Headspace	5	Carle 132	2	0	0	0
18X-2, 106–108	329.43	Headspace	5	Carle 132	5	1	0	0
21X-1, 112–114	357.42	Headspace	5	Carle 132	2	0	0	0

SITE 825 DOWNHOLE MEASUREMENTS

Reliability of Logs

Hole size and conditions were the most important controls of accuracy of logs from Hole 825B, and the caliper is the best indicator of these parameters. Most of the logged interval was greater than 15 in. (38 cm) in diameter, based on both mechanical and sonic calipers (see "Explanatory Notes" chapter, this volume). We had anticipated large hole sizes and had decided not to run the LDT, which requires pad contact against the borehole wall. Most other logs do not require pad contact and therefore are relatively insensitive to changes in the size of the borehole; gamma-ray and resistivity logs probably will change slightly with by post-cruise borehole correction.

As is often the case with ODP holes, the initial sonic logs from Hole 825B exhibited some zones in which cycle skipping caused unreliable swings in apparent velocity. The initial sonic logs from this site are the best that we could obtain during Leg 133 and reprocessing (see "Explanatory Notes" chapter, this volume) was successful in removing the few unreliable data. Because the short repeat up log reached deeper in the hole than the main up log, we created a composite reprocessed velocity log by combining the repeat and main up logs (Fig. 37). We think that the merged reprocessed log of Figure 37 is of very good quality.

The spectral gamma-ray tool is the only tool on the seismic stratigraphic combination string that can provide useful formation data even through pipe. At Hole 825B, through-pipe spectral gamma-ray logs were obtained only for the interval at 60 to 65 mbsf because of time constraints. For this through-pipe interval, total gamma-ray signal is above the noise level of the tool, but values for uranium, thorium, and potassium are all near or below the resolving power of the tool. Pipe-correction of the total gamma-ray data is warranted, but has not yet been undertaken. For the open-hole interval, replicate spectral gamma-ray logs exhibit modest agreement for uranium and almost no agreement for both potassium and thorium. The latter two elements are present in such low quantities at Hole 825B that their logs fluctuate about zero, and the total gamma-ray log is almost entirely attributable to uranium (Fig. 37).

Velocity and Resistivity

Velocity and resistivity correlate well throughout the entire logged interval at Hole 825B (Figs. 38 and 39). Because lithologic changes here are relatively minor and have been confined to variations in relative proportions of the geophysically similar minerals dolomite and calcite, log responses were controlled almost entirely by porosity.

An increase in velocity with depth appears to follow a simple compaction profile (Fig. 39), interrupted by several thin and low-porosity beds. Velocities increase from 1.7 to 1.8 km/s at 70 mbsf to 2.5 km/s at 400 mbsf, which is somewhat higher than the velocities of 1.7 and 2.2 km/s observed at similar depths in pelagic carbonates (Hamilton, 1979). Comparable data for near-reef carbonates are rare, but it may be that these velocities are higher because of a reef-derived component. The compaction profile does not indicate clearly whether mechanical compaction or diagenesis is more important for controlling most porosities at Site 825. Several thin zones exist in which resistivity and velocity decrease with increasing depth, contrary to the normal compaction profile. This agrees with drilling results, where soft intervals were encountered below hard layers, resulting in poor core recovery.

Velocity and resistivity ratios have been taken to remove the effects of water velocity and resistivity and to display differences between the two porosity-sensitive logs, which are usually assumed to move together (Fig. 38). Here, excursions to large positive A/B ratios indicate that velocity is high when compared to resistivity, as would be the case for a highly porous sediment in which the grain contacts had been cemented. No such zones are evident at Site 825. Excursions to low A/B ratios can be generated if the velocity remains constant and the resistivity increases, as might happen if the grains of an unconsolidated sediment became more platey at a constant porosity or if a cemented sediment had unconnected pores. Several zones of low A/B ratios are evident in Figure 38; these correspond with the highest resistivity intervals. These intervals are too high in velocity and resistivity to be unconsolidated, and the second possibility of unconnected pores probably is more likely. The log "Thin R" (Fig. 38) provides a qualitative indicator of frequency of thin beds (see "Site 812 chapter, this volume). This log delineates thin, resistive layers by taking a ratio of the shallow, high-rêsolution SFL and the deeper penetrating, but lower-resolution induction log. "Thin R" is seen as sensitive to instantaneous changes in resistivity caused by high-contrast thick beds, in addition to thin beds that are outside the resolving power of the measurements. Thin beds may be most plentiful in the interval at 128 to 208 mbsf and below 419 mbsf.

The reprocessed sonic log has been converted to an integrated traveltime log (Fig. 39) to facilitate depth-to-time conversion for comparing Site 825 data with seismic sequences. For the unlogged interval between the seafloor and 67.2 mbsf, we used a simple linear interpolation between water velocity at the seafloor and the first log value at 67.2 mbsf. We subjectively estimate that an error of 6 to 10 ms is associated with uncertainties of velocities in the top 67.2 mbsf. This estimated error is greater than at other Leg 133 sites because the trend of velocity as a function of depth does not extrapolate toward a water velocity of 1.5 km/s at the seafloor, suggesting that actual velocities above 67.2 mbsf might be faster than those assumed in Figure 39.

Log-Based Units

Based on log responses, Site 825 is composed of four units: log Unit I above 260 mbsf, log Unit II between 260 and 311 mbsf, log Unit III between 311 and 415 mbsf, and log Unit IV below 415 mbsf.

Based on log responses alone, the calcareous oozes (see "Site 825 Lithostratigraphy" section, this chapter) of log Unit I may be relatively homogeneous. In contrast, log Unit II includes intervals that are nearly identical with log Unit I, but it also has several thin (<5 m) beds that are highly cemented. The most prominent of these beds (at 306–308 mbsf is visible in cores as a hardground (see "Site 825 Lithostratigraphy" section, this chapter). These thin beds do not appear to be important permeability barriers to compaction, based on continuation of the log Unit I compaction trend through log Units II and III. Indeed, log Unit III may be just a more compacted continuation of log Unit II. Log Unit IV, like log Unit II, has intervals that constitute a continuation of the carbonate compaction trend, but log Unit IV is dominated by numerous thin beds of near-zero porosity. These thin and very dense beds in both log Units II and IV might be either dolomite or limestone; they are certainly diagenetic in origin. Some of the less dense beds may be rich in bioclasts, which are more lithified than the ooze. Because no FMS logs were obtained, we cannot distinguish between very dense beds that are too thin to resolve and thicker, less dense beds.

The bioclastic sands and packstones (see "Site 825 Lithostratigraphy" section, this chapter) of log Unit III, 311 to 415 mbsf, have relatively uniform log responses. Velocities in this unit are higher than can be accounted for by mechanical compaction of fine-grained carbonates, possibly because of some cementation *in-situ*, or alternatively, because of a high proportion of clasts. The homogeneity of porosities suggests that little or no shallow water was in the unit, nor any subaerial cementation.

Cavings prevented logging of the shallow basement penetration at this site.

Temperature

The L-DGO temperature tool was run at the bottom of the seismic stratigraphic tool string. Because hole temperatures are reduced by circulation during coring and by hole conditioning immediately prior to logging, one is unable to infer an equilibrium thermal profile reliably from a single temperature logging run. Our recorded maximum temperature of 18.7°C near the bottom of the hole thus is a minimum estimate of equilibrium temperature. Because of a battery problem in the tool, only the downgoing temperature log gave reliable pressure data; analysis of the upgoing log will have to wait for post-cruise merging of the Schlumberger time/depth data with the temperature-tool time/pressure data.

SITE 811 SEISMIC STRATIGRAPHY

The following section synthesizes the seismic stratigraphic data for Site 811 and compares the seismic analysis with the lithostratigraphic data.

The time-depth velocity plot shown in Figure 5 was calculated during the cruise for comparing seismic data with drilling results and to predict lithologies ahead of the drilling.

Our interpretation of the seismic stratigraphy at Site 811 is shown in Figure 40. Both seismic sections define the crossing for the originally proposed site together with the final position of the drill site. Six principal seismic reflectors were identified that can be tied around the site survey grid. These reflectors are numbered 1 through 6 and have been used to define the seismic stratigraphic sequences shown in Figures 40 and 41.

Sequence 1 occurs between reflector 1 and the seafloor and appears to drape over and smooth out all relief in the underlying unit throughout the site-survey area. This sequence equates with lithologic Unit I, which has been defined as composed dominantly of periplatform ooze and gravity-slide deposits of Pliocene to Pleistocene age.

Sequence 2 occurs between reflectors 1 and 2 and is characterized by having a more bedded appearance than sequence 3. This sequence can be divided into at least three coherent seismic subunits:

1. Subunit 1 is characterized by strongly mounded reflectors; the unit may comprise turbidites. The upper surface of Subunit 1 may have been truncated.
2. Subunit 2 is a transparent unit approximately 50 ms thick at the site, is bedded and chaotic, and bedded to the north and south. At the site, the unit may represent a pelagic ooze, but away from the site the unit may be turbiditic.
3. Subunit 3 at the base is composed of 50 ms of bedded sediments similar in character to seismic sequences 2 and 4 and therefore may represent turbidites. The subunit thickens and thins, but has some relief.

Sequence 2 is equivalent to lithologic Unit II, which has been defined as pelagic throughout its lower part and periplatform in its upper part. The age of this sequence is thus late Miocene to late Pliocene.

Sequence 3 occurs between reflectors 2 and 3 and is one of the thickest, most widespread, and most easily identified sequences throughout the site-survey area. Its seismic character is dominated at the site by its essentially transparent nature, with coherent and laterally continuous reflectors being limited to the base and near the top. Sequence 3 correlates with lithologic Unit III, which has been defined as periplatform ooze that contains abundant, bank-derived components

Table 9. Concentrations of total organic carbon, inorganic carbon, and carbon in sediments at Site 811.

Core, section, interval (cm)	Depth (mbsf)	Sample	Inorg. carbon (%)	$CaCO_3$ (%)	Total carbon (%)	TOC (%)
133-811A-						
1H-1, 97–98	0.97	PP	10.77	89.7		
1H-2, 86–87	2.36	PP	10.77	89.7		
1H-3, 85–86	3.85	PP	10.77	89.7		
1H-3, 143–145	4.43	Headspace	10.98	91.5	11.43	0.45
1H-4, 26–27	4.76	PP	11.32	94.3		
2H-1, 67–68	6.17	PP	11.41	95		
2H-2, 67–68	7.67	PP	11.02	91.8		
2H-3, 67–68	9.17	PP	11.45	95.4		
2H-4, 67–68	10.67	PP	11.21	93.4		
2H-5, 67–68	12.17	PP	11.37	94.7		
2H-5, 143–145	12.93	Headspace	11.25	93.7	11.36	0.11
2H-6, 67–68	13.67	PP	10.8	90		
3H-1, 102–104	16.02	PP	11.3	94.1		
3H-2, 66–68	17.16	PP	11.61	96.7		
3H-3, 66–68	18.66	PP	11.89	99		
3H-4, 66–68	20.16	PP	11.87	98.9		
3H-5, 66–68	21.66	PP	11.84	98.6		
3H-5, 143–145	22.43	Headspace	11.66	97.1	11.9	0.24
3H-6, 66–68	23.16	PP	11.82	98.5		
4H-1, 67–69	25.17	PP	11.53	96		
4H-2, 67–69	26.67	PP	11.26	93.8		
4H-3, 67–69	28.17	PP	11.39	94.9		
4H-4, 67–69	29.67	PP	11.4	95		
4H-4, 143–145	30.43	Headspace	11.23	93.5	11.46	0.23
4H-5, 67–69	31.17	PP	11.18	93.1		
4H-6, 67–69	32.67	PP	11.78	98.1		
5H-1, 137–140	35.37	PP	11.49	95.7		
5H-2, 140–142	36.9	PP	11.42	95.1		
5H-3, 127–130	38.27	PP	11.75	97.9		
5H-4, 130–132	39.8	PP	11.61	96.7		
5H-4, 143–145	39.93	Headspace	11.44	95.3	11.5	0.06
5H-5, 130–133	41.3	PP	11.28	94		
5H-6, 130–133	42.8	PP	11.33	94.4		
6H-1, 133–138	44.83	PP	11.29	94		
6H-2, 133–138	46.28	PP	11.61	96.7		
6H-3, 134–137	47.79	PP	11.34	94.5		
6H-4, 134–138	49.29	PP	11.41	95		
6H-5, 135–138	50.8	PP	11.28	94		
6H-5, 143–145	50.88	Headspace	11.31	94.2	11.66	0.35
6H-6, 134–137	52.29	PP	11.16	93		
7H-1, 137–139	54.37	PP	11.3	94.1		
7H-2, 135–138	55.85	PP	11.23	93.5		
7H-3, 136–138	57.36	PP	11.42	95.1		
7H-4, 136–138	58.86	PP	11.39	94.9		
7H-5, 99–101	59.99	PP	11.42	95.1		
7H-5, 143–145	60.43	Headspace	11.25	93.7	11.39	0.14
7H-6, 133–135	61.83	PP	11.48	95.6		
8H-1, 95–97	63.45	PP	11.46	95.5		
8H-2, 95–97	64.95	PP	11.22	93.5		
8H-3, 95–97	66.45	PP	11.49	95.7		
8H-4, 76–78	67.76	PP	11.32	94.3		
8H-5, 107–109	69.57	PP	11.56	96.3		
8H-5, 143–145	69.93	Headspace	11.5	95.8	11.83	0.33
8H-6, 105–107	71.05	PP	11.58	96.5		
8H-7, 34–36	71.84	PP	11.55	96.2		
9H-1, 101–104	73.01	PP	11.41	95		
9H-2, 101–104	74.51	PP	11.35	94.5		
9H-3, 101–104	76.01	PP	11.4	95		
9H-4, 101–104	77.51	PP	11.41	95		
9H-5, 101–104	79.01	PP	11.32	94.3		
9H-5, 143–145	79.43	Headspace	11.44	95.3	11.69	0.25
9H-6, 101–104	80.51	PP	11.49	95.7		
10H-1, 81–84	82.31	PP	11.31	94.2		
10H-2, 81–84	83.81	PP	11.43	95.2		
10H-3, 67–70	85.17	PP	11.33	94.4		
10H-4, 77–80	86.77	PP	11.43	95.2		
10H-4, 143–145	87.43	Headspace	11.02	91.8	11.34	0.32
10H-5, 77–80	88.27	PP	11.25	93.7		
11H-1, 104–107	92.04	PP	11.57	96.4		
11H-2, 104–107	93.54	PP	11.45	95.4		
11H-3, 105–108	95.05	PP	11.41	95		
11H-4, 105–108	96.55	PP	11.45	95.4		
11H-5, 105–108	98.05	PP	11.38	94.8		
11H-5, 143–145	98.43	Headspace	11.48	95.6	11.62	0.14
11H-6, 105–108	99.55	PP	11.42	95.1		
12H-1, 82–85	101.32	PP	11.41	95		

Table 9 (continued).

Core, section, interval (cm)	Depth (mbsf)	Sample	Inorg. carbon (%)	$CaCO_3$ (%)	Total carbon (%)	TOC (%)
12H-2, 82–85	102.82	PP	11.5	95.8		
12H-3, 82–85	104.32	PP	11.59	96.5		
12H-4, 96–99	105.96	PP	11.6	96.6		
12H-5, 0–2	106.5	Headspace	11.39	94.9	11.84	0.45
12H-5, 102–105	107.52	PP	11.67	97.2		
12H-6, 102–105	109.02	PP	11.2	93.3		
13H-1, 101–104	111.01	PP	11.37	94.7		
13H-2, 101–104	112.51	PP	11.45	95.4		
13H-3, 101–104	114.01	PP	11.55	96.2		
13H-4, 101–104	115.51	PP	11.57	96.4		
13H-4, 149–150	115.99	Headspace	11.54	96.1	11.84	0.3
13H-5, 101–104	117.01	PP	11.4	95		
13H-6, 101–104	118.51	PP	11.54	96.1		
14H-1, 101–104	120.51	PP	11.54	96.1		
14H-2, 101–104	122.01	PP	11.65	97		
14H-3, 101–104	123.51	PP	11.49	95.7		
14H-4, 101–104	125.01	PP	11.5	95.8		
14H-5, 101–104	126.51	PP	11.45	95.4		
14H-6, 0–2	127	Headspace	11.55	96.2	11.77	0.22
14H-6, 101–104	128.01	PP	11.66	97.1		
15H-1, 100–102	130	PP	11.51	95.9		
15H-2, 100–102	131.5	PP	11.46	95.5		
15H-3, 100–102	133	PP	11.55	96.2		
15H-4, 100–102	134.5	PP	11.57	96.4		
15H-5, 0–2	135	Headspace	11.53	96	11.62	0.09
15H-5, 100–102	136	PP	11.56	96.3		
15H-6, 100–102	137.5	PP	11.58	96.5		
16H-1, 101–103	139.51	PP	11.52	96		
16H-2, 101–103	141.01	PP	11.47	95.5		
16H-3, 101–103	142.51	PP	11.6	96.6		
16H-4, 101–103	144.01	PP	11.61	96.7		
16H-5, 0–2	144.5	Headspace	11.58	96.5	11.85	0.27
16H-5, 101–103	145.51	PP	11.56	96.3		
17H-1, 100–101	149	PP	11.47	95.5		
17H-2, 100–101	150.5	PP	11.54	96.1		
17H-3, 100–101	152	PP	11.43	95.2		
17H-4, 100–101	153.5	PP	11.66	97.1		
17H-5, 100–101	155	PP	11.69	97.4		
17H-5, 143–145	155.43	PP	11.67	97.2	11.79	0.12
17H-6, 100–101	156.5	PP	11.64	97		
18H-1, 101–104	158.51	PP	11.69	97.4		
18H-2, 101–104	160.01	PP	11.68	97.3		
18H-3, 101–104	161.51	PP	11.72	97.6		
18H-4, 101–104	163.01	PP	11.74	97.8		
18H-5, 0–2	163.5	Headspace	11.94	99.5	11.9	0.04
18H-5, 101–104	164.51	PP	11.68	97.3		
18H-6, 101–104	166.01	PP	11.76	98		
19H-1, 137–140	168.37	PP	11.67	97.2		
19H-2, 137–140	169.87	PP	11.66	97.1		
19H-3, 137–140	171.37	PP	11.65	97		
19H-4, 137–140	172.87	PP	11.63	96.9		
19H-5, 137–140	174.37	PP	11.36	94.6		
19H-6, 0–2	174.5	Headspace	11.82	98.5	12.09	0.27
19H-6, 137–140	175.87	PP	11.7	97.5		
20H-2, 130–133	179.3	PP	11.81	98.4		
20H-3, 130–133	180.8	PP	11.87	98.9		
20H-4, 130–133	182.3	PP	11.85	98.7		
20H-5, 130–133	183.8	PP	11.84	98.6		
20H-6, 0–2	184	Headspace	11.72	97.6	11.97	0.25
20H-6, 130–133	185.3	PP	11.73	97.7		
21H-1, 96–99	186.96	PP	11.74	97.8		
21H-2, 96–99	188.46	PP	11.69	97.4		
21H-3, 96–99	189.96	PP	11.68	97.3		
21H-4, 0–2	190.25	Headspace	11.57	96.4	11.79	0.25
21H-4, 96–99	191.21	PP	11.68	97.3		
21H-5, 96–99	192.71	PP	11.68	97.3		
21H-6, 94–97	194.19	PP	11.7	97.5		
22H-1, 125–127	196.75	PP	11.28	94		
22H-2, 125–127	198.25	PP	11.57	96.4		
22H-3, 125–127	199.75	PP	11.55	96.2		
22H-5, 0–2	201.5	Headspace	11.89	99	12.14	0.2
22H-5, 125–127	202.75	PP	11.6	96.6		
22H-6, 125–127	204.25	PP	11.78	98.1		
23H-1, 131–133	206.31	PP	11.67	97.2		
23H-2, 131–133	207.77	PP	11.75	97.9		
23H-3, 131–133	209.27	PP	11.76	98		
23H-4, 80–82	210.26	PP	11.78	98.1		
23H-5, 73–75	211.52	PP	11.73	97.7		

Table 9 (continued).

Core, section, interval (cm)	Depth (mbsf)	Sample	Inorg. carbon (%)	$CaCO_3$ (%)	Total carbon (%)	TOC (%)
133-811B-						
3X-1, 61–62	212.61	Headspace	11.64	97	11.82	0.18
7V-1, 13–14	250.43	Headspace	11.43	95.2	11.84	0.41
8V-1, 136–139	260.16	PP	11.82	98.5		
8V-2, 137–139	261.67	PP	11.81	98.4		
8V-3, 0–2	261.8	Headspace	11.54	96.1	11.77	0.23
8V-3, 137–139	263.17	PP	11.61	96.7		
9V-1, 0–2	263.7	Headspace	11.48	95.6	11.74	0.26
15X-CC, 11–12	298.51	PP	11.81	98.4		
16X-1, 92–93	308.92	PP	11.84	98.6		
16X-1, 148–150	309.48	Headspace	11.52	96	11.86	0.34
16X-2, 71–72	310.21	PP	11.89	99		
17X-1, 40–41	318.1	PP	11.83	98.5		
18X-1, 59–60	327.89	PP	11.87	98.9		
18X-2, 68–69	329.05	PP	11.83	98.5		
18X-2, 106–108	329.43	Headspace	11.87	98.9	12.01	0.14
19X-1, 7–8	337.07	PP	11.92	99.3		
20X-1, 49–50	347.09	PP	11.88	99		
21X-1, 70–71	357	PP	11.94	99.5		
21X-1, 112–114	357.42	Headspace	11.77	98	11.93	0.16

PP = physical property.

and few nannofossils of middle and late Miocene age. Gravity-flow deposits occur at the base and the top.

The reflector characteristics at the base and near the top may reflect turbidites related to changes in sea level. Throughout the site-survey area, the unit is mounded and almost certainly has been affected by current activity. This supports the shipboard biostratigraphers' conclusion that the low rate of sedimentation throughout much of this unit may result to some degree from current winnowing of pelagic and bank-derived materials.

Sequence 4 is defined as occurring between reflectors 3 and 4 and is characterized by easily identified, strong, continuous reflectors. The sequence blankets the underlying shallow-water units, and its internal character resembles sequence 2. It varies from 40 to 100 ms thick.

No lithologic unit identified at Site 811 corresponds to sequence 4. The sequence was recognized on the basis of the time-depth curve as it corresponded with the bottom part of lithologic Unit III of early middle Miocene age and is composed of chalks different from the rest of the unlithified lithologic unit above. These chalks are thought to have been deposited in an outer-shelf or upper-slope environment; thus, they indicate a substantial deepening of the platform unrelated to any previously proposed change in sea level. Such deepening thus may have been tectonically controlled. We propose that sequence 4 be formally recognized as a particular event within a lithostratigraphic expression different from the rest of lithologic Unit III. We think that sequence 4 defines the first major tectonically controlled subsidence pulse on the Queensland Plateau and is of early to middle Miocene age. We also note that the upper surface of sequence 4 (reflector 3) is undulating and irregular, suggesting that it may have been in some way affected by processes relating to a change in sea level, probably the middle Miocene decrease in sea level.

Sequence 5 occurs between reflectors 4 and 5 and varies in thickness from less than 50 ms to greater than 100 ms. However, its character is distinctive and is more bedded to the south of the drill site. To the north, the character of this sequence is dominated by a carbonate build-up. The sequence at the site thus may be related in composition to this or other adjacent build-ups. Sequence 5 corresponds to lithologic Unit IV, considered as of early Miocene and middle Miocene age. Cores from sequence 5 indicate that the sequence is composed of shallow-water reef and coral material. This material was probably derived from reef mounds comparable to those seen in the seismic section to the north and deposited in shallow water proximal to its reefal source. The sediments are unlikely to represent an open-shelf setting.

Sequence 6 occurs between reflectors 5 and 6 and represents the first flooding of the Queensland Plateau in the area. The unit corresponds with lithologic Unit V, defined as upper slope and dated as late Oligocene. Note, however, that the last core from Hole 811B (Core 133-811B-24X) produced a fragment that is middle Eocene in age and dominated by planktonic material and that was deposited in water depths of less than 100 m. The late Oligocene age for the upper part of the unit suggests that such sediments were probably deposited before the major decrease in sea level in the late Oligocene; seismic character differences between sequences 5 and 6 appear to support this contention. Reflector 5 almost certainly defines a major sequence boundary and probably represents the shallowing produced by the late Oligocene decline in sea level.

Sequence 7 occurs beneath reflector 6 and is interpreted as representing the continental basement in the area, which almost certainly consists of Palaeozoic sediments or metasediments. Geochemical data obtained from formation water samples during this cruise suggest that basement is not igneous.

SITES 811/825 SUMMARY AND CONCLUSIONS

Upper Neogene Sediments

At Site 811, a periplatform sequence was recovered during APC coring (Holes 811A and 811C) that was deposited during the late middle Miocene to the Pleistocene. The nearly 100% recovery of this material achieves one of the objectives for this site, i.e., to obtain a complete record of plateau deposition during the late Neogene. Unraveling the specific paleoceanographic and paleoclimatic signals contained within these sediments will have to wait for results of shore-based investigations; nevertheless, our shipboard studies of these sediments

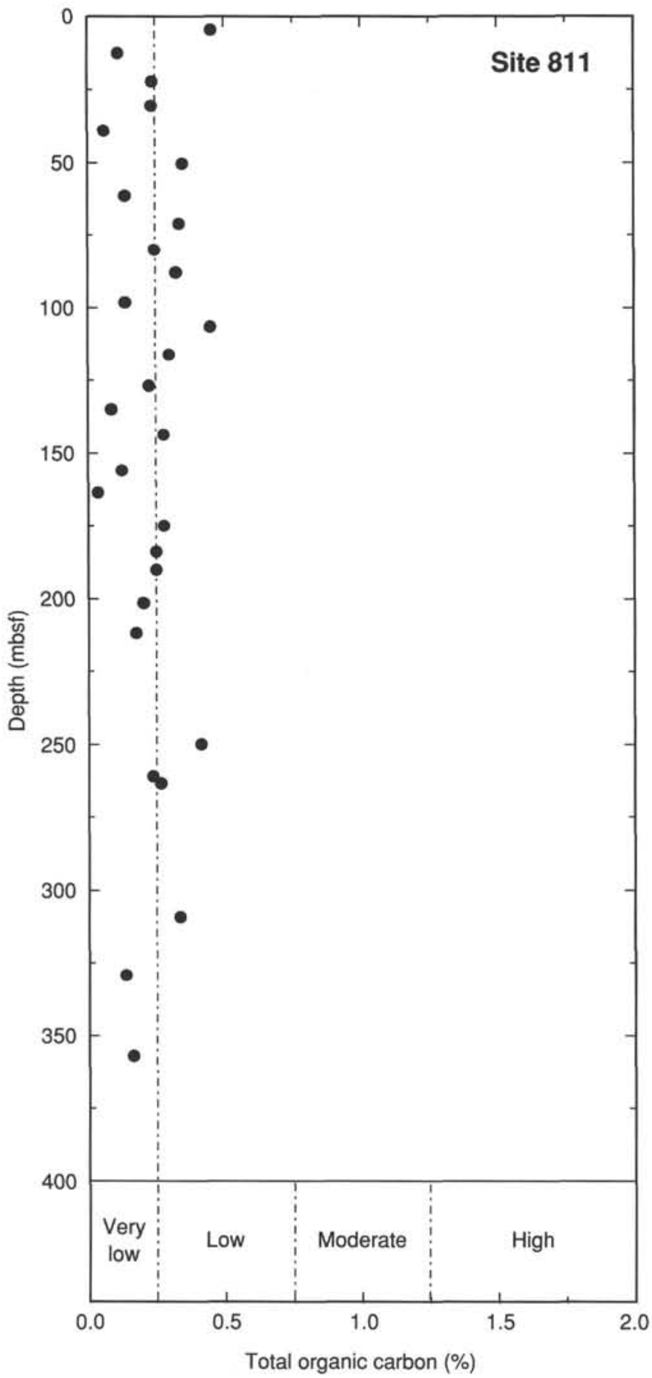

Figure 32. Total organic carbon contents of sediments at Site 811.

yielded pertinent data related to other objectives: determining the age and facies of periplatform deposits adjacent to Holmes Reef, a marginal reef build-up, and investigating sedimentation and diagenetic processes in an exclusively carbonate depositional system.

Environment of Deposition

The upper Neogene sediments are characterized by open-marine conditions on a carbonate platform slope at middle bathyal depths (600–1000 m) and exhibit a significant influx of carbonate bank-derived detritus. The excellent recovery between 0 and 205 mbsf provides us with a continuous sedimentary record of two periods of periplatform deposition during which shallow-water, bank-derived carbonates mixed with pelagic carbonates and an intervening period of pelagic deposition. The frequency and type of gravity-flow deposits help us divide the sequence into discrete units, which reflect export processes occurring on the bank, possibly in response to environmental changes induced by climatic and/or fluctuations in sea level.

Early Late Pliocene to Pleistocene Periplatform Sedimentation

The sediments contained in lithologic Unit I represent sedimentation during the late Pliocene to Pleistocene (2.5 Ma to the present), a climatic period characterized by intensive Northern Hemisphere glaciations. Unit I was divided into three subunits on the basis of the distribution of redeposited sediments. The upper Pleistocene periplatform oozes (Subunit IA) contain frequent 10- to 15-cm-thick intervals of bioclastic packstone layers, interpreted as calciturbidites. The number and distribution of these small-scale gravity deposits suggest that high-energy events, which transported material from the bank onto the slope, occurred frequently during this period. In contrast, the middle Pleistocene periplatform oozes (Subunit IB) contain no turbidites, although they are composed of up to 75% fine-grained calcareous, bank-derived sediment. This suggests that during this interval, material was being swept from the shallow banks but that only the finer-grained fraction reached the deeper slopes. One might infer that the reworking of bank-derived material was not related to high-energy events or that the coarser-grained fraction was trapped in the shallower regions.

Periplatform sedimentation processes during the late Pliocene to early Pleistocene (Subunit IC) were dramatically different from those represented in the overlying sediments. Ooze sedimentation was interrupted by the deposition of two debris-flow packages comprising unlithified bioclastic packstones, unlithified lithoclastic rudstones, and floatstones. Moldic porosity in some lithoclasts suggests meteoric diagenesis during periods of exposure of the carbonate bank source. The first debris flow was deposited between 2.3 and 1.8 Ma. The relationship between the occurrence of these debris flows and sea level is equivocal. Oxygen-isotope data indicate that Northern Hemisphere glaciation began at about 2.4 Ma, while

Table 10. Volatile hydrocarbon data from headspace analyses at Site 825.

Core, section, interval (cm)	Depth (mbsf)	Sample	Volume (mL)	Gas chromato.	C_1 (ppm)	C_{2+} (ppm)
133-825A-						
5H-5, 149–150	207.49	HS	5	CAR132	2	0
6H-4, 0–1	214	HS	5	CAR132	2	0
8H-5, 149–150	235.99	HS	5	CAR132	2	0
10X-2, 149–150	250.49	HS	5	CAR132	2	0
12X-1, 0–1	266.8	HS	5	CAR132	2	0

HS = headspace sample.

Table 11. Concentrations of total organic carbon, inorganic carbon, total carbon, total nitrogen, and sulfur in intertitial water and physical properties samples from Site 825.

Core, section, interval (cm)	Depth (mbsf)	Sample	Total organic carbon (%)	Total inorganic carbon (%)	Total carbon (%)	Total nitrogen (%)	Total sulfur (%)
133-825A-							
5H-3, 100–103	204	PP	0.27	11.98	12.25	0	0
6H-3, 100–103	213.5	PP	0.2	11.86	12.06	0	0
7H-3, 100–103	223	PP	0.16	11.94	12.1	0	0
8H-5, 140–145	235.9	IW	0.2	11.83	12.03	0	0
10X-2, 140–145	250.4	IW	0.21	11.86	12.07	0	0
11X-2, 100–103	259.6	PP	0.16	11.86	12.02	0	0
12X-1, 100–103	267.8	PP	0.12	11.88	12	0	0

PP = physical properties sample; IW = interstitial water sample.

the most recent eustatic sea-level curve derived from sequence stratigraphy shows a period of rising sea level from a lowstand at about 2.4 Ma to a highstand at about 1.8 Ma (Haq et al., 1987).

The sediments of Subunit IIA, deposited in the early late Pliocene (3.75–2.5 Ma), resemble those of Subunit IB. Gravity-flow deposits are missing, but the fine-grained fraction of the ooze contains up to 75% bank-derived calcareous component, which denotes it as a periplatform ooze. These sediments were deposited during a period of decreasing sea level, following the lower Pliocene highstand.

Aragonite is a characteristic carbonate component of periplatform sediments. Unit I sediments contained significant quantities of aragonite, up to 38% in the younger oozes, that decreases downward to only trace amounts in the older sediments. Thus, the dissolution of metastable aragonite and/or recrystallization to calcite apparently happens shortly after burial, within the upper 10 m of the sedimentary column. The monotonous uniformity of the interstitial-water geochemical profiles below 30 mbsf, in conjunction with a relatively elevated geothermal gradient, may indicate massive fluid circulation through the sediments.

The sedimentation rate throughout this interval of periplatform deposition was approximately 3 cm/k.y., twice as high as that for the underlying Subunit IIB pelagic sediments. The higher rates undoubtedly reflect the periplatform sedimentation processes, with enhanced influx of bank-derived detritus to the sediments.

Late Miocene to Early Pliocene Pelagic Sedimentation

The sediments of Subunit IIB, deposited at middle bathyal depths during the late Miocene to early Pliocene (8.75–3.75 Ma), are classified as pelagic in origin, based on a fine fraction content greater than 75% nannofossils. In addition, these sediments are devoid of calciturbiditic layers. Curiously, this interval covers a period having both intense glaciation (late Miocene) and warm climates (early Pliocene), implying that fluctuations in eustatic sea level did not influence the sedimentation pattern. The sedimentation rate for the lowermost Pliocene part of this pelagic interval was about 1.5 cm/k.y., less than for the periplatform sediments above and below.

Late Middle to Late Miocene Periplatform Sedimentation

Sediments of Unit III were recovered by APC coring in Holes 811A and 825A. These upper middle-to-upper Miocene (approximately 11–8.75 Ma) sediments are periplatform oozes and chalks that alternate with numerous 10- to 70-cm-thick, bioclastic foraminifer wackestone, packstone, lithoclast floatstone, and rudstone layers. These layers usually exhibit an upward-fining structure and thus are considered to be turbidites. The sedimentation rate in this interval was about 2.0 cm/k.y., not much higher than the rate for the overlying pelagic sediments. Considering the amount of redeposited material, this low rate may be anomalous. As benthic foraminifers indicate no significant change in the depth of the depositional environment, a possible explanation for this anomaly is that the comparatively low rate might reflect deposition in a current-swept environment, whereby the finer pelagic material was transported during winnowing and the coarser-grained detritus was concentrated.

Sea Level Control on Carbonate Platform Sedimentation

In an environment surrounding a carbonate platform, the amount of material available for transport and redeposition as periplatform sediments on the deeper slopes depends a great deal on the production rate on the bank tops and the mechanisms of off-bank transport. In turn, productivity is regulated by the location of the bank tops relative to the photic zone; maximum productivity occurs when they are situated within the upper part of the photic zone. If there is a relative decline in sea level, of course, bank-top productivity will cease when the banks are exposed. On the other hand, if a relatively rapid rise in sea level exceeds the keep-up rate of the platform, productivity will be drastically reduced with diminishing light penetration as the bank tops recede beneath the photic zone and are eventually drowned with increasing depth.

The late Neogene fluctuations from periplatform to pelagic back to periplatform sedimentation, which were recorded at Site 811 on the Queensland Plateau, may be a function of relative changes in sea level. The periods of periplatform sedimentation may correspond to times when the banks were actively producing carbonate material for transport and redeposition on the slopes. These periods occurred during the late middle to late Miocene (approximately 11–8.75 Ma) and early late Pliocene to Pleistocene (3.75 Ma to present). Although these time intervals have been recognized as times of major decreases in eustatic sea level, and although in particular the Pleistocene has been recognized as a time of glacial/interglacial fluctuations, we conclude that the carbonate banks were able to maintain a steady, although variable, influx of detritus to the slope environment.

In contrast, the period of pelagic sedimentation, late Miocene to early Pliocene (8.75–3.75 Ma), represents a time when the bank output was greatly diminished, if not completely stopped. This suggests either that the bank tops were subaerially exposed as a result of a relative decrease in sea level or that they were drowned as a result of a relative rise in sea level. Curiously, the late Miocene to early Pliocene corresponds to a time when both major decreases and in-

Table 12. Index properties data, Site 811.

Core, section, interval (cm)	Depth (mbsf)	Bulk density (g/cm^3)	Grain density (g/cm^3)	Porosity (%)	Water content (%)	Void ratio
133-811A-						
1H-1, 97–98	0.97	1.49	2.66	73.6	102.2	2.79
1H-2, 87–88	2.37	1.55	2.59	77.9	106.6	3.53
1H-4, 28–29	4.78	1.78	2.91	77.5	80.4	3.44
2H-1, 67–68	6.17	1.61	2.72	71.5	83.4	2.51
2H-2, 67–68	7.67	1.66	2.68	67.7	71.4	2.10
2H-3, 67–68	9.17	1.66	2.85	70.1	76.5	2.34
2H-4, 67–68	10.67	1.68	2.69	72.2	78.2	2.59
2H-5, 67–68	12.17	1.71	2.75	65.0	63.8	1.86
2H-6, 67–68	13.67	1.70	2.72	72.4	77.3	2.63
3H-1, 102–104	16.02	1.65	2.71	63.8	65.6	1.76
3H-2, 66–68	17.16	1.63	2.70	66.9	72.7	2.02
3H-3, 66–68	18.66	1.84	2.79	54.7	43.9	1.21
3H-4, 66–68	20.16	1.85	2.69	50.8	39.1	1.03
3H-5, 66–68	21.66	2.00	2.73	45.2	30.3	0.83
3H-6, 66–68	23.16	2.19	2.73	34.6	19.3	0.53
4H-1, 67–69	25.17	1.72	2.74	64.2	61.7	1.79
4H-2, 67–69	26.67	1.70	2.68	64.8	64.1	1.84
4H-3, 67–69	28.17	1.65	2.73	59.3	58.4	1.46
4H-6, 67–69	32.67	1.41	2.71	32.7	31.3	0.49
5H-1, 137–140	35.37	1.93	2.62	73.8	64.3	2.82
5H-2, 140–142	36.90	1.91	2.64	61.9	49.6	1.63
5H-3, 127–130	38.27	1.65	2.65	58.0	56.5	1.38
5H-4, 130–132	39.80	1.79	2.73	53.7	44.5	1.16
5H-5, 130–133	41.30	1.80	2.70	63.7	56.7	1.76
5H-6, 130–133	42.80	1.85	2.68	65.5	57.1	1.90
6H-1, 135–138	44.85	1.78	2.68	63.6	57.6	1.75
6H-3, 135–138	47.80	1.81	2.68	59.1	50.4	1.45
6H-4, 134–137	49.29	1.82	2.53	60.1	51.1	1.51
6H-5, 135–138	50.80	1.78	2.70	59.7	52.4	1.48
6H-6, 134–137	52.29	1.73	2.70	62.0	57.9	1.63
7H-1, 136–140	54.36	1.79	2.96	61.3	54.1	1.58
7H-2, 135–138	55.85	1.80	2.78	63.1	56.1	1.71
7H-3, 135–138	57.35	1.75	2.88	59.3	53.0	1.46
7H-4, 135–138	58.85	1.81	2.80	64.1	56.7	1.79
7H-5, 99–102	59.99	1.90	2.78	67.0	56.5	2.03
7H-6, 133–136	61.83	1.74	2.81	61.3	56.5	1.58
8H-1, 94–97	63.44	1.79	2.76	59.8	51.8	1.49
8H-2, 95–98	64.95	1.95	2.80	66.7	54.1	2.01
8H-3, 95–98	66.45	1.85	2.90	66.4	57.9	1.98
8H-4, 76–79	67.76	1.90	2.82	67.4	57.0	2.06
8H-6, 106–109	71.06	1.82	2.76	64.4	56.8	1.81
8H-7, 34–37	71.84	1.83	2.88	64.8	56.7	1.84
9H-1, 101–104	73.01	1.94	2.73	60.6	46.9	1.54
9H-4, 101–104	77.51	1.85	2.98	67.2	59.0	2.05
9H-6, 101–104	80.51	1.81	2.18	66.2	60.1	1.96
10H-1, 81–84	82.31	1.74	2.99	66.7	64.9	2.01
10H-4, 76–79	86.76	1.90	2.96	70.8	62.0	2.43
10H-5, 76–79	88.26	1.76	2.95	67.4	64.5	2.07
11H-2, 104–107	93.54	1.80	2.98	65.6	59.6	1.90
12H-3, 82–85	104.32	1.88	2.87	59.6	47.9	1.48
12H-5, 102–105	107.52	1.83	2.86	59.6	50.3	1.48
12H-6, 102–105	109.02	1.77	2.83	61.2	55.1	1.58
13H-3, 101–104	114.01	1.85	2.81	62.0	52.4	1.64
13H-4, 101–104	115.51	1.89	2.90	60.8	49.3	1.55
13H-6, 101–104	118.51	1.86	2.99	59.9	49.3	1.49
14H-1, 101–104	120.51	1.93	2.91	63.5	50.9	1.74
14H-2, 101–104	122.01	1.89	2.95	62.5	51.4	1.67
14H-5, 101–104	126.51	1.80	2.84	63.4	56.6	1.74
14H-6, 101–104	128.01	1.86	2.85	61.5	51.3	1.59
15H-1, 101–104	130.01	1.83	2.80	56.8	46.8	1.32
15H-2, 101–104	131.51	1.80	2.93	60.7	52.7	1.55
15H-3, 101–104	133.01	1.88	2.70	61.8	50.7	1.62
15H-4, 101–104	134.51	1.87	2.78	59.7	48.5	1.48
15H-5, 101–104	136.01	1.82	2.96	59.9	50.9	1.50
16H-1, 101–104	139.51	1.88	2.86	62.3	51.4	1.66
16H-2, 101–104	141.01	1.90	2.76	64.0	52.6	1.78
16H-3, 101–104	142.51	1.94	2.95	63.5	50.5	1.74
16H-4, 101–104	144.01	2.12	2.99	68.8	49.7	2.20
16H-5, 101–104	145.51	1.88	2.79	59.2	47.7	1.45
17H-1, 100–103	149.00	1.81	2.67	62.3	54.4	1.65
17H-2, 100–103	150.50	1.83	2.76	65.1	57.5	1.86
17H-4, 100–103	153.50	1.94	2.80	61.3	47.8	1.59
17H-5, 100–103	155.00	1.81	2.10	57.7	48.6	1.37
17H-6, 100–103	156.50	1.85	2.76	57.5	46.6	1.35

Table 12 (continued).

Core, section, interval (cm)	Depth (mbsf)	Bulk density (g/cm^3)	Grain density (g/cm^3)	Porosity (%)	Water content (%)	Void ratio
18H-1, 101–104	158.51	1.85	2.72	57.4	46.5	1.35
18H-2, 101–104	160.01	1.90	2.91	59.7	47.4	1.48
18H-3, 101–104	161.51	1.83	2.70	57.2	47.1	1.34
18H-4, 101–104	163.01	1.96	2.93	61.0	46.8	1.56
18H-5, 101–104	164.51	2.05	2.97	69.8	53.5	2.32
18H-6, 101–104	166.01	2.10	2.96	64.8	46.4	1.84
19H-1, 137–140	168.37	1.98	2.80	53.5	38.4	1.15
19H-2, 137–140	169.87	1.85	2.72	58.2	47.6	1.39
19H-3, 137–140	171.37	2.01	2.85	51.4	35.4	1.06
19H-4, 137–140	172.87	1.80	2.84	49.7	39.3	0.99
19H-5, 137–140	174.37	1.84	2.75	59.9	50.0	1.50
20H-2, 130–133	179.30	1.93	2.76	56.1	42.3	1.28
20H-3, 130–133	180.80	1.97	2.74	51.3	36.5	1.05
20H-4, 130–133	182.30	1.88	2.74	53.4	41.1	1.15
20H-5, 130–133	183.80	1.84	2.74	55.9	45.1	1.27
20H-6, 130–133	185.30	1.85	2.75	57.5	46.6	1.35
21H-1, 96–99	186.96	1.93	2.73	52.8	38.9	1.12
21H-2, 96–99	188.46	1.97	2.77	51.4	36.4	1.06
21H-3, 96–99	189.96	1.99	2.79	50.7	35.4	1.03
21H-4, 96–99	191.21	1.94	2.74	53.4	39.3	1.15
21H-5, 96–99	192.71	2.09	2.87	56.4	38.2	1.29
21H-6, 94–97	194.19	1.97	2.87	57.0	42.1	1.32
22H-1, 125–127	196.75	1.89	2.74	55.3	42.7	1.24
22H-2, 125–127	198.25	1.91	2.75	56.2	43.2	1.29
22H-3, 125–127	199.75	1.96	2.81	58.4	43.9	1.40
22H-5, 125–127	202.75	1.91	2.89	60.5	47.9	1.53
23H-1, 131–133	206.31	1.82	2.78	54.1	43.8	1.18
23H-2, 131–133	207.77	1.83	2.74	58.5	48.6	1.41
23H-3, 131–133	209.27	1.81	2.77	56.4	46.9	1.29
23H-4, 80–82	210.26	2.06	2.79	45.9	29.5	0.85
23H-5, 73–75	211.52	2.03	2.78	54.0	37.5	1.18

creases in eustatic sea level occurred. What factors controlled bank-top carbonate production and off-bank transport during this time period regardless of changes in eustatic sea level? For now, we can only speculate that either the eustatic rises and declines were too rapid or that a tectonic factor controlled the relative position of the banks with respect to sea level. In either case, the rate of change might have been too fast to permit the carbonate banks to respond quickly enough to remain viable carbonate sources.

Subsidence data from exploration and scientific drill holes off northeastern Australia indicate that the region has not subsided wholly as a result of uniform post-rift thermal cooling. These data indicate that subsidence pulses have occurred at different times. DSDP Site 209 (Burne, Andrews, et al., 1973) suggested that the subsidence history of the Queensland Plateau has been characterized by progressively increased rates of subsidence. An initial slow rate (20 m/m.y.) was followed by an increase to 40 m/m.y. after the middle Miocene. The bottom part of lithologic Unit III of early middle Miocene age indicates that it is composed of chalks and represents a marked increase in paleobathymetry, compared to the shallow-water sediments below. This change probably represents the first pulse of more rapid tectonic subsidence of the Queensland Plateau and confirms that a sharply increased subsidence pulse occurred in the early middle Miocene. Results from the other Leg 133 sites on the Queensland Plateau will determine whether subsidence has been uniform over the Plateau or whether distinct areas experienced different tectonic histories. Indeed, it will be particularly interesting to compare the subsidence of northern and southern sites to test whether the plateau has tilted to the north, as advocated by earlier scientists (Mutter and Karner, 1980).

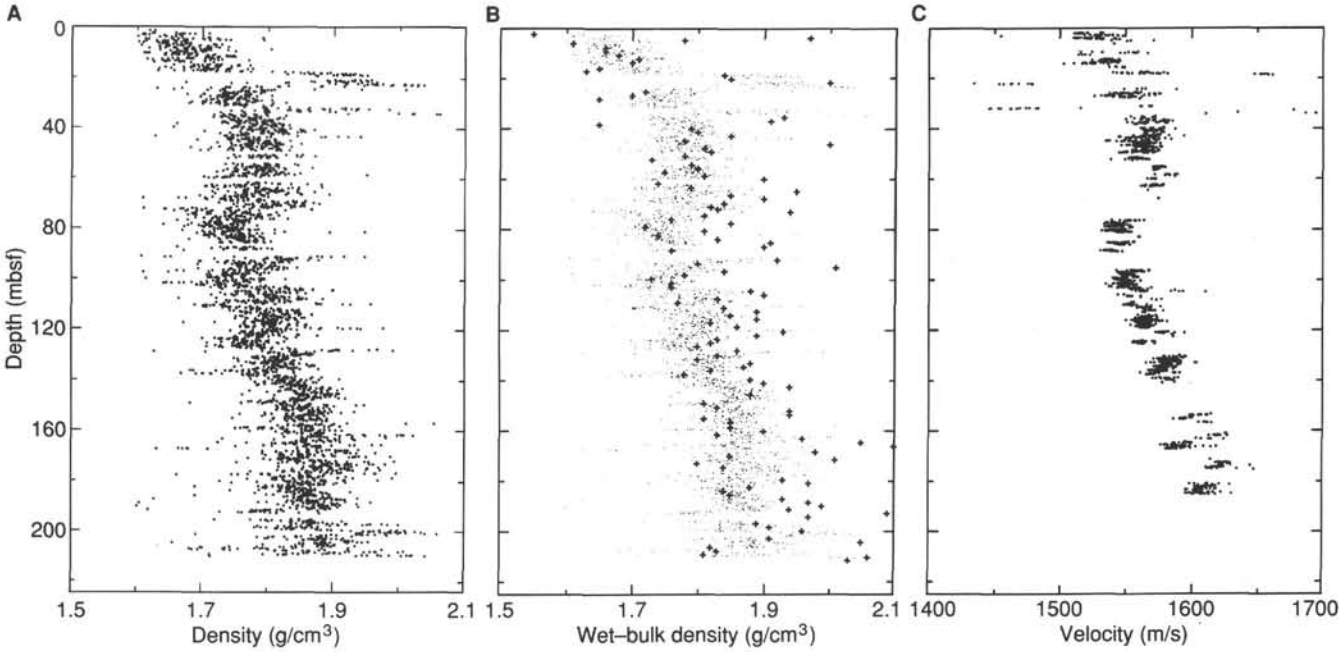

Figure 33. **A.** GRAPE bulk density for Hole 811A. **B.** Comparison of GRAPE bulk density (dots) with discrete data (crosses). **C.** *P*-wave velocities from MST logger, Site 811.

Paleogene–Lower Neogene Sediments

The poor recovery of underlying Paleogene to lower Neogene sediments in Holes 811B and 825A was disappointing, but sufficient material was retrieved to give an impression of the evolving environment at Sites 811/825 on the Queensland Plateau from the Paleogene (early to middle Eocene) to the early Neogene (middle Miocene). The sparse recovery provides us with a cursory view of the depositional processes that must have occurred during the late Paleogene and early Neogene. Based on an initial interpretation, sediments deposited during the early-to-middle Miocene apparently represent a major change in water depth from the overlying periplatform shelf deposits in a middle bathyal environment to shallow-water deposits in a tropical fore- or back-reef environment with water depths less than 50 m. Neritic deposits are indicated by the occurrence of larger benthic foraminifers in the lower Miocene section. In addition to the benthic foraminifers, Unit IV (early to middle Miocene) contains redeposited sand and rubble composed mostly of skeletal grains, such as coral debris, alcyonarian spicules, mollusk fragments, echinoids, crustaceans, bryozoans, and red algae, all of which document the passage to a neritic environment.

In the lower section of Hole 811B, the recovery of a fine-grained skeletal packstone (Unit V) that contains upper Oligocene planktonic foraminifers indicates that cooler, open-marine waters prevailed and promoted environmental conditions considerably different from the overlying tropical water sediments. Drilling at Hole 825B recovered middle Eocene to lower Miocene, temperate-to-subtropical sediments that contain coralline algae, echinoids, mollusks, and small branching corals, apparently deposited on an inner neritic shelf. At Site 825, the lowermost sediments probably represent the transgressive facies overlying the continental basement, which is composed of Paleozoic(?) metasedimentary rocks. The relatively rapid transition from temperate to tropical sedimentsreflects the initiation of the southward flow of tropical waters from the equatorial Pacific, combined with the northward movement of the Australian Plate.

REFERENCES

Adams, C. G., 1970. A reconsideration of the East Indian Letter Classification. *Bull. Br. Mus. Nat. Hist. (Geol.),* 19:87–137.

Andrews, J. E., 1973. Correlation of seismic reflectors. *In* Burns, R. E., Andrews, J. E., et al., *Init. Repts. DSDP,* 21: Washington (U.S. Govt. Printing Office), 459–479.

Baker, P. A., and Bloomer, S. H., 1988. The origin of celestite in deep-sea carbonate sediments. *Geochim. Cosmochim. Acta,* 52:335–339.

Berggren, W. A., Kent, D. V., and Van Couvering, J. A., 1985. The Neogene: Part 2. Neogene geochronology and chronostratigraphy. *In* Snelling, N. J. (Ed.), *The Chronology of the Geological Record.* Geol. Soc. London Mem., 10:211–260.

Boersma, A., 1984. *A Handbook of Common Tertiary* Uvigerina: Stony Point, NY (Microclimates Press).

Chaproniere, G.C.H., 1981. Australasian mid-Tertiary larger foraminiferal associations and their bearing on the East Indian Letter Classification. *J. Aust. Geol. Geophys.,* 6:145–151.

Droxler, A. W., Bruce, C. H., Sager, W. W., and Watkins, D. H., 1988. Pliocene-Pleistocene variations in aragonite content and planktonic oxygen-isotope record in Bahamian periplatform ooze, Hole 633A. *In* Austin, J. A., Jr., Schlager, W., et al., *Proc. ODP, Sci. Results,* 101: College Station, TX (Ocean Drilling Program), 221–244.

Droxler, A. W., Haddad, G. A., Mucciarone, D. A., and Cullen, J. L., 1990. Pliocene-Pleistocene aragonite cyclic variations in Holes 714A and 716B (The Maldives) compared with Hole 633A (The Bahamas): records of climate-induced $CaCO_3$ preservation at intermediate water depths. *In* Duncan, R. A., Backman, J., Peterson, L. C., et al., *Proc. ODP, Sci. Results,* 115: College Station, TX (Ocean Drilling Program), 539–577.

Droxler, A. W., and Schlager, W., 1985. Glacial/interglacial sedimentation rates and turbidite frequency in the Bahamas. *Geology,* 13:799–802.

Feary, D. A., Pigram, C. J., Davies, P. J., Symonds, P. A., Droxler, A. W., and Peerdeman, F., 1990. Ocean drilling Project–Leg 133 safety package. *Bur. Miner. Res. Aust. Rec.,* 1990/6.

Gieskes, J. M., 1981. Deep-sea drilling interstitial water studies: implications for chemical alteration of the oceanic crust, layers I and II. *In* Warme, J. E., Douglas, R. G., and Winterer, E. L. (Eds.), *The Deep Sea Drilling Project: A Decade of Progress*. Soc. Econ. Paleontol. Mineral. Spec. Publ., 32:149–167.
Hamilton, E. L., 1979. Sound velocity gradients in marine sediments. *J. Acoust. Soc. Am.*, 65:909–922.
Haq, B. U., Hardenbol, J., and Vail, P. R., 1987. Chronology of fluctuating sea levels since the Triassic. *Science*, 235:1156–1167.
McDuff, R. E., 1981. Major cation gradients in DSDP interstitial waters: the role of diffusive exchange between seawater and upper oceanic crust. *Geochim. Cosmochim. Acta*, 45:1705–1713.
Mutter, J. C., and Karner, G. D., 1980. The continental margin off northeast Australia. *In* Henderson, R. A., and Stephenson, P. J. (Eds.), *The Geology and Geophysics of Northeast Australia:* Brisbane (Geol. Soc. of Australia, Queensland Division), 47–69.
Schlager, W., and James, N. P., 1978. Low-magnesian calcite limestones forming at the deep-sea floor, Tongue of the Ocean, Bahamas. *Sedimentology*, 15:675–702.
Shackleton, N. J., and Hall, M. A., 1989. Stable isotope history of the Pleistocene at ODP Site 677. *In* Becker, K., Sakai, H., et al., *Proc. ODP, Sci. Results*, 111: College Station, TX (Ocean Drilling Program), 295–316.
Shipboard Scientific Party, 1973. Site 209. *In* Burns, R. E., Andrews, J. E., et al., *Init. Repts. DSDP*, 21: Washington (U.S. Govt. Printing Office), 333–367.
Swart, P. K., and Burns, S. J., 1990. Pore-water chemistry and carbonate diagenesis in sediments from Leg 115: Indian Ocean. *In* Duncan, R. A., Backman, J., Peterson, L. C., et al., *Proc. ODP, Sci. Results*, 115: College Station, TX (Ocean Drilling Program), 629–645.
Swart, P. K., and Guzikowski, M., 1988. Interstitial-water chemistry and diagenesis of periplatform sediments from the Bahamas, ODP Leg 101. *In* Austin, J. A., Jr., Schlager, W., et al., *Proc. ODP, Sci. Results*, 101: College Station, TX (Ocean Drilling Program), 363–380.
Symonds, P. A., and Davies, P. J., 1988. Structure, stratigraphy, evolution and regional framework of the Townsville Trough and Marion Plateau region–research cruise proposal, project 9131.11. *Bur. Miner. Res. Aust. Rec.*, 1988/48.
van Morkhoven, F.P.C.M., Berggren, W. A., and Edwards, A. S., et al., 1986. Cenozoic cosmopolitan deep-water benthic foraminifera. *Bull. Cent. Rech. Explor.-Prod. Elf-Aquitaine*, Mem. 11.

Ms 133-104

NOTE: All core description forms ("barrel sheets") and core photographs have been printed on coated paper and bound separately as Part 2 of this volume, beginning on page 813.

Table 13. Compressional wave velocities from the Hamilton Frame, Site 811.

Core, section, interval (cm)	Depth (mbsf)	Distance (mm)	Traveltime (μs)	Velocity (m/s)
133-811A-				
5H-1, 137–140	35.37	26.10	21.53	1341
5H-2, 139–142	36.89	27.37	21.52	1407
5H-3, 127–130	38.27	29.11	21.52	1497
5H-4, 130–133	39.80	23.09	19.90	1295
5H-5, 130–133	41.30	27.18	19.88	1526
5H-6, 130–133	42.80	25.40	18.82	1516
6H-1, 133–138	44.83	26.93	19.70	1527
6H-2, 133–138	46.28	28.39	20.97	1502
6H-3, 134–137	47.79	27.80	19.88	1561
6H-4, 134–138	49.29	27.53	19.60	1570
6H-5, 135–138	50.80	27.85	19.93	1559
6H-6, 134–137	52.29	28.01	19.94	1567
7H-1, 136–140	54.36	27.58	19.65	1569
7H-2, 135–138	55.85	27.36	19.49	1570
7H-3, 135–138	57.35	27.40	19.33	1587
7H-4, 135–138	58.85	27.06	19.40	1561
7H-5, 99–102	59.99	23.48	16.87	1586
7H-6, 133–136	61.83	27.62	19.79	1559
8H-1, 94–97	63.44	27.64	19.43	1592
8H-2, 95–98	64.95	27.88	19.41	1608
8H-3, 95–98	66.45	27.54	19.63	1568
8H-4, 76–79	67.76	27.23	21.94	1370
8H-5, 106–109	69.56	27.66	20.27	1520
8H-6, 106–109	71.06	28.80	20.06	1601
8H-7, 34–37	71.84	27.60	19.56	1578
9H-1, 101–104	73.01	26.27	21.49	1353
9H-2, 101–104	74.51	29.71	24.11	1348
9H-3, 101–104	76.01	29.01	23.81	1334
9H-4, 101–104	77.51	27.18	19.73	1539
9H-5, 101–104	79.01	27.15	19.63	1546
9H-6, 101–104	80.51	26.67	19.16	1560
10H-1, 81–84	82.31	27.46	19.78	1550
10H-2, 81–84	83.81	28.42	20.64	1530
10H-3, 66–69	85.16	29.11	23.58	1353
10H-4, 76–79	86.76	27.45	19.78	1550
10H-5, 76–79	88.26	26.79	19.57	1531
11H-1, 104–107	92.04	28.02	21.58	1436
11H-2, 104–107	93.54	29.15	23.46	1356
11H-3, 105–108	95.05	27.89	22.40	1372
11H-4, 105–108	96.55	27.38	19.47	1573
11H-5, 105–108	98.05	27.85	19.96	1557
11H-6, 105–108	99.55	27.66	22.54	1351
12H-1, 82–85	101.32	28.56	20.54	1546
12H-2, 82–85	102.82	27.80	19.91	1558
12H-3, 82–85	104.32	25.42	17.91	1605
12H-4, 96–99	105.96	26.97	19.05	1588
12H-5, 102–105	107.52	26.23	18.83	1565
12H-6, 102–105	109.02	28.24	19.97	1578
13H-1, 101–104	111.01	28.85	20.96	1527
13H-2, 101–104	112.51	27.62	19.56	1579
13H-3, 101–104	114.01	26.36	18.87	1569
13H-4, 101–104	115.51	27.86	19.87	1565
13H-5, 101–104	117.01	28.58	20.23	1574
13H-6, 101–104	118.51	26.71	19.13	1566
14H-1, 101–104	120.51	27.28	19.47	1568
14H-2, 101–104	122.01	26.93	19.28	1565
14H-3, 101–104	123.51	27.40	19.63	1560
14H-4, 101–104	125.01	27.28	19.62	1554
14H-5, 101–104	126.51	28.07	22.74	1358
14H-6, 101–104	128.01	23.26	16.63	1597
15H-1, 101–104	130.01	28.26	20.23	1556
15H-2, 101–104	131.51	23.52	17.16	1558
15H-3, 101–104	133.01	28.58	22.58	1393
15H-4, 101–104	134.51	29.36	21.13	1540
15H-5, 101–104	136.01	28.22	19.97	1576
15H-6, 101–104	137.51	27.41	19.49	1573
16H-1, 101–104	139.51	27.06	19.46	1556
16H-2, 101–104	141.01	25.71	18.68	1548
16H-3, 101–104	142.51	24.75	17.56	1598
16H-4, 101–104	144.01	11.99	9.39	1638
16H-5, 101–104	145.51	23.09	16.23	1630
18H-1, 101–104	158.51	26.88	19.93	1505
18H-2, 101–104	160.01	28.24	19.93	1581
18H-3, 101–104	161.51	25.44	18.43	1555

Table 13 (continued).

Core, section, interval (cm)	Depth (mbsf)	Distance (mm)	Traveltime (μs)	Velocity (m/s)
18H-4, 101–104	163.01	26.75	18.95	1585
18H-5, 101–104	164.51	23.22	16.70	1587
18H-6, 101–104	166.01	27.14	18.74	1628
19H-1, 137–140	168.37	28.36	19.66	1612
19H-2, 137–140	169.87	27.59	22.31	1363
19H-4, 137–140	172.87	27.94	19.35	1617
19H-5, 137–140	174.37	28.58	19.87	1605
19H-6, 137–140	175.87	28.49	19.69	1617
20H-2, 130–133	179.30	28.59	19.71	1621
20H-3, 130–133	180.80	29.15	20.03	1623
20H-4, 130–133	182.30	28.59	19.80	1612
20H-5, 130–133	183.80	27.98	19.36	1618
20H-6, 130–133	185.30	28.20	19.42	1625
21H-1, 96–99	186.96	27.90	19.42	1608
22H-1, 125–127	196.75	29.51	22.58	1610
22H-2, 125–127	198.25	29.51	22.60	1608
22H-3, 125–127	199.75	30.02	23.05	1597
22H-5, 125–127	202.75	29.72	22.59	1621
22H-6, 125–127	204.25	29.34	22.80	1582
23H-1, 131–133	206.31	25.05	19.97	1594
23H-2, 131–133	207.77	28.59	20.56	1753
23H-3, 131–133	209.27	26.23	20.89	1576
23H-5, 73–75	211.52	28.58	22.38	1576

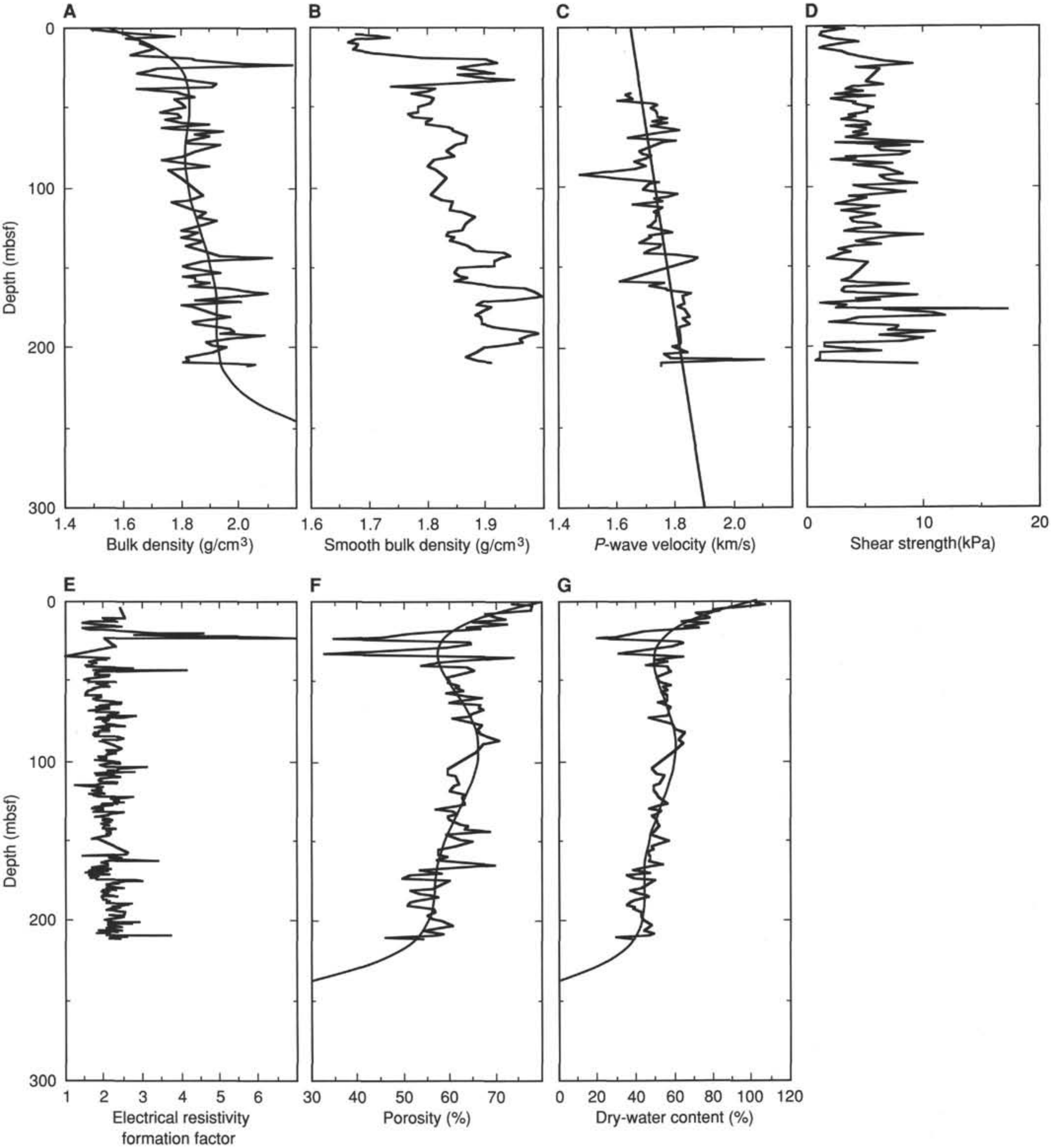

Figure 34. Physical properties data vs. depth, Hole 811A. **A.** Wet bulk density, regression equation $y = 1.5516 + 1.7574 \times 10^{-2}X - 3.9633 \times 10^{-4}X^2 + 3.9116 \times 10^{-6}X^{3\text{-}1}0.7065 \times 10^{-8}X^4 + 2.7259 \times 10^{-11}X^5$ for Y = bulk density (g/cm^3) and X = depth (mbsf), with regression coefficient $R = 0.81$. **B.** Smoothed pycnometer bulk density. **C.** Hamilton frame *P*-wave velocity, (values < 1400 km/s removed). Regression equation $Y = 1.5238 + 4.2324 \times 10^{-4}X$ for Y = *P*-wave velocity (km/s) and X = depth (mbsf) with regression coefficient $R = 0.74$. **D.** Shear strength. **E.** Formation factor. **F.** Porosity. Regression equation $Y = 79.92 - 1.75X - 4.5946 \times 10^{-2}X^{2\text{-}4}0.7757 \times 10^{-4}X^3 + 2.1473 \times 10^{-6}X^{4\text{-}3}0.5233 \times 10^{-9}X^5$, where Y = porosity (%), X = depth (mbsf), and regression coefficient $R = 0.80$. **G.** Dry-water content. Regression equation $Y = 102.11 - 3.7564X + 9.16 \times 10^{-2}X^{2\text{-}9}0.3014 \times 10^{-4}X^3 + 4.1503 \times 10^{-6}X^{4\text{-}6}0.7859 \times 10^{-9}X^5$, where Y = water content (%), X = depth (mbsf), and regression coefficient $R = 0.91$.

Table 14. Vane shear strength data, Site 811.

Core, section, interval (cm)	Depth (mbsf)	Torque (deg.)	Strain (deg.)	Shear str. (kPa)
133-811A-				
1H-1, 76–78	0.76	7	2	1.5
1H-2, 93–95	2.43	15	6	3.2
1H-3, 93–95	3.93	6	3	1.3
1H-4, 58–60	5.08	6	1	1.3
2H-1, 95–96	6.45	5	32	1.1
2H-2, 94–95	7.94	11	18	2.3
2H-3, 94–95	9.44	21	17	4.5
2H-4, 94–95	10.94	14	13	3.0
2H-5, 97–98	12.47	7	14	1.5
2H-6, 96–97	13.96	5	23	1.1
3H-1, 96–97	15.96	14	18	3.0
3H-2, 96–97	17.46	17	16	3.6
3H-5, 103–104	22.03	31	21	6.6
3H-6, 101–104	23.51	43	21	9.1
4H-1, 95–96	25.45	20	19	4.2
4H-2, 96–97	26.96	29	23	6.2
5H-1, 101–102	35.01	24	22	5.1
5H-2, 102–103	36.52	31	20	6.6
5H-3, 102–103	38.02	19	20	4.0
5H-4, 101–102	39.51	16	15	3.4
5H-5, 102–103	41.02	23	17	4.9
5H-6, 101–102	42.51	12	22	2.5
5H-7, 77–78	43.77	28	13	5.9
6H-1, 86–87	44.36	16	15	3.4
6H-2, 100–101	45.95	10	23	2.1
6H-3, 100–101	47.45	20	11	4.2
6H-4, 100–101	48.95	19	16	4.0
6H-5, 100–101	50.45	27	16	5.7
6H-6, 100–101	51.95	25	17	5.3
7H-1, 99–100	53.99	25	16	5.3
7H-2, 99–100	55.49	17	17	3.6
7H-3, 99–100	56.99	20	18	4.2
7H-4, 99–100	58.49	14	14	3.0
7H-5, 99–100	59.99	24	17	5.1
7H-6, 99–100	61.49	26	15	5.5
7H-7, 62–63	62.62	16	6	3.4
8H-1, 91–92	63.41	24	13	5.1
8H-2, 91–92	64.91	24	18	5.1
8H-3, 91–92	66.41	19	12	4.0
8H-4, 91–92	67.91	25	18	5.3
8H-5, 85–86	69.35	16	27	3.4
8H-6, 95–96	70.95	24	15	5.1
8H-7, 58–59	72.08	47	17	10.0
9H-1, 89–90	72.89	12	13	2.5
9H-2, 89–90	74.39	42	17	8.9
9H-3, 89–90	75.89	28	17	5.9
9H-4, 89–90	77.39	30	13	6.4
9H-5, 89–90	78.89	42	16	8.9
9H-6, 89–90	80.39	38	15	8.1
9H-7, 19–20	81.19	16	18	3.4
10H-1, 91–92	82.41	20	14	4.2
10H-2, 91–92	83.91	10	9	2.1
10H-3, 71–72	85.21	35	18	7.4
10H-4, 91–92	86.91	19	16	4.0
10H-5, 91–92	88.41	31	16	6.6
11H-1, 91–92	91.91	39	19	8.3
11H-2, 92–93	93.42	29	23	6.2
11H-3, 92–93	94.92	32	23	6.8
11H-4, 92–93	96.42	34	15	7.2
11H-5, 92–93	97.92	45	13	9.5
11H-6, 92–93	99.42	19	15	4.0
12H-1, 92–93	101.42	26	15	5.5
12H-2, 92–93	102.92	40	18	8.5
12H-3, 92–93	104.42	33	16	7.0
12H-4, 105–106	106.05	17	14	3.6
12H-5, 93–94	107.43	24	16	5.1
12H-6, 93–94	108.93	18	18	3.8
13H-1, 93–94	110.93	12	18	2.5
13H-2, 93–94	112.43	29	17	6.2
13H-3, 93–94	113.93	20	17	4.2
13H-4, 93–94	115.43	14	14	3.0
13H-5, 93–94	116.93	28	15	5.9
13H-6, 93–94	118.43	24	15	5.1
14H-1, 94–95	120.44	18	15	3.8
14H-2, 94–95	121.94	19	12	4.0
14H-3, 94–95	123.44	27	16	5.7
14H-4, 94–95	124.94	30	13	6.4
14H-5, 94–95	126.44	21	12	4.5
14H-6, 94–95	127.94	15	13	3.2
15H-1, 94–95	129.94	47	14	10.0
15H-2, 94–95	131.44	35	17	7.4
15H-3, 94–95	132.94	25	11	5.3
15H-4, 94–95	134.44	20	15	4.2
15H-5, 94–95	135.94	30	13	6.4
15H-6, 94–95	137.44	20	11	4.2
16H-1, 93–94	139.43	13	15	2.8
16H-2, 93–94	140.93	18	15	3.8
16H-3, 81–82	142.31	14	13	3.0
16H-4, 81–82	143.81	11	9	2.3
16H-5, 92–93	145.42	8	5	1.7
16H-6, 100–101	147.00	25	18	5.3
17H-6, 100–101	156.50	18	13	3.8
18H-1, 99–100	158.49	14	10	3.0
18H-2, 98–99	159.98	20	12	4.2
18H-3, 91–92	161.41	41	8	8.7
18H-4, 91–92	162.91	15	11	3.2
18H-5, 91–92	164.41	14	15	3.0
18H-6, 91–92	165.91	15	8	3.2
18H-7, 41–42	166.91	32	13	6.8
19H-1, 125–126	168.25	45	10	9.5
19H-2, 103–104	169.53	20	15	4.2
19H-3, 103–104	171.03	29	16	6.2
19H-4, 103–104	172.53	5	19	1.1
19H-5, 103–104	174.03	16	23	3.4
19H-6, 103–104	175.53	12	24	2.5
19H-7, 70–71	176.70	81	17	17.2
20H-1, 75–76	177.25	31	12	6.6
20H-2, 91–92	178.91	51	19	10.8
20H-3, 91–92	180.41	56	20	11.9
20H-4, 91–92	181.91	21	14	4.5
20H-5, 91–92	183.41	16	19	3.4
20H-6, 91–92	184.91	9	12	1.9
21H-1, 91–92	186.91	37	22	7.9
21H-2, 91–92	188.41	36	15	7.6
21H-3, 91–92	189.91	33	16	7.0
21H-4, 91–92	191.16	52	16	11.0
21H-5, 99–100	192.74	29	22	6.2
21H-6, 99–100	194.24	47	27	10.0
22H-1, 99–100	196.49	38	16	8.1
22H-2, 99–100	197.99	7	31	1.5
22H-3, 99–100	199.49	7	33	1.5
22H-4, 99–100	200.99	13	11	2.8
22H-5, 99–100	202.49	30	10	6.4
22H-6, 99–100	203.99	5	18	1.1
23H-1, 99–100	205.99	5	9	1.1
23H-2, 99–100	207.45	5	8	1.1
23H-3, 99–100	208.95	4	14	0.8
23H-4, 85–86	210.31	45	23	9.5

Shear str. = shear strength; deg. = degrees.

Table 15. Electrical resistivity formation factors, Site 811.

Core, section, interval (cm)	Depth (mbsf)	Seawater (ohms)	Sample (ohms)	Formation factor
133-811A-				
1H-4, 20	4.70	3.9	9.5	2.42
2H-4, 10	10.10	3.3	8.4	2.56
2H-4, 40	10.40	3.3	6.5	1.98
2H-4, 70	10.70	3.3	7.5	2.29
2H-4, 120	11.20	3.3	7.4	2.27
2H-5, 20	11.70	3.5	7.1	2.03
2H-5, 70	12.20	3.5	8.1	2.32
2H-5, 121	12.71	3.6	8.5	2.34
2H-6, 20	13.20	3.9	6.4	1.66
2H-6, 70	13.70	3.9	5.6	1.45
2H-6, 117	14.17	4.0	5.8	1.47
3H-1, 20	15.20	3.7	6.6	1.81
3H-1, 70	15.70	3.2	7.8	2.45
3H-1, 124	16.24	3.2	7.9	2.44
3H-2, 20	16.70	4.7	6.8	1.46
3H-2, 118	17.68	4.1	6.8	1.67
3H-3, 20	18.20	4.1	8.2	2.01
3H-3, 70	18.70	3.7	10	2.67
3H-4, 20	19.70	2.6	8.8	3.35
3H-4, 70	20.20	2.5	11.6	4.58
3H-4, 120	20.70	2.7	11.3	4.23
3H-5, 13	21.13	4.1	11.3	2.79
3H-5, 73	21.73	3.8	15.4	4.01
3H-5, 120	22.20	3.9	20.5	5.31
3H-6, 64	23.14	3.9	27	6.99
3H-6, 124	23.74	3.9	7.8	2.02
4H-3, 20	27.70	3.1	6.8	2.21
4H-3, 120	28.70	3.1	7.2	2.32
5H-1, 44	34.44	7.0	7.2	1.02
5H-2, 20	35.70	3.1	6.6	2.13
5H-2, 70	36.20	3.5	6.9	1.97
5H-2, 120	36.70	3.3	6.8	2.05
5H-3, 20	37.20	4.1	7.7	1.87
5H-3, 70	37.70	4.1	6.9	1.67
5H-3, 120	38.20	4.2	6.8	1.63
5H-4, 20	38.70	4.1	7.5	1.81
5H-4, 70	39.20	4.2	7.1	1.7
5H-4, 120	39.70	4.2	7	1.68
5H-5, 20	40.20	4.4	6.7	1.52
5H-5, 70	40.70	4.1	7.2	1.76
5H-5, 120	41.20	4.1	6.9	1.68
5H-6, 20	41.70	4.6	7.3	1.59
5H-6, 120	42.70	3.5	9.6	2.74
5H-7, 20	43.20	4.2	7.4	1.76
5H-7, 70	43.70	4.3	7.5	1.74
6H-1, 20	43.70	3.5	14.5	4.14
6H-1, 70	44.20	3.7	7	1.89
6H-1, 133	44.83	3.8	7.1	1.87
6H-2, 20	45.15	3.8	6.8	1.79
6H-2, 70	45.65	3.8	7	1.84
6H-2, 120	46.15	3.8	6.8	1.79
6H-3, 20	46.65	3.2	6.8	2.13
6H-3, 70	47.15	3.3	7	2.12
6H-3, 120	47.65	3.4	7.1	2.09
6H-4, 20	48.15	4.2	6.9	1.64
6H-4, 70	48.65	4.3	6.9	1.6
6H-4, 120	49.15	4.5	6.6	1.47
6H-5, 20	49.65	4.5	7.3	1.62
6H-5, 70	50.15	4.5	7	1.56
6H-5, 120	50.65	4.5	7.2	1.6
6H-6, 20	51.15	3.1	7.2	2.32
6H-6, 20	51.15	3.8	7.4	1.95
6H-6, 70	51.65	3.4	7.2	2.12
6H-6, 70	51.65	3.8	7.6	2
6H-6, 120	52.15	3.4	6.9	2.03
6H-6, 120	52.15	4.1	7.4	1.8
7H-1, 60	53.60	3.7	8	2.16
7H-1, 120	54.20	3.9	7.6	1.94
7H-2, 20	54.70	4.3	7.5	1.75
7H-2, 70	55.20	4.4	7.8	1.78
7H-2, 120	55.70	4.4	7.2	1.64
7H-3, 20	56.20	4.7	7.6	1.61
7H-3, 70	56.70	4.8	7.6	1.59
7H-3, 120	57.20	4.9	7.7	1.57
7H-4, 20	57.70	4.9	7.6	1.55

Table 15 (continued).

Core, section, interval (cm)	Depth (mbsf)	Seawater (ohms)	Sample (ohms)	Formation factor
7H-4, 70	58.20	4.9	7.6	1.56
7H-4, 120	58.70	4.9	7.5	1.54
7H-5, 20	59.20	3.8	7.3	1.94
7H-5, 70	59.70	3.8	6.9	1.8
7H-5, 120	60.20	3.8	7.2	1.88
7H-6, 20	60.70	4.1	7.9	1.95
7H-6, 70	61.20	4.1	7	1.72
7H-7, 20	62.20	3.8	7.1	1.87
7H-7, 70	62.70	3.8	6.8	1.8
8H-1, 40	62.90	3.4	8.3	2.47
8H-2, 20	64.20	3.3	8	2.41
8H-2, 70	64.70	3.3	7.3	2.18
8H-2, 90	64.90	3.4	8.1	2.36
8H-2, 120	65.20	3.4	6.6	1.91
8H-3, 20	65.70	3.8	8.2	2.16
8H-3, 70	66.20	3.8	7	1.82
8H-3, 120	66.70	3.9	7.2	1.85
8H-3, 130	66.80	3.5	7.4	2.12
8H-4, 20	67.20	3.6	7.8	2.15
8H-4, 70	67.70	3.6	7.4	2.09
8H-4, 120	68.20	3.6	5.9	1.63
8H-5, 20	68.70	3.8	6.8	1.8
8H-5, 70	69.20	3.9	7.1	1.82
8H-5, 120	69.70	3.9	7.6	1.94
8H-6, 6	70.06	3.3	7.9	2.4
8H-6, 70	70.70	3.3	7.4	2.27
8H-6, 120	71.20	3.3	7.3	2.21
8H-7, 20	71.70	3.5	7.4	2.09
8H-7, 64	72.14	3.7	8.1	2.22
9H-1, 20	72.20	3.8	10.8	2.82
9H-1, 68	72.68	3.9	9.6	2.46
9H-1, 120	73.20	3.9	7.2	1.88
9H-2, 20	73.70	3.8	7	1.83
9H-2, 70	74.20	3.8	8	2.13
9H-2, 120	74.70	3.8	8	2.11
9H-3, 20	75.20	3.8	7.6	1.97
9H-3, 70	75.70	3.8	7.8	2.07
9H-4, 20	76.70	3.9	8	2.07
9H-4, 70	77.20	4.0	8.4	2.11
9H-4, 120	77.70	3.8	9.8	2.57
9H-5, 20	78.20	3.9	8.1	2.06
9H-5, 70	78.70	3.9	7	1.78
9H-5, 120	79.20	3.9	8.4	2.16
9H-6, 20	79.70	3.9	7.6	1.94
9H-6, 70	80.20	3.9	7.8	2.02
9H-6, 120	80.70	3.9	8.4	2.12
9H-7, 20	81.20	3.9	8.4	2.16
10H-1, 20	81.70	4.0	7.5	1.89
10H-1, 70	82.20	3.8	7	1.84
10H-1, 120	82.70	3.9	7	1.78
10H-2, 20	83.20	4.0	6.8	1.73
10H-2, 70	83.70	3.9	7.4	1.87
10H-2, 120	84.20	3.9	7	1.79
10H-3, 20	84.70	3.4	8	2.33
10H-3, 70	85.20	3.4	8.6	2.5
10H-4, 20	86.20	3.1	7.1	2.3
10H-4, 70	86.70	3.6	7.1	1.99
10H-4, 120	87.20	3.6	7.2	1.99
10H-5, 20	87.70	3.7	7.1	1.91
10H-5, 70	88.20	3.7	7.3	1.98
11H-1, 70	91.70	3.9	9.6	2.45
11H-1, 120	92.20	3.9	9.6	2.45
11H-2, 20	92.70	3.4	8.1	2.36
11H-2, 70	93.20	3.4	6.9	2.06
11H-2, 120	93.70	3.5	8	2.31
11H-3, 20	94.20	3.8	8.2	2.17
11H-3, 70	94.70	3.8	7.9	2.12
11H-3, 120	95.20	3.8	8.7	2.3
11H-4, 70	96.20	3.9	8.2	2.08
11H-4, 120	96.70	3.9	8	2.05
11H-5, 20	97.20	3.9	7.8	1.98
11H-5, 70	97.70	3.9	7.2	1.85
11H-5, 120	98.20	3.9	7.5	1.92
11H-6, 20	98.70	3.9	8	2.05
11H-6, 70	99.20	3.9	7.8	2.01
11H-6, 120	99.70	4.0	7.1	2.37
12H-1, 20	100.70	3.3	7.7	2.37

Table 15 (continued).

Core, section, interval (cm)	Depth (mbsf)	Seawater (ohms)	Sample (ohms)	Formation factor
12H-1, 70	101.20	3.3	8	2.41
12H-1, 120	101.70	3.4	7.3	2.14
12H-2, 20	102.20	3.9	7.5	1.92
12H-2, 70	102.70	4.0	7.5	1.88
12H-2, 120	103.20	3.9	7.9	2.05
12H-3, 20	103.70	3.9	12	3.11
12H-3, 70	104.20	3.9	9.2	2.39
12H-3, 120	104.70	3.7	8.7	2.38
12H-4, 20	105.20	3.9	9.2	2.36
12H-4, 70	105.70	3.9	8.3	2.1
12H-4, 120	106.20	3.9	8.3	2.11
12H-5, 20	106.70	3.9	10.9	2.79
12H-5, 70	107.20	4.0	10.2	2.56
12H-5, 120	107.70	4.0	7	1.77
12H-6, 20	108.20	4.1	9.2	2.25
12H-6, 70	108.70	4.0	7.2	1.8
12H-6, 120	109.20	4.1	8.7	2.13
13H-1, 30	110.30	4.1	9.9	2.43
13H-1, 80	110.80	4.2	8	1.9
13H-2, 20	111.70	4.2	8.1	1.92
13H-2, 70	112.20	4.3	7.9	1.86
13H-2, 120	112.70	4.3	8.4	1.95
13H-3, 20	113.20	4.3	9.9	2.33
13H-3, 70	113.70	4.3	9.8	2.3
13H-3, 120	114.20	4.1	7.9	1.94
13H-4, 20	114.70	4.1	7.5	1.82
13H-4, 70	115.20	6.2	7.8	1.26
13H-4, 120	115.70	4.2	7.6	1.82
13H-5, 20	116.20	4.4	8.1	1.86
13H-5, 70	116.70	4.2	8.3	1.99
13H-5, 120	117.20	4.4	8	1.83
13H-6, 20	117.70	4.2	7.5	1.82
13H-6, 70	118.20	4.1	8	1.94
13H-6, 120	118.70	4.5	7.6	1.71
14H-1, 70	120.20	4.4	9	2.04
14H-1, 120	120.70	4.5	7.3	1.62
14H-2, 20	121.20	4.5	8.6	1.9
14H-2, 70	121.70	4.9	8.5	1.74
14H-2, 120	122.20	4.5	8.5	1.9
14H-3, 20	122.70	2.9	8.1	2.74
14H-3, 70	123.20	3.3	7.5	2.26
14H-3, 120	123.70	3.4	7.4	2.19
14H-4, 20	124.20	3.2	7.7	2.39
14H-4, 70	124.70	3.4	7.8	2.28
14H-4, 120	125.20	3.4	7.8	2.28
14H-5, 20	125.70	3.1	7.6	2.49
14H-5, 70	126.20	3.3	7.6	2.27
14H-5, 120	126.70	3.6	8.4	2.35
14H-6, 20	127.20	4.3	8.5	1.98
14H-6, 70	127.70	4.4	8.4	1.92
14H-6, 120	128.20	4.1	9	2.21
15H-1, 24	129.24	4.6	8.1	1.76
15H-1, 70	129.70	4.7	7.9	1.68
15H-1, 120	130.20	4.2	8.4	2
15H-2, 20	130.70	4.2	8.3	1.98
15H-2, 70	131.20	4.2	7.8	1.86
15H-2, 120	131.70	4.7	8.2	1.74
15H-3, 20	132.20	3.9	9.9	2.53
15H-3, 70	132.70	4.0	8.8	2.18
15H-3, 120	133.20	4.1	8.8	2.17
15H-4, 20	133.70	4.2	8.8	2.08
15H-4, 70	134.20	4.1	8.7	2.1
15H-4, 120	134.70	4.5	7.9	1.76
15H-5, 20	135.20	4.5	9	1.99
15H-5, 70	135.70	4.2	8.4	2
15H-5, 120	136.20	4.2	8.5	2.02
15H-6, 20	136.70	4.3	9	2.11
15H-6, 70	137.20	4.3	9.6	2.24
15H-6, 120	137.70	4.3	8.6	2
16H-1, 20	138.70	3.8	8.4	2.2
16H-1, 70	139.20	4.0	7.9	1.96
16H-1, 120	139.70	3.9	7.6	1.93
16H-2, 20	140.20	4.0	8.5	2.15
16H-2, 70	140.70	3.9	8	2.04
16H-2, 120	141.20	4.0	8.2	2.02
16H-3, 20	141.70	4.0	8.2	2.03
16H-3, 70	142.20	3.9	7.8	1.97

Table 15 (continued).

Core, section, interval (cm)	Depth (mbsf)	Seawater (ohms)	Sample (ohms)	Formation factor
16H-3, 120	142.70	3.9	9	2.29
16H-4, 20	143.20	4.0	8.2	2.06
16H-4, 70	143.70	4.0	8.7	2.15
16H-4, 120	144.20	4.4	9.4	2.15
16H-5, 20	144.70	4.5	9.5	2.12
16H-5, 70	145.20	4.5	9.9	2.2
16H-5, 120	145.70	4.5	9.8	2.18
16H-6, 20	146.20	4.5	9.2	2.05
16H-6, 70	146.70	4.7	9.7	2.08
16H-6, 120	147.20	4.5	9.5	2.13
17H-1, 20	148.20	4.5	8.6	1.91
17H-1, 70	148.70	4.5	7.5	1.68
17H-1, 120	149.20	4.6	8.6	1.87
18H-1, 20	157.70	3.6	9.5	2.62
18H-1, 70	158.20	3.6	9.2	2.57
18H-1, 120	158.70	3.8	10	2.6
18H-2, 20	159.20	4.6	6.6	1.43
18H-2, 70	159.70	4.0	8.4	2.12
18H-2, 120	160.20	3.9	9.5	2.47
18H-3, 20	160.70	3.9	8.4	2.15
18H-3, 70	161.20	4.1	9.3	2.3
18H-3, 120	161.70	4.0	9.1	2.27
18H-4, 20	162.20	3.9	13.5	3.42
18H-4, 70	162.70	3.9	9.3	2.4
18H-4, 100	163.00	3.9	8.3	2.13
18H-5, 20	163.70	4.1	8.1	1.95
18H-5, 70	164.20	4.1	8.2	1.99
18H-5, 120	164.70	4.0	8.4	2.09
18H-6, 20	165.20	4.2	8.7	2.07
18H-6, 70	165.70	4.2	8.9	2.1
18H-6, 120	166.20	4.2	8.1	1.92
18H-7, 20	166.70	5.0	8.5	1.69
18H-8, 60	167.10	5.1	8.9	1.75
19H-1, 60	167.60	5.5	12.1	2.2
19H-1, 60	167.60	5.3	9.9	1.87
19H-1, 120	168.20	5.4	9.5	1.76
19H-2, 20	168.70	5.4	8.8	1.63
19H-2, 60	169.10	4.7	9.8	2.09
19H-2, 120	169.70	5.5	8.5	1.55
19H-3, 20	170.20	5.6	9.6	1.71
19H-3, 60	170.60	5.1	10.9	2.14
19H-3, 120	171.20	5.4	8.8	1.63
19H-4, 20	171.70	5.3	8.7	1.64
19H-4, 70	172.20	5.3	8.8	1.66
19H-4, 120	172.70	5.3	9.8	1.85
19H-5, 20	173.20	5.4	8.9	1.66
19H-5, 70	173.70	5.5	10	1.82
19H-5, 120	174.20	5.4	9.7	1.8
19H-6, 20	174.70	3.1	8.7	2.8
19H-6, 70	175.20	3.4	10.1	2.99
19H-6, 120	175.70	3.5	9	2.55
19H-7, 20	176.20	4.1	9	2.22
19H-7, 63	176.63	3.9	9.3	2.39
20H-1, 60	177.10	4.3	8.9	2.07
20H-2, 20	178.20	4.3	9.3	2.16
20H-2, 70	178.70	4.3	9.2	2.13
20H-2, 120	179.20	4.3	10.8	2.51
20H-3, 20	179.70	4.4	9.1	2.07
20H-3, 70	180.20	4.3	9.9	2.3
20H-3, 120	180.70	4.2	8.3	1.98
20H-4, 20	181.20	4.3	9.3	2.16
20H-4, 70	181.70	4.3	8.7	2.02
20H-4, 120	182.20	4.4	8.4	1.94
20H-5, 20	182.70	4.4	9.1	2.08
20H-5, 70	183.20	4.3	9.1	2.1
20H-5, 120	183.70	4.3	8.5	2
20H-6, 20	184.20	4.3	8.5	1.98
20H-6, 70	184.70	4.3	10.1	2.35
20H-6, 120	185.20	4.3	8.3	1.93
21H-1, 20	186.20	4.4	8.8	2
21H-1, 70	186.70	4.3	8.5	1.98
21H-1, 120	187.20	4.3	8.8	2.05
21H-2, 20	187.70	4.3	8.9	2.07
21H-2, 70	188.20	4.3	9.3	2.16
21H-2, 120	188.70	4.3	8.8	2.05
21H-3, 20	189.20	3.2	8.7	2.72
21H-3, 70	189.70	3.2	7.6	2.38

Table 15 (continued).

Core, section, interval (cm)	Depth (mbsf)	Seawater (ohms)	Sample (ohms)	Formation factor
21H-3, 120	190.20	3.3	8.7	2.64
21H-4, 20	190.45	3.7	9.4	2.54
21H-4, 70	190.95	3.7	8.2	2.22
21H-4, 120	191.45	3.7	9	2.43
21H-5, 20	191.95	3.8	8.7	2.29
21H-5, 70	192.45	3.8	8.5	2.24
21H-5, 120	192.95	3.9	8	2.05
21H-6, 20	193.45	3.9	8.5	2.18
21H-6, 70	193.95	3.9	9.7	2.49
21H-6, 117	194.42	3.9	10	2.56
22H-1, 70	196.20	3.9	9.8	2.51
22H-1, 120	196.70	3.9	8.3	2.13
22H-2, 20	197.20	4.0	9.6	2.42
22H-2, 70	197.70	4.0	10	2.5
22H-2, 120	198.20	4.0	9	2.25
22H-3, 20	198.70	4.0	9	2.27
22H-3, 70	199.20	4.0	8.1	2.03
22H-3, 120	199.70	4.0	8.7	2.18
22H-4, 20	200.20	4.0	8.4	2.1
22H-4, 70	200.70	4.0	11.7	2.93
22H-4, 120	201.20	3.9	10	2.56
22H-5, 20	201.70	4.0	10.9	2.73
22H-5, 70	202.20	4.0	8.5	2.13
22H-5, 120	202.70	4.0	8.4	2.1
22H-6, 20	203.20	4.0	8.4	2.1
22H-6, 70	203.70	4.0	9.8	2.45
22H-6, 120	204.20	4.0	8.7	2.18
23H-1, 20	205.20	4.0	8.3	2.08
23H-1, 70	205.70	4.0	9.8	2.45
23H-1, 120	206.20	4.0	7.4	1.85
23H-2, 24	206.70	4.0	9.4	2.35
23H-2, 67	207.13	4.0	8.7	2.18
23H-2, 124	207.70	4.0	7.3	1.83
23H-3, 20	208.16	4.0	8.5	2.13
23H-3, 70	208.66	4.0	8.3	2.08
23H-3, 120	209.16	4.0	15	3.75
23H-4, 20	209.66	4.0	9	2.25
23H-4, 70	210.16	4.0	10.3	2.58
23H-4, 120	210.66	4.0	8.7	2.18
23H-5, 20	210.99	4.1	8.8	2.15
23H-5, 70	211.49	4.1	10	2.44
23H-5, 94	211.73	4.3	10.1	2.35

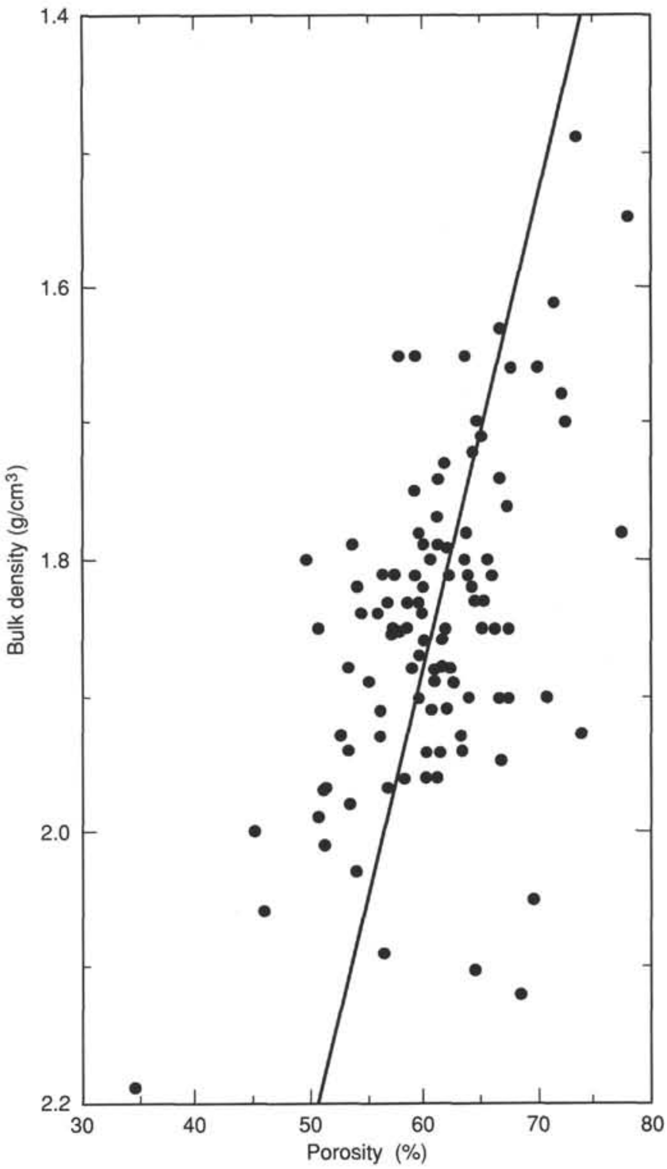

Figure 35. Porosity vs. bulk density, Hole 811A; regression equation $Y = 114.29 - 28.891X$, where Y = porosity (%) and X = bulk density (g/cm^3), and regression coefficient $R = 0.71$.

Table 16. Index properties data, Site 825.

Core, section, interval (cm)	Depth (mbsf)	Bulk density (g/cm^3)	Grain density (g/cm^3)	Porosity (%)	Water content (%)	Void radio
133-825A-						
5H-1, 100–103	201.00	1.87	2.76	52.5	40.3	1.11
5H-2, 100–103	202.50	1.89	2.70	53.6	41.0	1.15
5H-3, 100–103	204.00	2.02	2.65	43.4	28.2	0.77
5H-4, 100–103	205.50	1.82	2.70	55.0	44.7	1.22
5H-5, 100–103	207.00	1.86	2.73	52.0	40.1	1.09
5H-6, 100–103	208.50	1.91	2.68	65.6	54.2	1.91
6H-1, 100–103	210.50	1.87	2.64	54.0	41.9	1.17
6H-2, 100–103	212.00	1.86	2.68	52.6	40.9	1.11
6H-3, 100–103	213.50	1.85	2.71	51.8	40.2	1.07
6H-4, 100–103	215.00	1.84	2.69	56.5	45.8	1.30
6H-5, 100–103	216.50	1.79	2.63	56.4	47.5	1.29
6H-6, 100–103	218.00	1.89	2.67	55.1	42.6	1.23
7H-1, 100–103	220.00	1.79	2.70	50.0	39.9	1.00
7H-2, 100–103	221.50	1.97	2.69	50.4	35.5	1.02
7H-3, 100–103	223.00	1.82	2.62	50.0	39.3	1.00
7H-4, 100–103	224.50	1.90	2.70	52.7	39.6	1.11
7H-5, 100–103	226.00	1.88	2.71	53.6	41.4	1.16
7H-6, 100–103	227.50	1.84	2.68	54.8	43.8	1.21
8H-1, 100–103	229.50	1.78	2.63	55.7	47.3	1.26
8H-2, 100–103	231.00	1.84	2.69	54.2	43.2	1.18
8H-3, 100–103	232.50	1.91	2.71	50.7	37.4	1.03
8H-4, 100–103	234.00	1.83	2.68	54.3	43.8	1.19
8H-5, 100–103	235.50	1.90	2.65	50.8	37.8	1.03
8H-6, 100–103	237.00	1.88	2.67	50.1	37.5	1.01
10X-1, 100–103	248.50	1.81	2.69	55.0	45.3	1.22
10X-2, 100–103	250.00	1.97	2.68	49.8	34.9	0.99
10X-3, 100–103	251.50	1.92	2.58	49.7	36.2	0.99
10X-4, 100–103	253.00	1.96	2.69	47.9	33.5	0.92
11X-1, 100–103	258.10	1.89	2.64	49.4	36.7	0.98
11X-2, 100–103	259.60	1.92	2.70	50.3	36.7	1.01
12X-1, 100–103	267.80	1.97	2.68	46.9	32.2	0.88

Table 17. Compressional-wave velocity data, Site 825.

Core, section, interval (cm)	Depth (mbsf)	Distance (mm)	Traveltime (μs)	Velocity (m/s)
133-825A-				
6H-1, 100–103	210.50	28.24	19.28	1683
6H-2, 100–103	212.00	28.42	19.34	1688
6H-3, 100–103	213.50	29.07	19.83	1678
6H-5, 100–103	216.50	26.78	18.79	1641
6H-6, 100–103	218.00	28.12	19.26	1678
7H-1, 100–103	220.00	29.37	20.40	1640
7H-3, 100–103	223.00	29.33	19.79	1698
7H-4, 100–103	224.50	29.99	20.33	1683
7H-5, 100–103	226.00	29.37	20.08	1671
7H-6, 100–103	227.50	28.98	19.90	1665
8H-1, 100–103	229.50	28.24	19.63	1647
8H-2, 100–103	231.00	27.76	19.35	1646
8H-3, 100–103	232.50	29.54	20.12	1677
8H-5, 100–103	235.50	28.02	19.23	1674
10X-1, 100–103	248.50	29.16	19.96	1670
10X-2, 100–103	250.00	28.42	19.06	1718
10X-3, 100–103	251.50	29.63	19.64	1732
10X-4, 100–103	253.00	29.61	19.88	1706
11X-1, 100–103	258.10	28.63	19.70	1664
11X-2, 100–103	259.60	27.80	18.90	1696
12X-1, 100–103	267.80	27.59	18.84	1689

Table 18. Vane shear strength data, Site 825.

Core, section, interval (cm)	Depth (mbsf)	Spring number	Torque (degrees)	Strain (degrees)	Shear strength (kPa)
133-825A-					
5H-1, 77–78	200.77	2	8	7	3.8
5H-2, 90–91	202.40	2	10	6	4.7
5H-3, 90–91	203.90	2	4	6	1.9
5H-4, 90–91	205.40	2	8	10	3.8
5H-5, 90–91	206.90	2	9	10	4.2
5H-6, 91–92	208.41	2	4	9	1.9
6H-1, 92–93	210.42	2	7	5	3.3
6H-2, 89–90	211.89	2	8	11	3.8
6H-3, 89–90	213.39	2	7	10	3.3
6H-4, 91–92	214.91	2	7	10	3.3
6H-5, 91–92	216.41	2	4	9	1.9
6H-6, 91–92	217.91	2	6	8	2.8
7H-1, 91–92	219.91	2	5	9	2.4
7H-2, 91–92	221.41	2	4	8	1.9
7H-3, 91–92	222.91	2	6	8	2.8
7H-4, 91–92	224.41	2	5	6	2.4
7H-5, 91–92	225.91	2	5	7	2.4
7H-6, 91–92	227.41	2	6	8	2.8
8H-1, 91–92	229.41	2	3	2	1.4
8H-2, 91–92	230.91	2	7	6	3.3
8H-3, 91–92	232.41	2	5	4	2.4
8H-4, 91–92	233.91	2	6	9	2.8
8H-5, 91–92	235.41	2	11	10	5.2
8H-6, 91–92	236.91	2	7	8	3.3
10X-1, 91–92	248.41	2	4	2	1.9
10X-2, 91–92	249.91	2	8	4	3.8
10X-3, 91–92	251.41	2	6	9	2.8
11X-1, 91–92	258.01	2	11	15	5.2
11X-2, 91–92	259.51	2	9	9	4.2
12X-1, 91–92	267.71	2	7	9	3.3

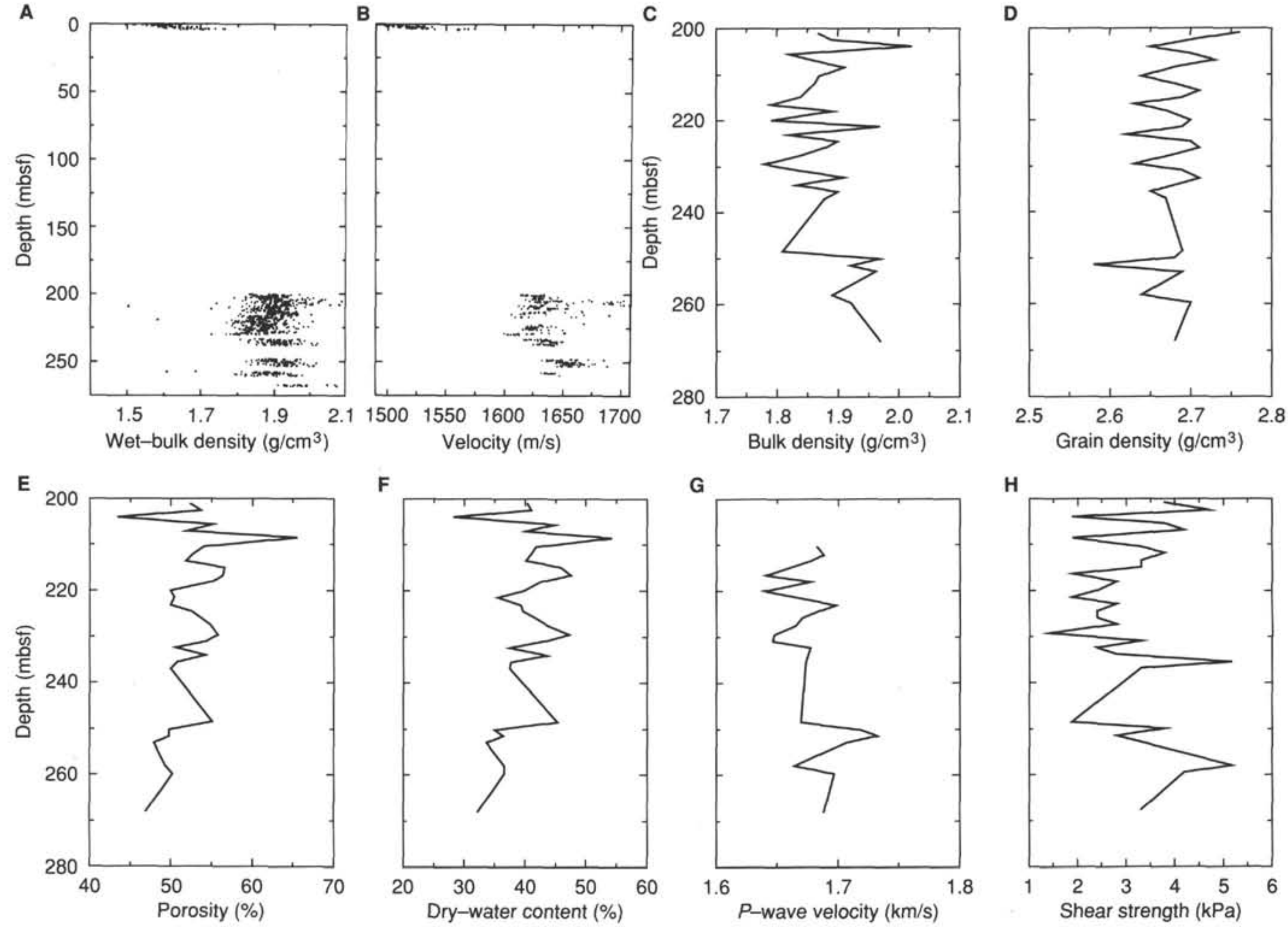

Figure 36. **A.** Physical properties vs. depth, Site 825. GRAPE bulk density measurements; data values have been averaged at 5-cm intervals. **B.** MST sonic velocity, raw data values having amplitudes greater than 30 have been averaged in 5-cm intervals. **C.** Bulk density; the data were obtained from mass and volume measurements for samples taken from split cores. **D.** Grain density. **E.** Porosity; the data were obtained from mass and volume measurements for samples taken from split cores. **F.** Dry-water content; the data were obtained from mass and volume measurements for samples taken from split cores. **G.** *P*-wave velocity; data were obtained from samples taken from split cores using the Hamilton frame. **H.** Shear strength; the data were obtained from split cores using the Wykeham-Farrance motorized vane apparatus.

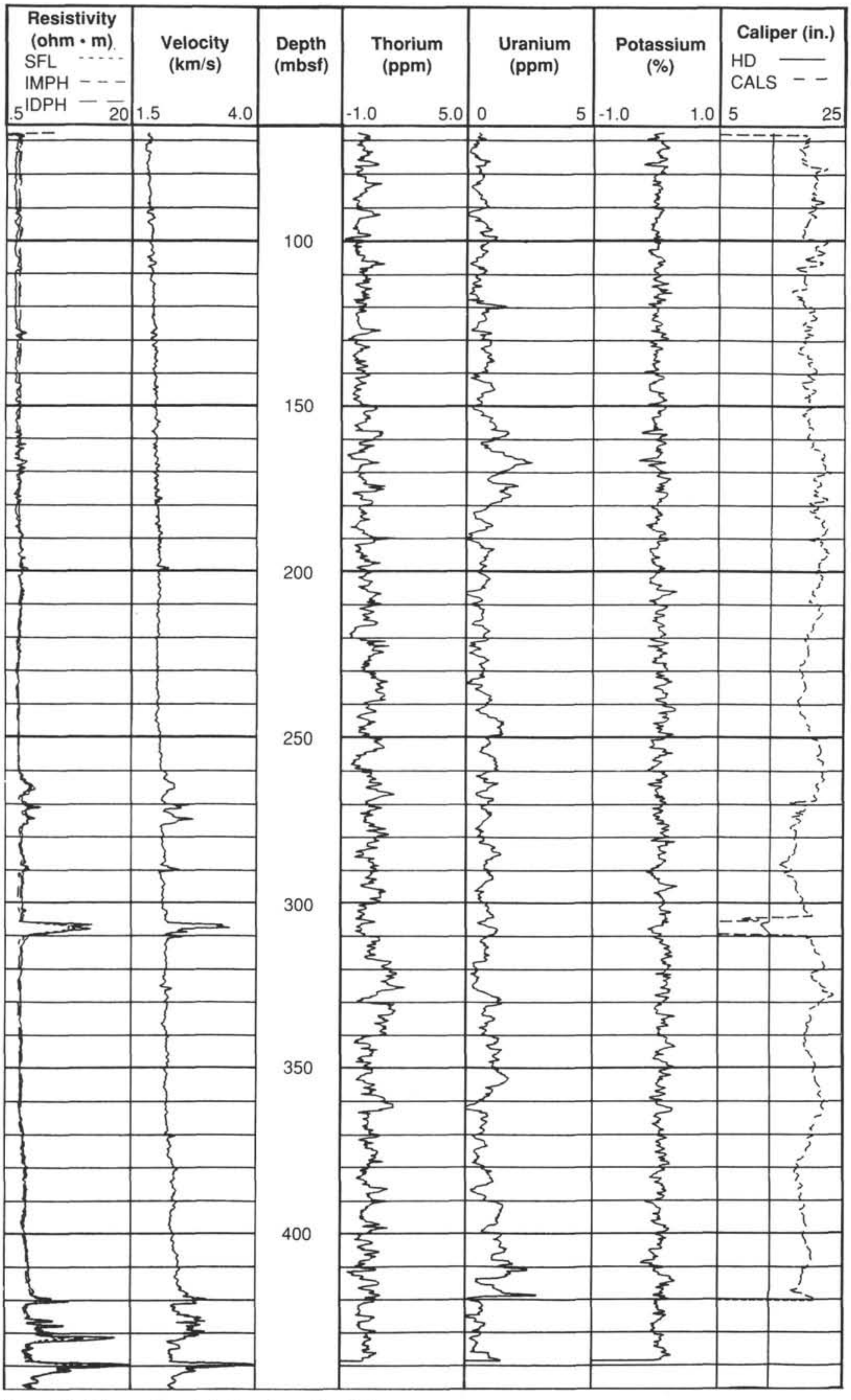

Figure 37. Primary downhole logs from Site 825.

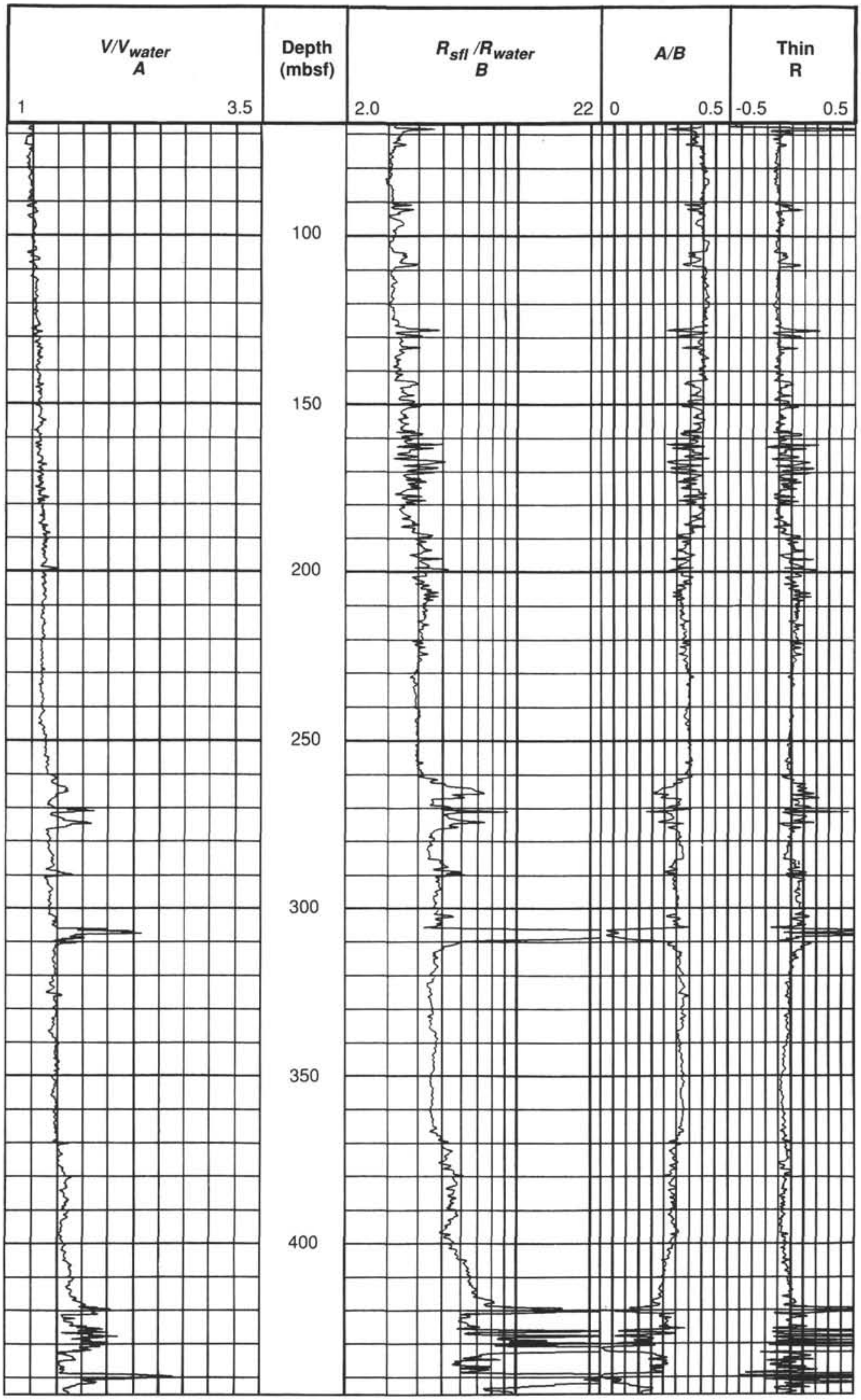

Figure 38. Velocity and resistivity for Site 825, plotted as ratios to highlight variations in cementation.

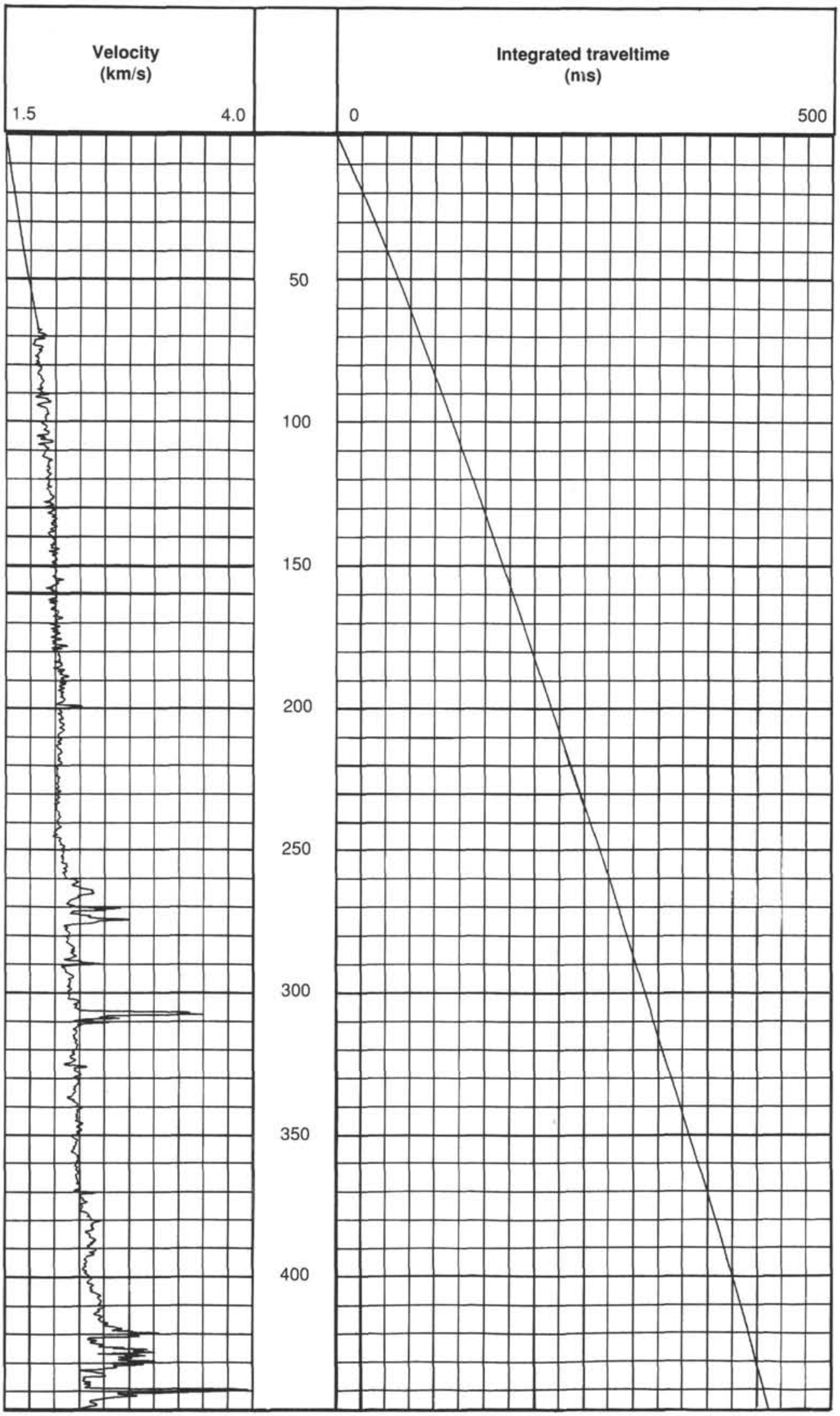

Figure 39. Velocity log and integrated two-way traveltime function that it implies, for comparison of core-derived information from Site 825 with the seismic sections across the site.

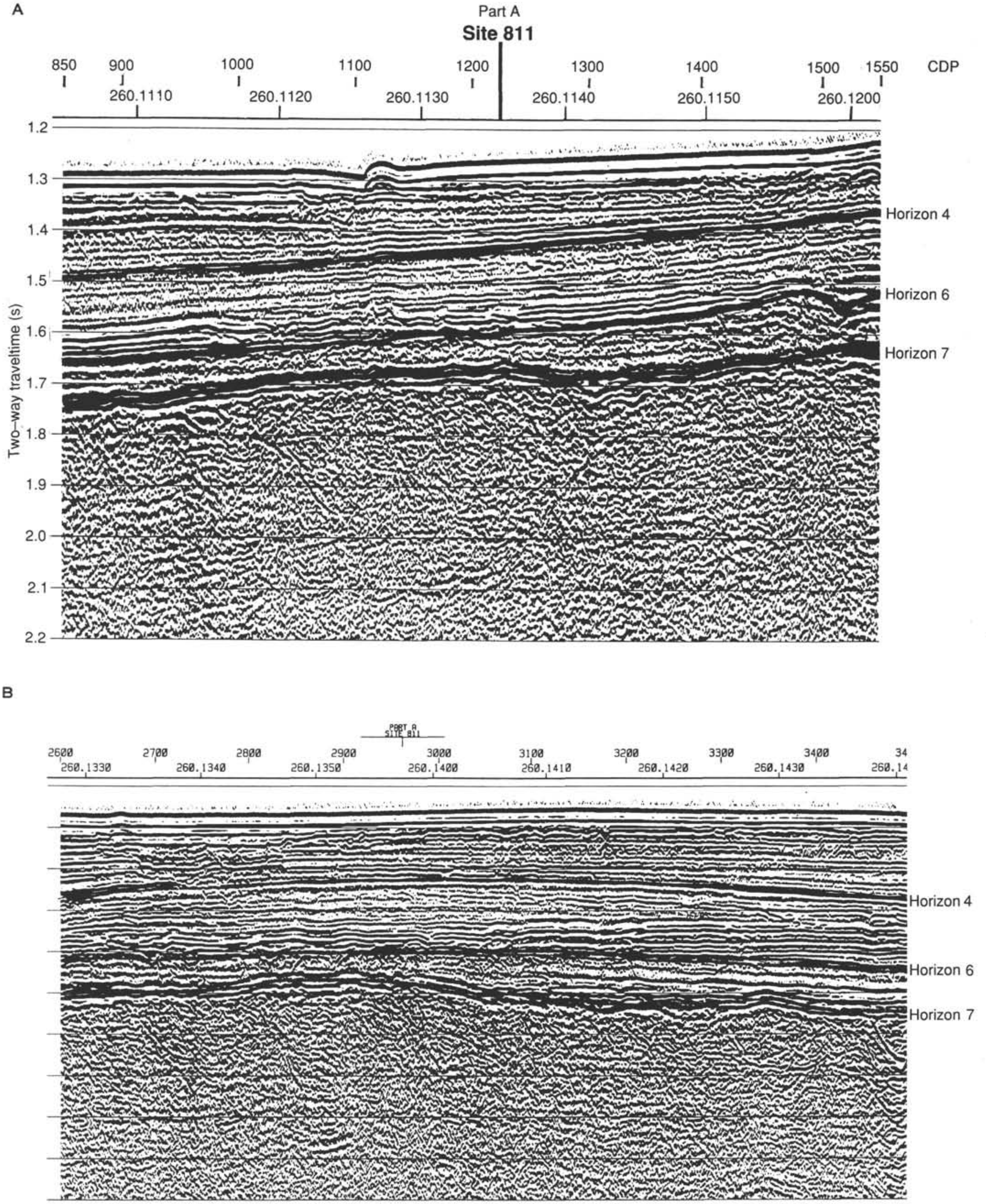

Figure 40. **A.** Part of BMR Line 75/037 Part A in the vicinity of Site 811. For the exact position of tie line consult Figure 4. **B.** Part of BMR seismic Line 75/037 Part C, showing the drill site and the reflectors defining the seismic sequences.

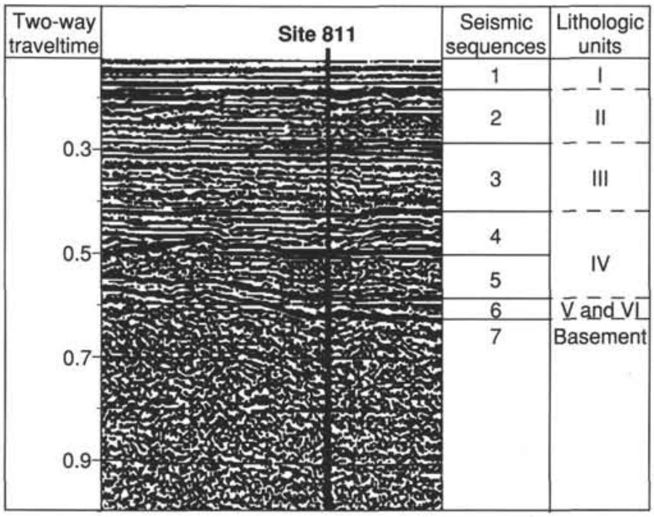

Figure 41. Seismic stratigraphic section at Site 811 showing the principal sequences and their lithostratigraphic equivalents.

Hole 825B: Resistivity-Sonic-Natural Gamma Ray Log Summary

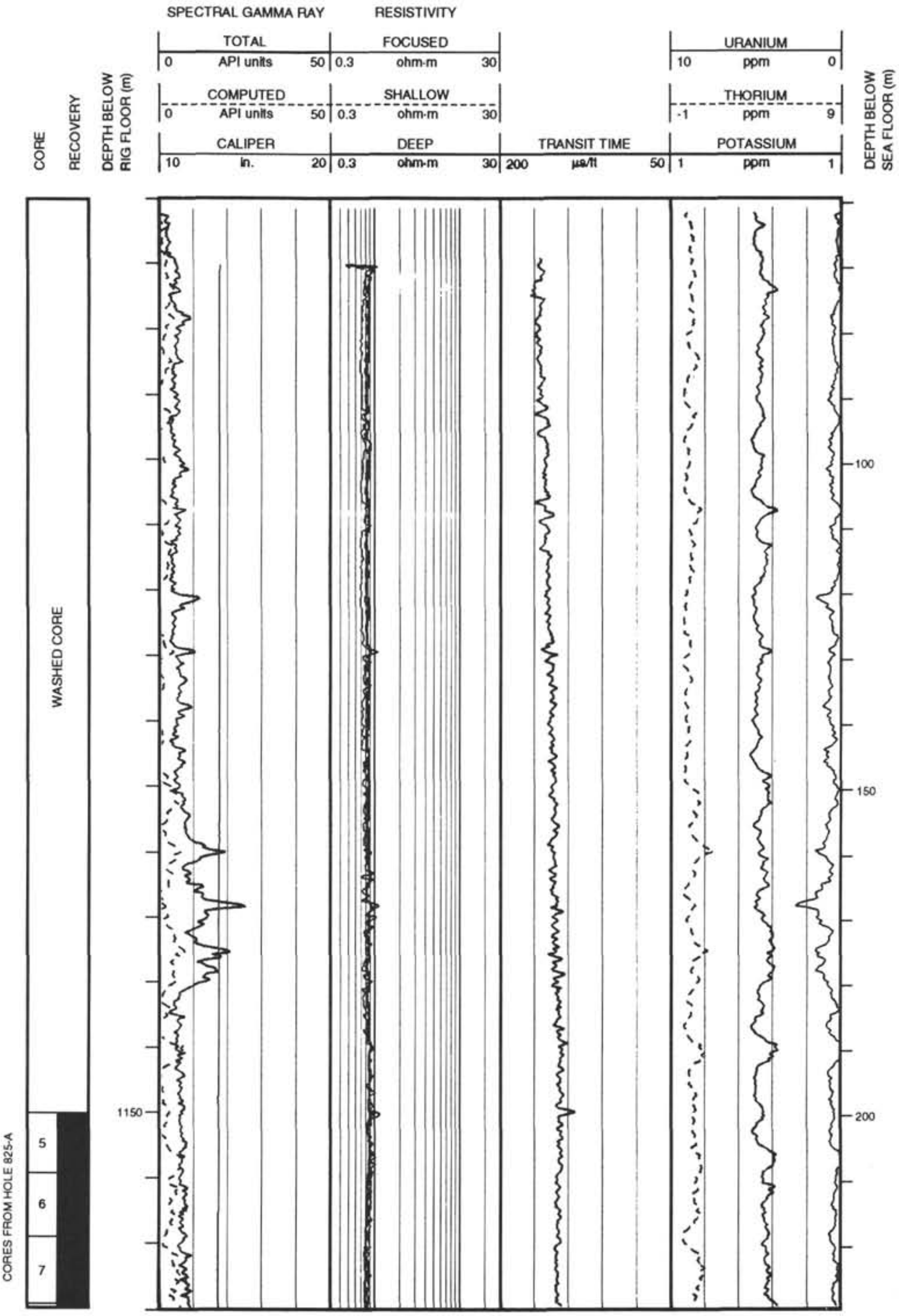

Hole 825B: Resistivity-Sonic-Natural Gamma Ray Log Summary (continued)